2013-07-19

Demand Response-Enabled Model Predictive HVAC Load Control in Buildings using Real-Time Electricity Pricing

Mesut Avci
University of Miami, avcimesut@gmail.com

UNIVERSITY OF MIAMI

DEMAND RESPONSE-ENABLED MODEL PREDICTIVE HVAC LOAD CONTROL IN BUILDINGS USING REAL-TIME ELECTRICITY PRICING

By

Mesut Avci

A DISSERTATION

Submitted to the Faculty
of the University of Miami
in partial fulfillment of the requirements for
the degree of Doctor of Philosophy

Coral Gables, Florida

August 2013

UNIVERSITY OF MIAMI

A dissertation submitted in partial fulfillment of
the requirements for the degree of
Doctor of Philosophy

DEMAND RESPONSE-ENABLED MODEL PREDICTIVE HVAC LOAD CONTROL IN BUILDINGS USING REAL-TIME ELECTRICITY PRICING

Mesut Avci

Approved:

_____
Shihab S. Asfour, Ph.D.
Professor and Associate Dean
College of Engineering

_____
M. Brian Blake, Ph.D.
Dean of the Graduate School

_____
Murat Erkoc, Ph.D.
Associate Professor of Industrial
Engineering

_____
Moataz Eltoukhy, Ph.D.
Post-Doctoral Associate of
Industrial Engineering

_____
Amir Rahmani, Ph.D.
Assistant Professor of Mechanical and
Aerospace Engineering

AVCI, MESUT (Ph.D., Industrial Engineering)

Demand Response-Enabled Model Predictive HVAC Load Control in Buildings Using Real-Time Electricity Pricing (August 2013)

Abstract of a dissertation at the University of Miami.

Dissertation supervised by Professor Shihab S. Asfour.
No. of pages in text. (148)

A practical cost and energy efficient model predictive control (MPC) strategy is proposed for HVAC load control under dynamic real-time electricity pricing. The MPC strategy is built based on a proposed model that jointly minimizes the total energy consumption and hence, cost of electricity for the user, and the deviation of the inside temperature from the consumer's preference. An algorithm that assigns temperature set-points (reference temperatures) to price ranges based on the consumer's discomfort tolerance index is developed. A practical parameter prediction model is also designed for mapping between the HVAC load and the inside temperature. The prediction model and the produced temperature set-points are integrated as inputs into the MPC controller, which is then used to generate signal actions for the AC unit. To investigate and demonstrate the effectiveness of the proposed approach, a simulation based experimental analysis is presented using real-life pricing data. An actual prototype for the proposed HVAC load control strategy is then built and a series of prototype experiments are conducted similar to the simulation studies. The experiments reveal that the MPC strategy can lead to significant reductions in overall energy consumption and cost savings for the consumer. Results suggest that by providing an efficient response strategy for the

consumers, the proposed MPC strategy can enable the utility providers to adopt efficient demand management policies using real-time pricing. Finally, a cost-benefit analysis is performed to display the economic feasibility of implementing such a controller as part of a building energy management system, and the payback period is identified considering cost of prototype build and cost savings to help the adoption of this controller in the building HVAC control industry.

DEDICATION

I would like to dedicate this work to my father Sait Avci, mother Salime Avci, sister Hafsa Oksuz, and wife Ipek Avci. I thank them kindly for their unconditional support, resolute understanding, and steadfast patience during the coursework, research, and writing of this dissertation.

ACKNOWLEDGMENTS

I would like to send my deepest thanks to my advisor, Dr. Shihab Asfour for his financial and emotional support and enduring patience. My deepest thanks also go to Dr. Murat Erkoc for his friendship and support both academically and emotionally. Without his input, this research would not have been possible.

I would also like to thank Dr. Amir Rahmani for his technical support and Mr. Joel Zahlan for his emotional support and friendship.

My appreciation also extends to the U.S. Department of Energy on behalf of its grant to the University of Miami Industrial Assessment Center (MIIAC). The knowledge gained while working under Dr. Shihab Asfour, the director of MIIAC, is greatly appreciated and valued.

My ultimate thanks go to my parents, Sait Avci and Salime Avci, for their unconditional love and support. I thank them for their prayers and I wish I could repay them for what they have done for me.

Last but not least, I could not have gone through this experience without the help and support of my wife, Ipek Avci. She has supported me throughout this entire scholastic endeavor. I will forever be grateful to her.

TABLE OF CONTENTS

LIST OF FIGURES

LIST OF TABLES

Page

CHAPTER 1: INTRODUCTION

The U.S. consumed approximately 97.8 quads of energy in 2010 which represents 19% of global energy consumption, making it the second largest share of world energy consumption by any country (U. S. DOE, 2011). In the United States, the buildings sector accounted for about 41% of primary energy consumption in 2010, compared to 30% for the industrial sector and 29% for the transportation sector (U. S. DOE, 2011). Figure 1-1 below displays the distribution of global energy and the breakdown of energy consumption in the U.S and within the U.S. buildings sector in 2010.

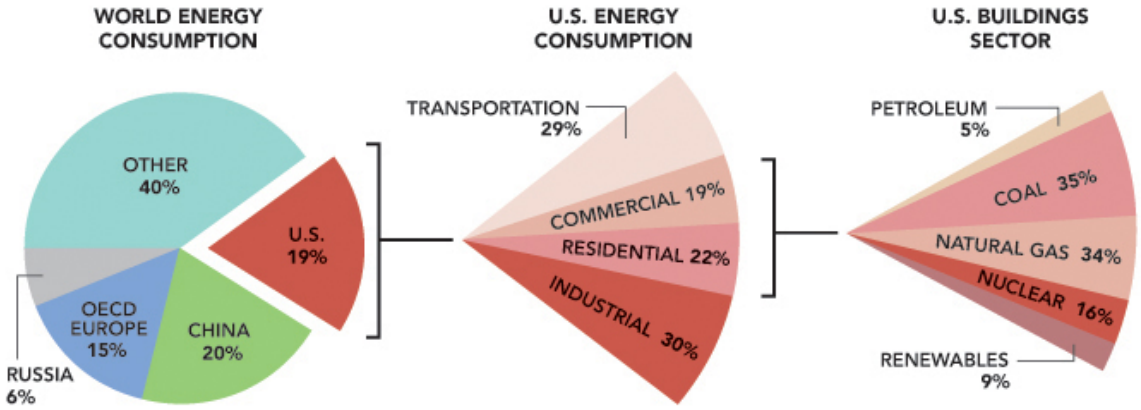

Figure 1-1 Distribution of global energy and the breakdown of energy consumption in the U.S. and within the U.S. buildings sector in 2010 (U. S. DOE, 2011)

Primary energy consumption in U.S. buildings increased by 48% between 1980 and 2009 (U. S. DOE, 2011). The Energy Information Administration (EIA) projects that total primary energy consumption will increase 17% over 2009 levels by 2035 (U. S. DOE, 2011). Figure 1-2 illustrates actual and projected primary energy consumption in the U.S. building sector.

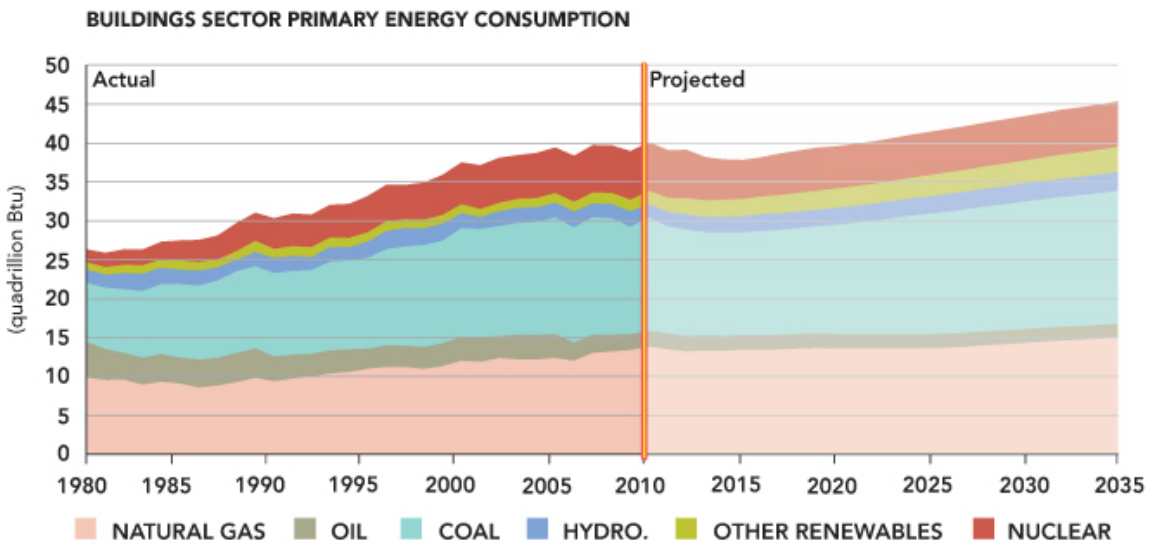

Figure 1-2 Actual and projected primary energy consumption in the U.S. building sector (U. S. DOE, 2011)

According to the U.S. DOE Buildings Energy Data Book, heating, ventilation, and air conditioning (HVAC) systems generated about 50% total building energy consumption in 2010 (U. S. DOE, 2011). Water heating, lighting, consumer electronics, kitchen appliances, and other end uses made up to the remainder (U. S. DOE, 2011). Figure 1-3 shows buildings site energy consumption by end use in 2010. It should be noted that Figure 1-3 is generated according to delivered energy which does not include energy lost during production, transmission, or distribution to customers.

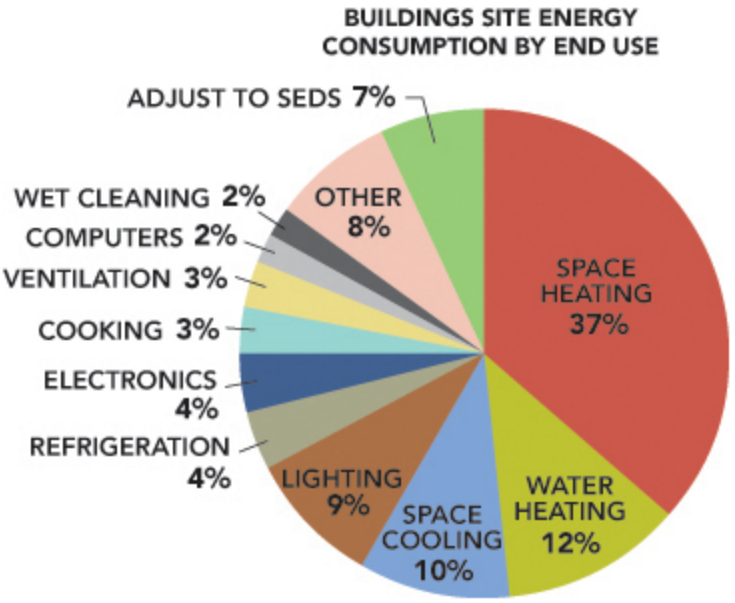

Figure 1-3 Buildings site energy consumption by end use in 2010 (U. S. DOE, 2011)

Electricity represents the largest source of energy for heating, cooling and ventilation systems in buildings. Figure 1-4 presents the breakdown of buildings HVAC primary energy consumption by fuel type. In 2010, 59% of total HVAC energy consumption in buildings was electricity driven (U. S. DOE, 2011). Figure 1-5 displays buildings HVAC energy end-use expenditure splits by fuel type in 2010. As it can be seen in Figure 1-5, electricity accounted for 9.84 quads of energy in building HVAC systems in 2010 (U. S. DOE, 2011).

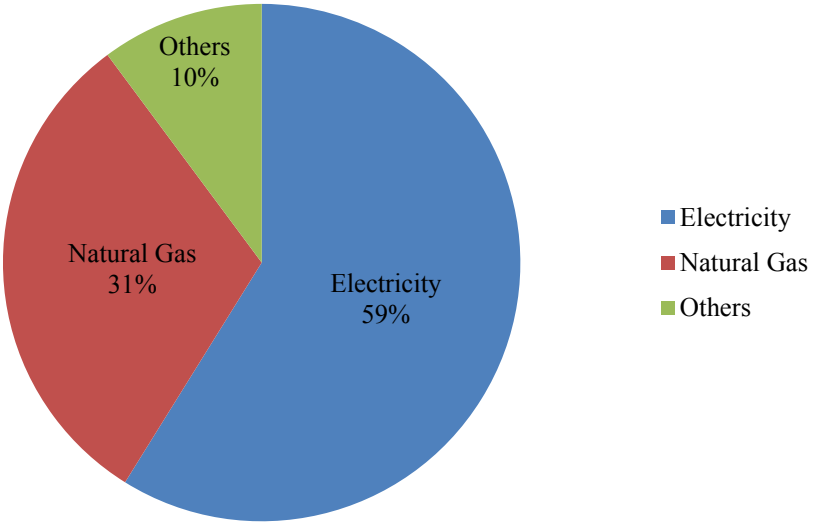

Figure 1-4 Buildings HVAC primary energy consumption by fuel type in 2010

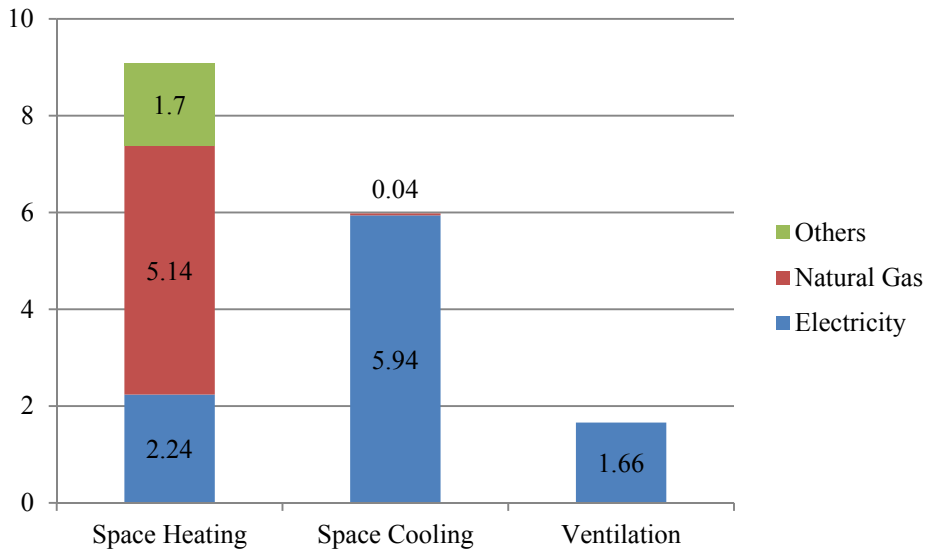

Figure 1-5 Buildings HVAC energy end-use expenditure splits by fuel type in 2010

Additionally, buildings are one of the major sources of carbon dioxide emissions. In 2010, buildings were responsible for 40% of greenhouse gas emissions in the United States (U. S. DOE, 2011). Figure 1-6 illustrates the end-use breakdown of carbon dioxide emissions in buildings in 2010. As it can be seen from Figure 1-6, HVAC accounted for the largest percent (43%) of carbon dioxide emissions in buildings (U. S. DOE, 2011).

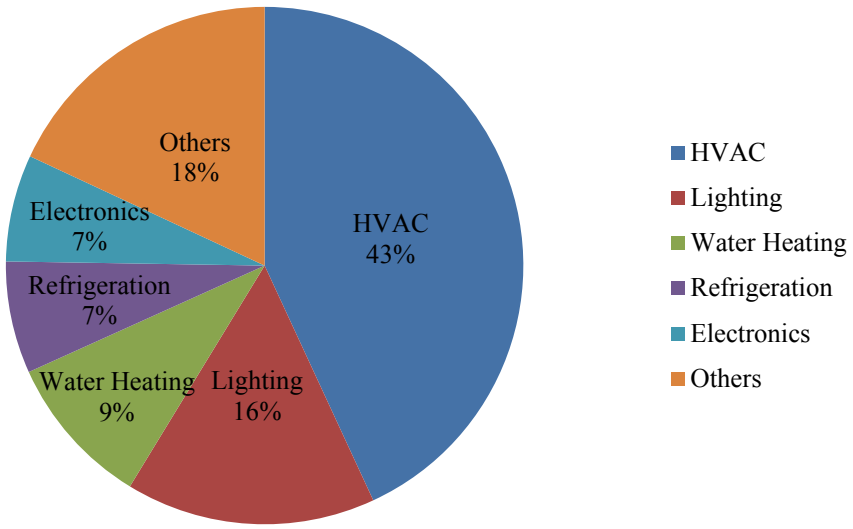

Figure 1-6 Buildings carbon dioxide emissions by end use in 2010

Electricity represents the largest source of carbon dioxide emissions for heating, cooling and ventilation systems in buildings. Figure 1-7 displays the breakdown of buildings HVAC carbon dioxide emissions by fuel type. In 2010, 61% of total HVAC carbon dioxide emissions in buildings were caused by electricity driven systems (U. S. DOE, 2011). Figure 1-8 displays buildings HVAC energy end-use carbon dioxide emissions splits by fuel type in 2010. As it can be seen in Figure 1-8, electricity accounted for 566.2 million metric tons of carbon dioxide emissions in building HVAC systems in 2010 (U. S. DOE, 2011).

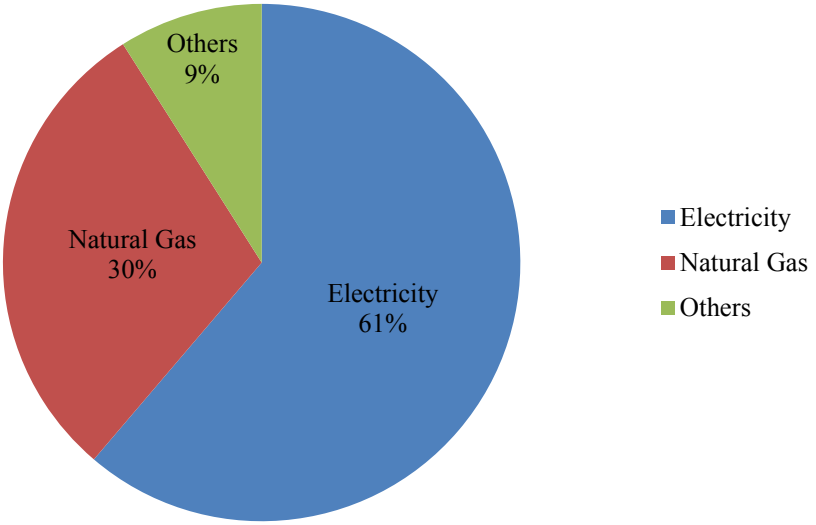

Figure 1-7 Buildings HVAC carbon dioxide emissions by fuel type in 2010

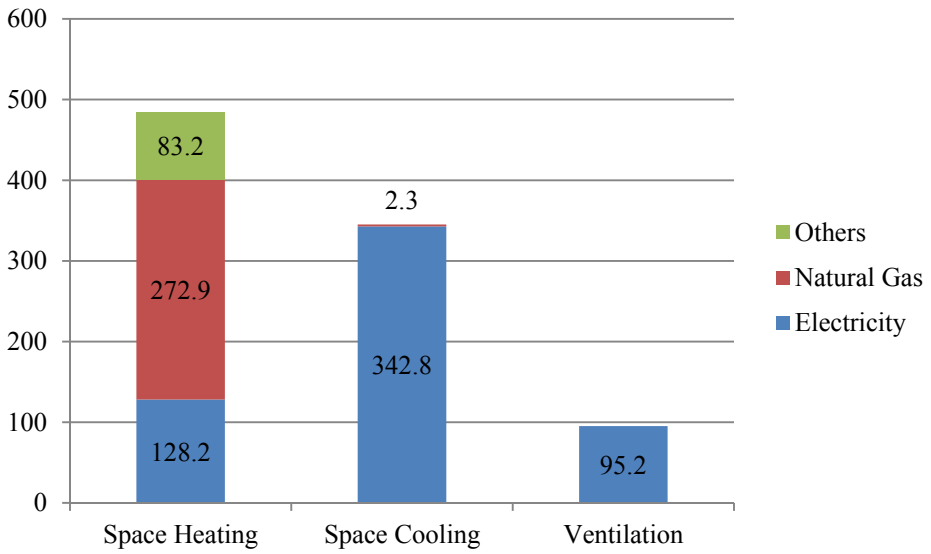

Figure 1-8 Buildings HVAC energy end-use carbon dioxide emissions splits by fuel type in 2010

From the statistics provided above, it can be concluded that it is both economically and environmentally significant to reduce HVAC energy consumption in buildings. The simplest and most effective way to reduce HVAC energy is to improve control strategies without having to replace existing equipment, which is often a slow process with considerable infrastructure investments (Dawson-Haggerty, Ortiz, Jiang, Hsu, Shankar, & Culler, 2010). According to a recent report from the Department of Energy's Pacific Northwest National Laboratory (PNNL), commercial buildings can experience significant energy savings by implementing more efficient control strategies for HVAC systems (Wang, Katipamula, Huang, & Brambley, 2011). Figure 1-9 displays estimated cost saving ranges for U.S. commercial building HVACs with efficiency controls (Wang et. al, 2011). The results of the PNNL report show that commercial building owners could save an average of 38% on their HVAC bills just by installing a few new controls onto their HVAC systems (Wang et. al, 2011). Therefore, it is not only encouraging for researchers to develop more efficient HVAC control strategies, but also important for manufacturers to produce these advanced controllers.

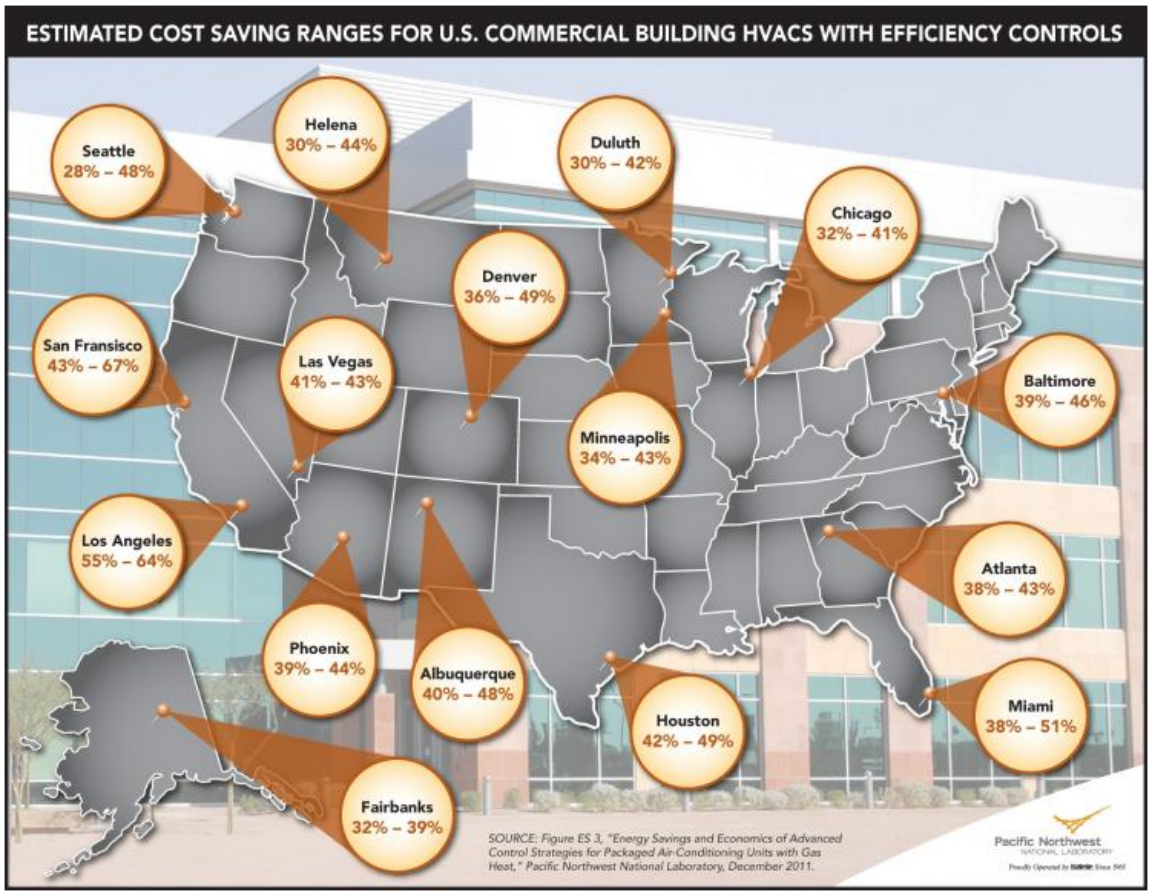

Figure 1-9 Estimated cost saving ranges for U.S. commercial building HVACs with efficiency controls (Wang et. al, 2011)

Demand Response

Regulating the use of energy has recently become critical for government and utility companies due to the concerns of the energy crisis with increasingly frequent power curtailment and scheduled blackouts during peak demand periods such as hot days of summer. While energy efficiency is the most prominent component of growing efforts to supply affordable, reliable, secure, and clean electric power, demand response is a key pillar of utility and regional resource plans, and its importance is growing. Figure 1-10 shows linkages between the electricity value chains and their key features those are necessary for a robust technology framework and depicts energy efficiency and demand response as more of a continuum (Piette, 2009).

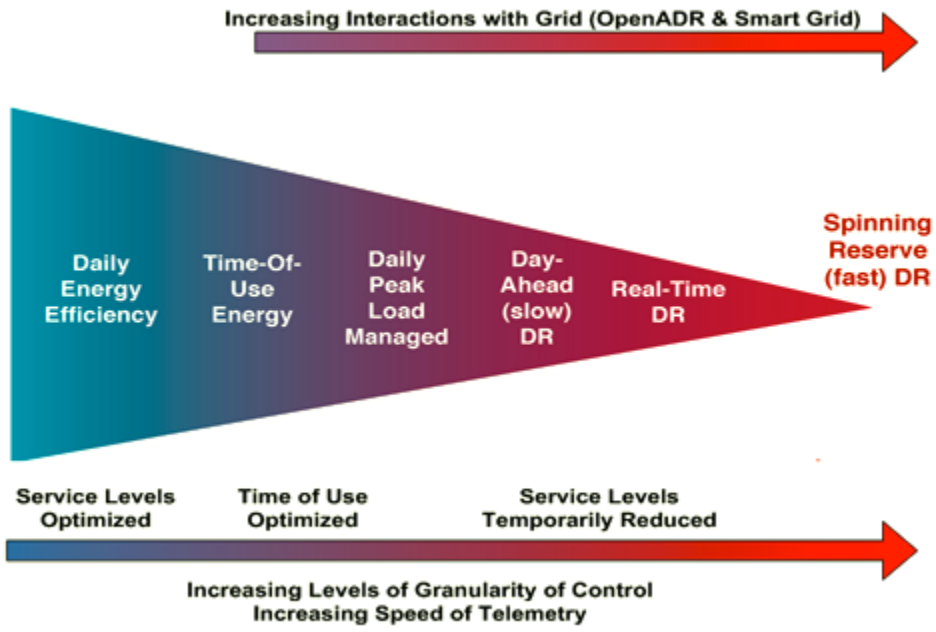

Figure 1-10 Conceptual perspective of energy efficiency and demand response (Piette, 2009)

The left side of the Figure 1-10 underlines that most hours of the year customers are concerned with continuous energy efficiency which focuses on optimizing each hour energy use relative to the energy services begin delivered (Piette, 2009). Looking to the right, few hours of the year are included and customers begin to reduce building service levels in demand response periods, likely requiring additional investment to execute real-time or fast demand response options (Piette, 2009). The second bar in the Figure 1-10 adds a level of describing control system granularity (Piette, 2009). The ability to provide fine grain controls into end-use building systems improves both energy management and demand responsiveness (Piette, 2009).

Unlike gas, water or other substance; electricity cannot be stored economically on a large scale. It needs to be used right after it is generated and transmitted. As a result, supply and demand must remain in balance in real time. Electricity shortages occur when supply cannot meet demand. It is possible to avoid electricity shortages by offering more supply through constructing additional power generation systems or reducing the peak demand by managing the use of electricity. The investments in constructing new power plants and transmission lines to satisfy every possible supply and demand scenario cannot be covered easily by increasing the price of electricity because the critical peak demand occurs less than 1% of the time in a whole year (California Energy Commission, 2002). Additionally, environmental impact of that would be tremendous. Demand response (also known as load response) works from the other side of the equation – instead of increasing power generation to meet demand, it entails end-use electric customers reducing or shifting their electricity consumption during times of peak demand in response to changes in the price of electricity over time or to incentive payments designed to induce lower

electricity use when wholesale market prices are high or system reliability is in jeopardy. Utilities pay for demand response capacity because it is typically cheaper and easier to procure than traditional generation.

The ability to reduce electricity demand and shift peak loads during shortages through better demand-side management and optimal control on HVAC systems is the main approach to relieve the global energy crisis. It is estimated that a 5% lowering of demand would have resulted in a 50% price reduction during the peak hours of the California electricity crisis in 2000/2001 (International Energy Agency, 2003). According to California energy demand report, most of the peaks of electricity consumption in the summer are caused by the wide use of electricity-driven air conditioners and central air conditioner systems (California Energy Commission, 2000). This problem can be mitigated by methods of engaging customers in demand response efforts. This includes offering a retail electricity rate that reflects the time-varying nature of electricity costs and/or programs that provide incentives to reduce load at critical times (time-based rates) such as real-time electricity pricing and developing HVAC control mechanisms for utility customers to respond to those rates. Advanced metering infrastructure expands the range of time-based rate programs that can be offered to consumers and smart customer systems such as in-home displays or home-area-networks can make it easier for consumers to changes their behavior and reduce peak period consumption from information on their power consumption and costs. These programs also have the potential to help electricity providers save money through reductions in peak demand and the ability to defer construction of new power plants and power delivery systems - specifically, those reserved for use during peak times. Many of the Recovery Act projects

involve deployment of enabling technologies and customer information/feedback systems to facilitate demand response. These include both information and control technologies such as in-home displays and programmable and communicating thermostats with corresponding demand response programs. A number of consumer behavior studies on the use of the installed equipment were performed in order to examine factors that influence the participation of consumers in dynamic pricing programs, as well as the influence of these programs and enabling technologies on customer response.

According to information provided by respondents to The Federal Energy Regulatory Commission (FERC) 2012 Demand Response and Advanced Metering Survey (2012 FERC Survey), significant progress was achieved in the past year for both wholesale and retail electricity demand response and advanced metering, supported by the actions of state regulators, federal regulators and federal funding under the American Recovery and Reinvestment Act, the development of interoperability standards, and efforts of industry and customers (Federal Energy Regulatory Commission, 2012). 2012 FERC Survey indicates that the potential demand response resource contribution from all U.S. demand response programs is estimated to be nearly 72,000 MW (MW), or about 9.2 percent of U.S. peak demand (Federal Energy Regulatory Commission, 2012). This is an increase of about 13,000 MW from the 2010 FERC Survey which represents a 25 percent increase in reported potential peak reductions from demand response (Federal Energy Regulatory Commission, 2012). Figure 1-11 illustrates a steady national increase in demand response capability (potential peak reduction) across all FERC survey years (Federal Energy Regulatory Commission, 2012).

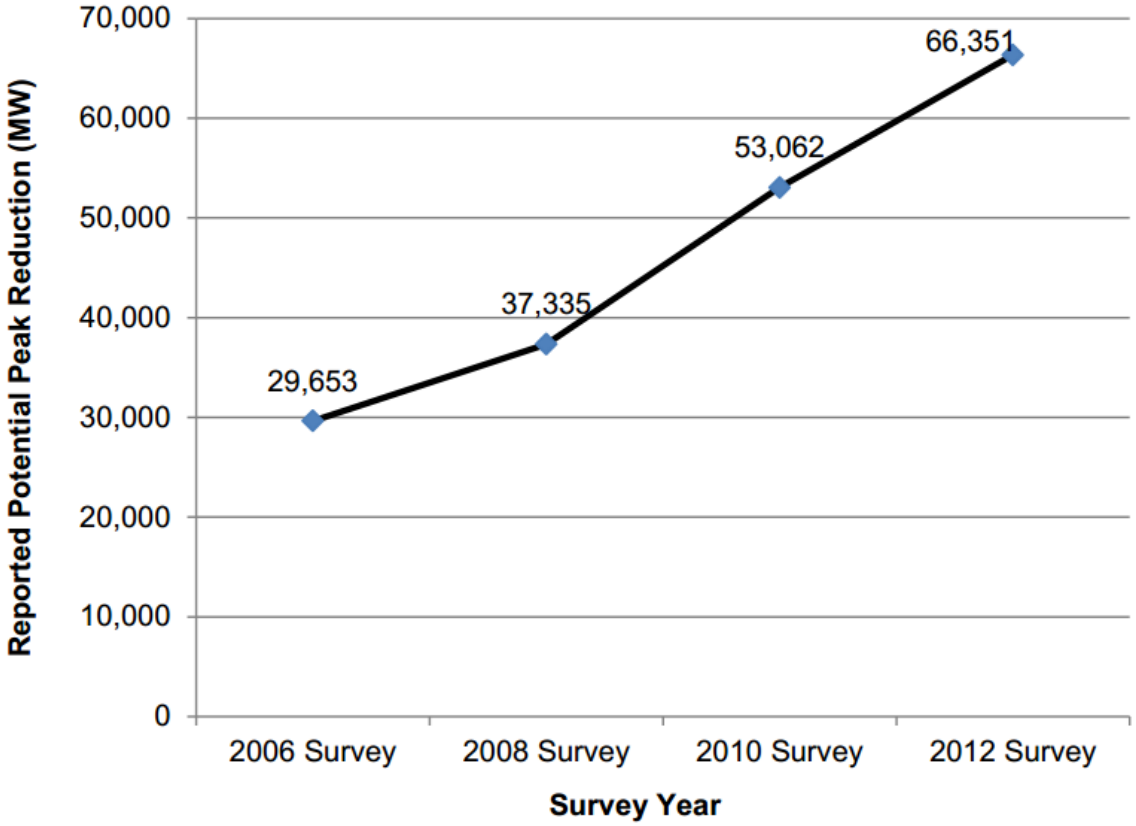

Figure 1-11 Total reported potential peak reduction in the 2006 through 2012 FERC Surveys (Federal Energy Regulatory Commission, 2012)

Additionally, advanced metering penetration (i.e., the fraction of all installed meters that are advanced meters) reached approximately 22.9 percent in 2011 in the United States, compared to approximately 8.7 percent in the 2010 FERC Survey (covering calendar year 2009) (Federal Energy Regulatory Commission, 2012).

However, according to a Federal Energy Regulatory Commission (FERC or Commission) staff report – A National Assessment of Demand Response Potential (National Assessment), submitted to Congress in June 2009 – current demand response programs tap less than a quarter of the total market potential for demand response (Federal Energy Regulatory Commission, 2009). Figure 1-12 displays a comparison of the demand response estimates under four demand response scenarios (business-as-usual,

expanded BAU, achievable participation, full participation) illustrating the potential impact of demand response on peak demand over the analysis horizon (Federal Energy Regulatory Commission, 2009). Because current efforts have missed a significant portion of the cost-effective demand response potential, it is evident that action needs to be taken to either create new programs or expand existing ones where cost-effective.

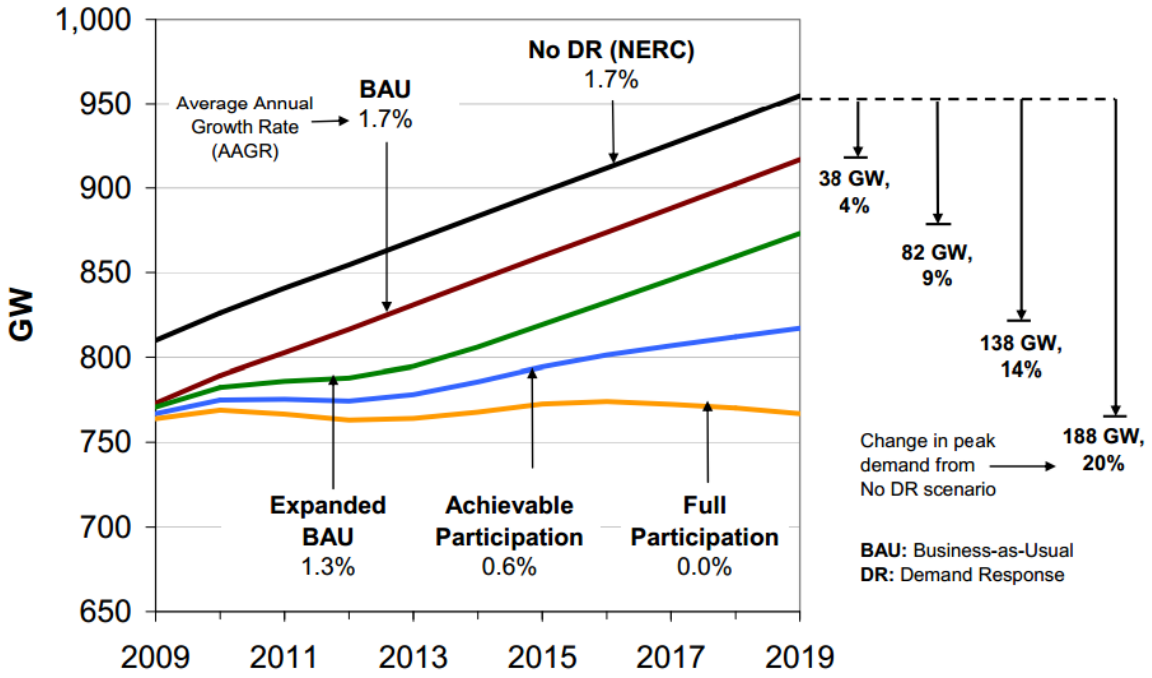

Figure 1-12 U.S. summer peak demand forecast by scenario (Federal Energy Regulatory Commission, 2009)

Since most demand response programs in effect today are event-driven and designed primarily to curtail or shift load for short periods of time, customers tend to assume that demand response events occur for limited periods that are called by the grid operator. However, real-time electricity pricing programs also produce measurable reductions in customers' total energy use and cost and are growing in prevalence and impact.

Real-Time Electricity Pricing

The marginal costs for electricity provided during consumers' actual consumptions vary continuously with the supply demand interaction affected by weather conditions and human activity. At present, many utility consumers are billed at a static average rate for the total amount of electricity consumed which does not correspond to the actual wholesale prices during the time of their actual consumption. Furthermore, the average hourly market price over a year is typically lower than the standard utility flat rates. Figure 1-13 is a snapshot of a random summer day that shows how the market-based "real-time" price of electricity shoots high above or dips far below the traditional utility fixed rate.

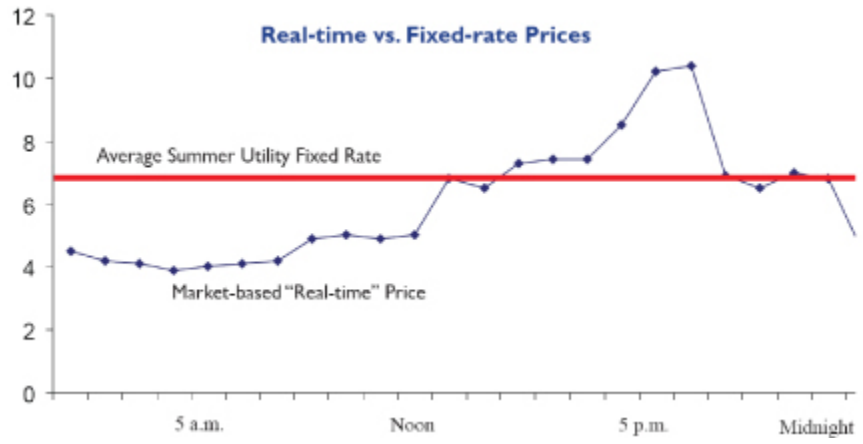

Figure 1-13 Real-time vs. fixed-rate electricity prices on a summer day

Under the traditional pricing policy, with a constant rate, consumers have no incentive to modify their electricity consumption behavior in response to the marginal cost. In recent years, utility companies have started to adopt dynamic pricing rates for end-consumers. Dynamic electricity pricing models help utility companies better distribute the price with respect to demand-supply interaction while encouraging

consumers to reduce their electricity consumption during peak times - when market power prices are at their highest - according to price variations in order to achieve financial benefits. Figure 1-14 presents the number of entities that reported offering real-time pricing programs by region and entity type (Federal Energy Regulatory Commission, 2012). In 2012, twenty-eight entities reported offering real-time pricing, a slight increase from the 25 entities reporting in 2010 (Federal Energy Regulatory Commission, 2012).

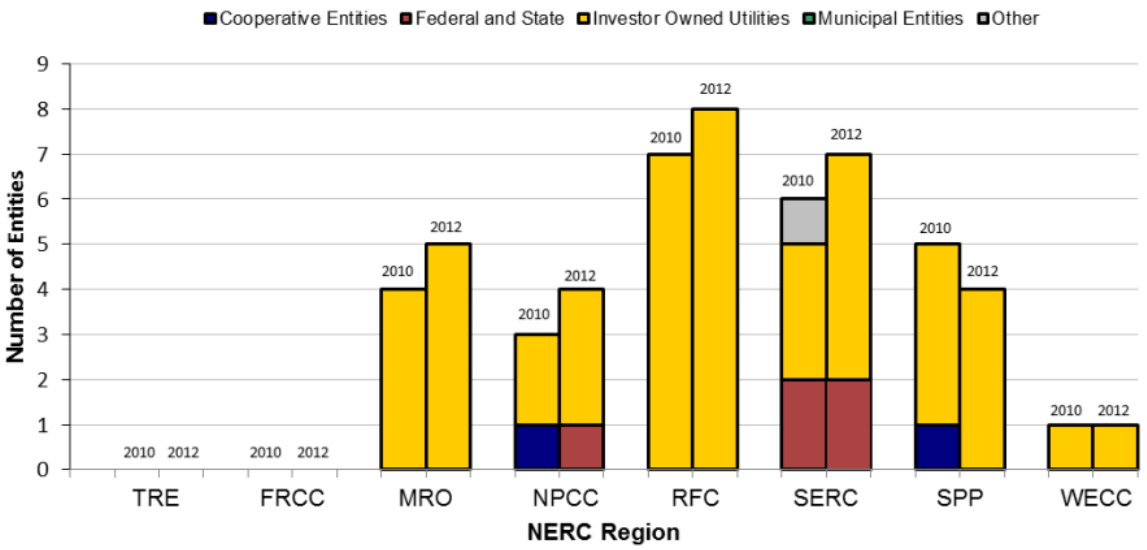

Figure 1-14 Number of entities reporting retail real-time pricing by region and entity type in 2010 and 2012 (Federal Energy Regulatory Commission, 2012)

Moreover, according to a Federal Energy Regulatory Commission (FERC or Commission) staff report – A National Assessment of Demand Response Potential (National Assessment), submitted to Congress in June 2009 – the largest gains in demand response impacts can be made through pricing programs, particularly when offered with enabling technologies at the national level (Federal Energy Regulatory Commission, 2009). Figure 1-15 below more pronounces this in the Full Participation scenario, where

roughly 70 percent of the impacts come from pricing programs (Federal Energy Regulatory Commission, 2009).

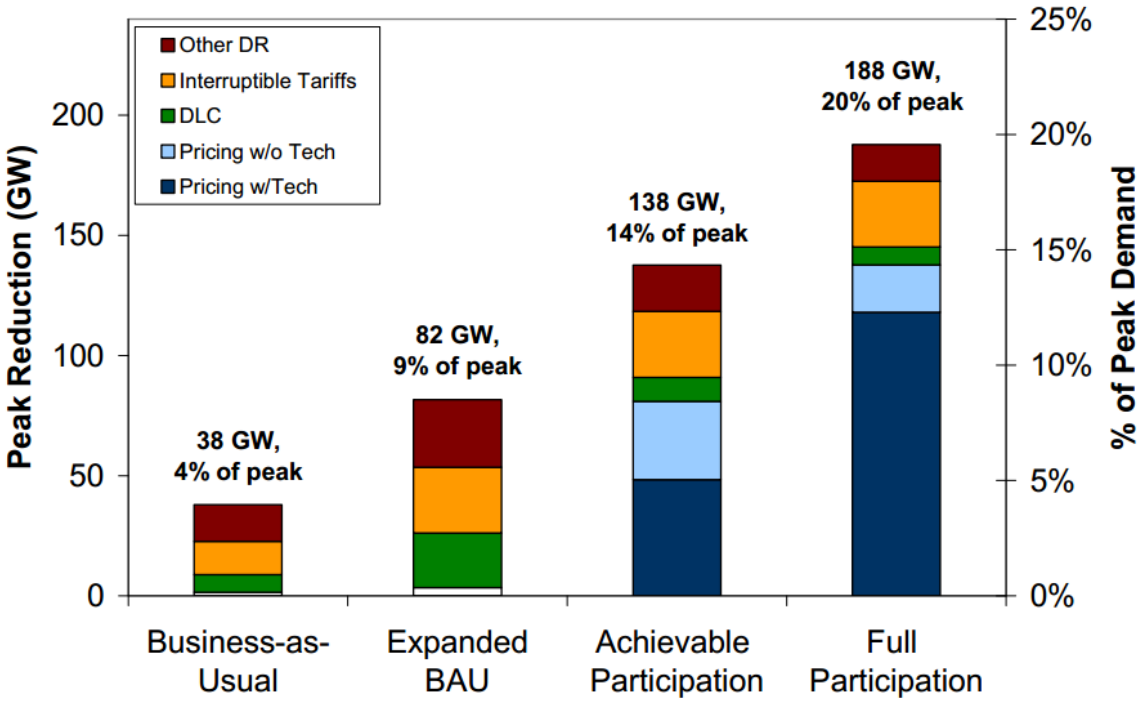

Figure 1-15 U.S. demand response potential by program type (2019) (Federal Energy Regulatory Commission, 2009)

Real-time pricing (RTP) is a dynamic pricing model where the retail price of energy is different for various hours of the day along with the different days and seasons. In RTP, upcoming hourly energy prices are announced to the end-consumers an hour or a day ahead. This allows end-consumers to be aware what the electricity is worth at different hours of the day. By providing accurate information about electricity rates real-time pricing allows consumers to use that information to make decisions about electricity use. End-consumers, however, do not have the necessary knowledge about how to efficiently schedule the operation of their appliances in response to the hourly updated

pricing information they may receive from the utilities in an RTP program in order to achieve financial benefits. Moreover, building automation systems (BAS) are not fully adapted to coordinate with RTP models. Thus, the benefits of RTP are not fully utilized in current practice.

The fact that the building envelope itself forms a thermal storage makes it possible to shift electricity demand of thermal appliances from high price to low price periods or from high loading to low loading periods respectively. As demand becomes increasingly price-responsive due to demand shifting through dynamic pricing, the spot electricity markets can also be expected to investigate different bidding strategies which may lead to lower wholesale electricity prices (International Energy Agency, 2003), (CooKE, 2011).

The advantage of RTP would be best realized with automated controllers that can efficiently manage the HVAC load in response to price shifts. While such controllers should be advanced enough to execute efficient control mechanisms, they need to be designed for practical use by consumers. In this research, such a controller based on model predictive control (MPC) is proposed for HVAC usage in a retail electricity market with RTP.

Model Predictive Control (MPC)

MPC is a simple yet effective approach for constrained process control which was initially developed in the late seventies and early eighties in the process industries (oil refineries, chemical plants, etc.), and has been successfully applied in many areas both within the research community and in industry over the last decades (Morari & Lee, 1999), (Maciejowski, 2002), (Fernandez-Camacho & Bordons-Alba, 1995), and (Mayne & Rawlings, 2009). In recent years it has also been used in power system balancing

models (Arnold & Andersson, 2011). Model predictive controllers make explicit use of a dynamic model of the process which is obtained by system identification, in order to generate the control signal by minimizing an objective function. The main advantage of MPC is that it takes future timeslots into account while optimizing the current timeslot. This is achieved by optimizing a finite time-horizon, but only implementing the current timeslot.

The main idea of MPC is to utilize a mathematical model of the process to predict the future behavior of the system over a determined horizon (prediction horizon) and to compute control actions by optimizing a cost function depending on these predictions subject to some constraints. Only the first element of the open-loop control sequence is employed in the system, then the plant state is sampled again based on feedback from the previous period and current measurements. Calculations are then repeated starting from the now current state, yielding a new control and new predicted state path. The prediction horizon keeps being shifted forward and for this reason MPC is also called receding horizon control. The chosen length of the prediction horizon should be greater than the system settling time in order to account for behavior with significant dynamics. The methodology of MPC strategy is represented in Figure 1-16.

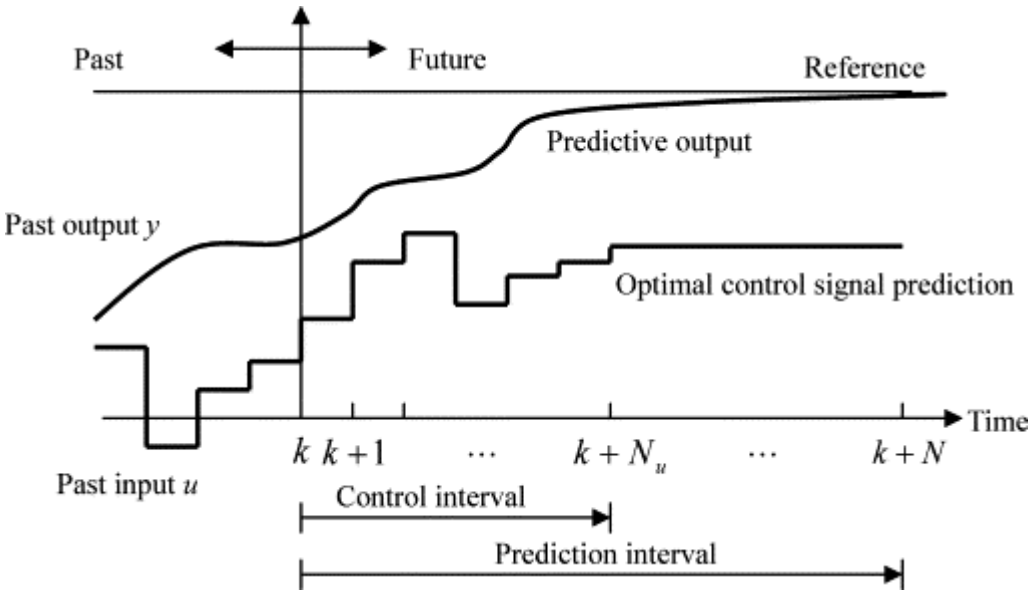

Figure 1-16 Basic principle of MPC

One of the goals of the cost function to be optimized is to keep the process as close as possible to the reference trajectory (set-point). This criterion is usually represented as a quadratic function of the errors between the predicted output signal and the predicted reference trajectory in the cost function.

Figure 1-17 shows the basic structure used to implement MPC strategy. The optimizer calculates the optimal future control actions taking into account the cost function as well as the constraints. Based on these actions and past and current values, future plant outputs are predicted using the prediction model.

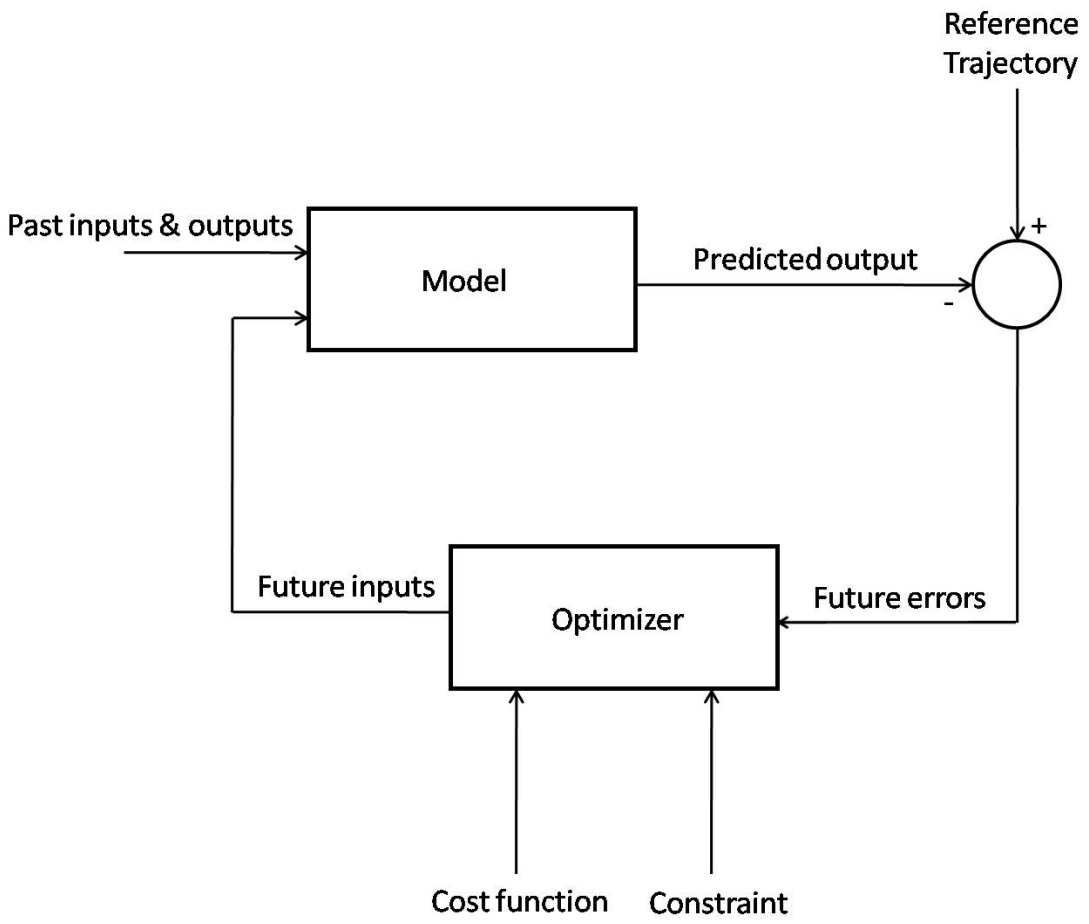

Figure 1-17 Basic structure of MPC

The process model plays a decisive role in the MPC controller. The chosen model must be able to capture the process dynamics to precisely predict the future outputs and while being simple to implement and understand. It may not be necessary to model all the physics, chemistry and internal behavior of the process in order to get a model that gives reliable prediction, and in fact all this detail should not be modeled if it is not required. Majority of applications use linear MPC approaches with the feedback mechanism of the MPC compensating for prediction errors due to structural mismatch between the model and the process. This simplifies the control problem to a series of direct matrix algebra calculations that are fast and robust.

In HVAC systems control, MPC is a well suited control methodology due to the following properties of HVAC systems: the plant is a multiple input, multiple output system and its inputs are constrained. Moreover, disturbances acting on the plant like varying outdoor air temperature are measurable. Furthermore, time constants are relatively large which makes it easy to perform the required optimization of the MPC strategy in time. The objective of MPC in HVAC systems is to design a control strategy that minimizes the HVAC energy consumption (or operational costs) while satisfying occupants' thermal comfort. The achievements of MPC used for HVAC control are derived from efficient use of thermal mass or thermal storage of a building.

Contributions of This Research

In this research, real-time pricing is incorporated into the model predictive control strategy. A practical cost and energy efficient strategy is proposed for HVAC load control with dynamic real-time electricity pricing. The proposed MPC strategy aims to reduce the total energy consumption and hence, cost of electricity for the user, while considering the thermal comfort of the consumers by concurrently minimizing the deviation of the inside temperatures from the consumer's choice of reference temperatures. A mechanism that bolsters the energy efficiency and cost savings by coupling smart load shifting in response to changing prices with dynamically setting the temperature set-points based on consumer preferences is designed. The proposed system enforces effective and practical use of MPC by providing an efficient parameter prediction process and an algorithm for temperature set-point determination. The predicted input/output mapping and the produced temperature set-points serve as inputs for the proposed MPC controller, which eventually generates signal actions for the AC

unit according to the aforementioned objective. The signal action is composed of a duty cycle that represents the proportion of "on" time for the AC during any given time period.

The parameter prediction model is built in linear form for the mapping between the signal action and the inside temperature. To determine the reference temperatures for the planning horizon (usually a day), an algorithm is developed for temperature set-point assignment. For this, a discomfort tolerance index that models the consumer's attitude towards thermal comfort in reference to cost of comfort is first developed. Based on the index value, the algorithm assigns temperature set-points to price ranges constructed from the RTP data.

To investigate and demonstrate the effectiveness of the proposed approach a simulation based experimental analysis is carried out using real-life pricing data. An actual prototype for the proposed HVAC load control strategy is then built and a series of prototype experiments is conducted similar to the simulation studies. In both cases the MPC process is compared to the conventional two-position control approach. The latter strategy is used as a benchmark since two-position control is very common in practice. The experiment is first conducted assuming fixed temperature set-points. This way, the impact of MPC on energy consumption and costs with only load shifting option can be singled out. It is observed that while the MPC process leads to energy reduction and cost savings for the consumer under this setting, in general, with only load shifting, the benefits are not too promising. The temperature set-point assignment algorithm is employed to determine the temperature set-points in the second part of the analysis where temperature set-points are treated as endogenous parameters. In this case, the experiments reveal that with the MPC strategy, reduction in energy consumption (both for total

electricity use and for peak time consumption) and cost savings significantly improve. The obtained results suggest that the proposed MPC strategy, when controlling both the load and the temperature set-points, allows the consumers effectively take advantage of the dynamic pricing and enjoy significant cost savings in electricity usage. As such, this strategy can be instrumental in facilitating an effective demand response framework, which enables the utility providers adopt efficient demand management policies using real-time pricing.

CHAPTER 2: REVIEW OF LITERATURE

Temperature Regulation in Residential Buildings

Many people spend most of their days indoor and each day they spend about half of the day in their residences. Therefore the thermal comfort of the residential building is very important and the control of the heating, ventilation and cooling (HVAC) system should satisfy the thermal comfort and energy efficiency requirements. It is also a very important issue to reduce and optimize the HVAC energy consumption in the residential sector in the context of the global warming effect, since HVAC is the largest contributor to a home's energy bills and carbon emissions, accounting for 43% of residential energy consumption in the U.S. and 61% in Canada and U.K., which have colder climates (Energy Information Administration, 2009), (Energy, E. P. B. E. S., 1997) and (Rathouse & Young, 2004). Although most of the research and implementation of advanced control schemes for the HVAC systems are on the commercial buildings, laboratories or hospitals, there have been a number of researches conducted on the HVAC control systems for the residential buildings.

Most residential buildings in the United States use a single-zone, two position HVAC control system which is simple and easy to manage. However, this control system has its disadvantage for its unsatisfactory thermal comfort and energy efficiency. Kulkarni & Hong presented a proportional control system for the residential building by setting up the dynamic simulation for the building and the control system (Kulkarni & Hong, 2004). They used the state-space method to model the building system and implemented the simulation code on MATLABTM, which makes the optimization of the controller possible (Kulkarni & Hong, 2004). They compared the thermal comfort and energy

efficiency under different proportional control scheme and traditional two-position control schemes (Kulkarni & Hong, 2004). Their results indicated that proportional control is advantageous to the two-position control for the thermal comfort while there is not much difference in energy consumption between two control schemes (Kulkarni & Hong, 2004).

Chen et al. introduced an autonomous thermostat system, the Demand Response Electrical Appliance Manager (DREAM), to control residential HVAC systems aiming to improve price-based demand responsiveness in residences (Chen, Jang, Auslander, Peffer, & Arens, 2008). Using a disaggregated set of energy and environmental sensors, they implemented control strategies to optimize electricity cost and user's comfort (Chen et al., 2008). To perform optimization, the system starts from default values and learns the dynamic behavior of a house and HVAC system (Chen et al., 2008). They used computer simulation, lab tests and field tests to validate the system infrastructure and control strategies (Chen et al., 2008). Their tests indicated that the DREAM responds automatically to price signals with appropriate energy saving behavior reducing electricity consumption during peak price hours without significantly decreasing thermal comfort (Chen et al., 2008). Figure 2-1 illustrates the DREAM concept schematic in a home.

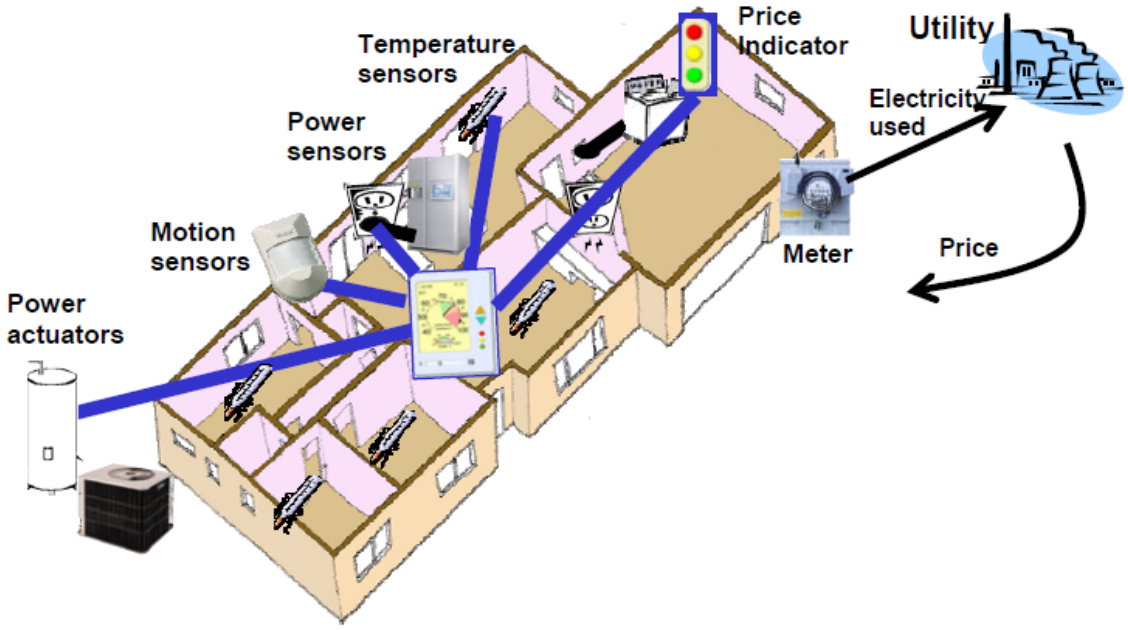

Figure 2-1 Schematic of the Demand Response Electrical Appliance Manager (Chen et al., 2008)

Lu et al. introduced the Smart Thermostat that uses simple sensing technology to automatically sense occupancy and sleep patterns in a home, and using these patterns saves energy by automatically turning off the home's HVAC system (Lu, Sookoor, Srinivasan, Gao, Holben, Stankovic, Field, & Whitehouse, 2010). In order to evaluate this approach, they installed sensors in 8 homes and compared the expected energy usage of their algorithm against existing approaches (Lu et al., 2010). Their results shows that the Smart Thermostat can provide larger energy savings and more comfort than existing baseline solutions (Lu et al., 2010). They indicated that their approach will save 28% of residential HVAC energy consumption on average, at a cost of approximately $25 in sensors (Lu et al., 2010).

Tiptipakorn et al. introduced a residential consumer-centered control strategy of air conditioner/heater and water heater in real-time electricity pricing environment

(Tiptipakorn & Lee, 2007) and (Tiptipakorn, Lee, & Wang, 2009). They demonstrated the results of their strategy in the MATLAB simulations using the pseudo real-time pricing of ERCOT and actual outdoor temperature data (Tiptipakorn & Lee, 2007). The performances of the proposed load control strategy show that it is effective compared to those from the optimization problems and no load control strategies, in a way that it can be applied in real-time while the optimization problems face the difficulty in acquiring the valid and accurate data of future time frames (Tiptipakorn & Lee, 2007). Figure 2-2 illustrates the proposed real-time air conditioning load control strategy.

Tiptipakorn et al. introduced a load control strategy in which "price naming" concept serves as a supporting tool for the developments of the residential consumer's demand response (Tiptipakorn, Lee, Mao, & Lu, 2010). They simulated samples of hourly home appliance load profiles using the Market Clearing Price Energy (MCPE) of ERCOT as pseudo real-time prices (Tiptipakorn et al., 2010).

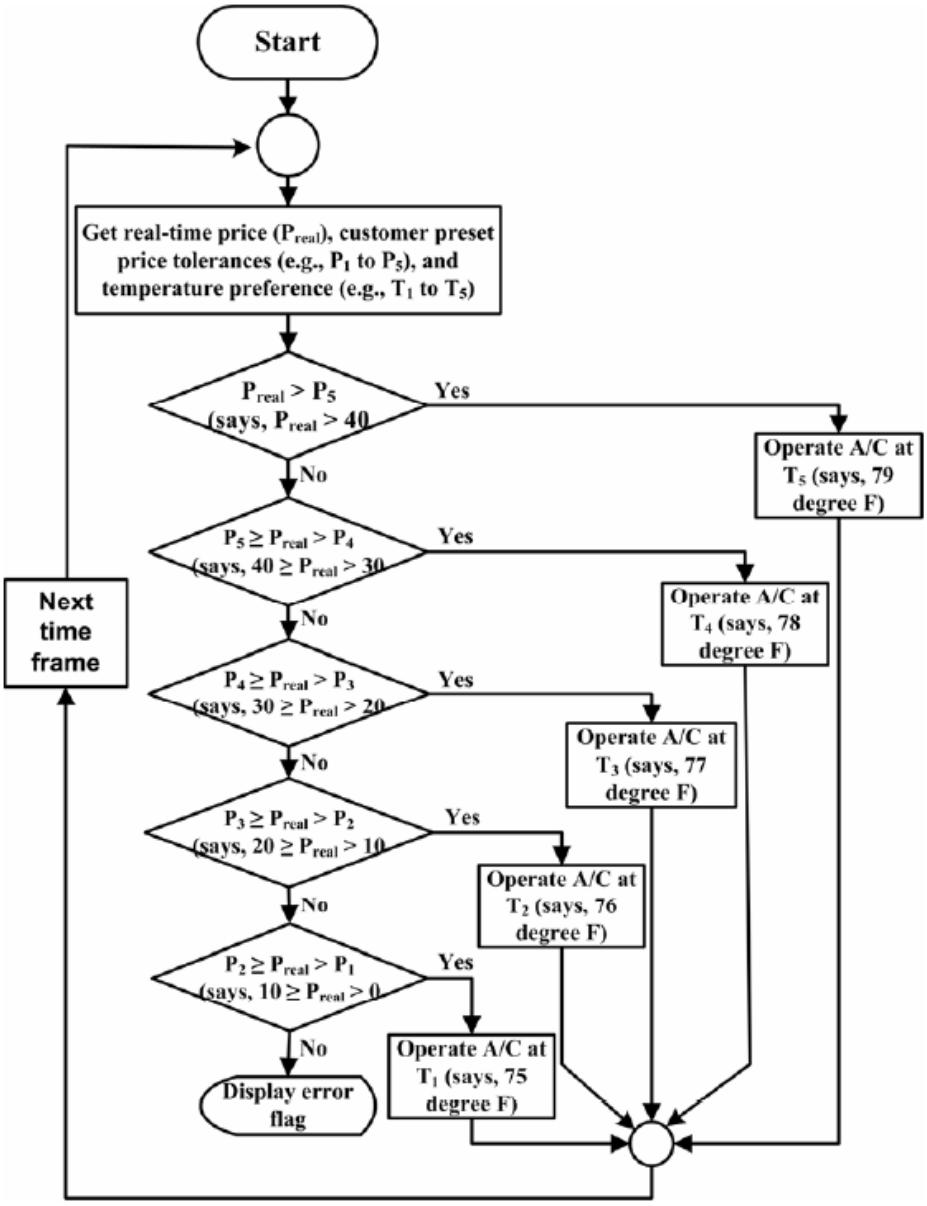

Figure 2-2 Real-time air conditioning load control strategy (Tiptipakorn & Lee, 2007)

Mohsenian-Rad & Leon-Garcia proposed an optimal and automatic residential energy consumption scheduling framework which attempts to achieve a desired trade-off between minimizing the electricity payment and minimizing the waiting time for the operation of each appliance in household based on the needs declared by the users (Mohsenian-Rad & Leon-Garcia, 2010). They considered a scenario where real-time pricing is combined with inclining block rates in order to have more balanced residential load with a low peak-to-average ratio (Mohsenian-Rad & Leon-Garcia, 2010). They also developed a weighted average electricity price predictor filter to the actual hourly-based price values used by the Illinois Power Company in order to effectively implement their residential load control strategy (Mohsenian-Rad & Leon-Garcia, 2010). They obtained the optimal choices of the coefficients for each day of the week to be used by the price predictor filter (Mohsenian-Rad & Leon-Garcia, 2010). They found that the combination of their proposed energy consumption scheduling design and the price predictor filter leads to significant reduction in both users' payments and the resulting peak-to-average ratio in load demand for various load scenarios (Mohsenian-Rad & Leon-Garcia, 2010). Figure 2-3 illustrates smart meter operation and wireless home area network (WHAN) in the design proposed by Mohsenian-Rad & Leon-Garcia.

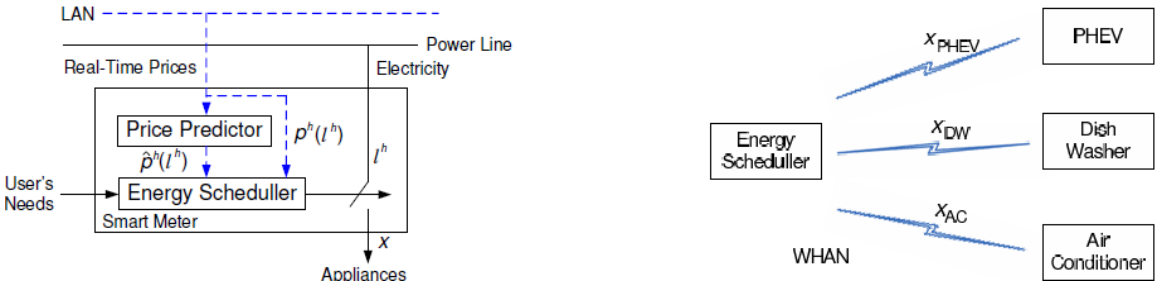

Figure 2-3 Smart meter operation and wireless home area network (WHAN) (Mohsenian-Rad & Leon-Garcia, 2010)

Space heating is a major factor in residential energy use. It uses more energy than any other residential energy expenditure including air conditioning, water heating, and appliances (Energy Information Administration, 2009). Scott et al. developed a system, PreHeat, to more efficiently heat homes by using occupancy sensing and occupancy prediction to automatically control home heating (Scott, Brush, Krumm, Meyers, Hazas, Hodges, & Villar, 2011). They applied their system in five homes in both US and UK and compared their prediction algorithm with a static program over an average 61 days per house, measuring actual gas consumption and occupancy (Scott et al., 2011). They indicated that their system both saved gas and reduced MissTime (the time that the house was occupied but not warm) while removing the need for users to program thermostat schedules (Scott et al., 2011).

Boait & Rylatt proposed an approach to the user interface of home heating systems that simplifies the user interaction with the system (Boait, & Rylatt, 2010). They used electricity consumption and hot water use to automatically determine time settings (Boait, & Rylatt, 2010). They also provided a temperature set point that adapts to user activity levels and external temperature (Boait, & Rylatt, 2010). Their practical results from a prototype control system showed useful energy savings (Boait, & Rylatt, 2010). Figure 2-4 shows the user interface of prototype control system.

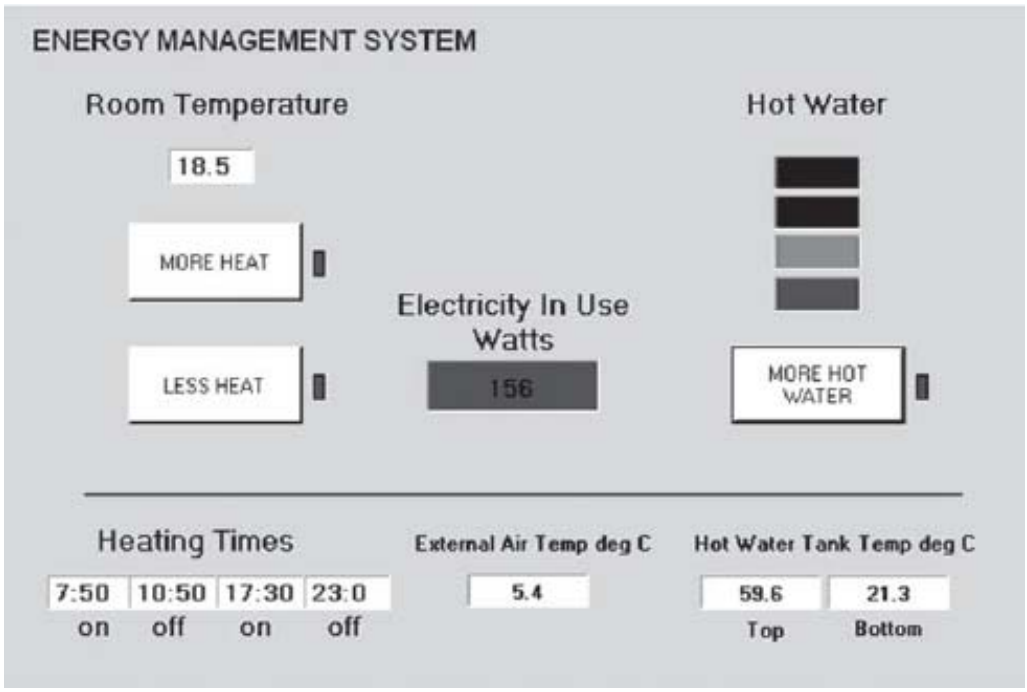

Figure 2-4 User interface of prototype domestic energy management system (Boait, & Rylatt, 2010)

Mozer et al. presented an adaptive controller, Neurothermostat, which learns to regulate indoor air temperature automatically in a residence by observing and detecting patterns in the occupants' schedules and comfort preferences (Mozer, Vidmar, & Dodier, 1997). Although they focused on the problem of air heating with a whole-house furnace, it is indicated that the same approach could be taken with alternative or multiple heating devices, as well as to the problems of cooling and ventilation (Mozer et al., 1997). They defined the task as an optimal control problem in which both comfort and energy costs are considered as part of the control objective, and used a hybrid neural net/look-up table to predict occupancy pattern (Mozer et al., 1997). The Neurothermostat searches for a decision sequence that minimizes the expected cost over a fixed planning horizon at each discrete time step (Mozer et al., 1997). They conducted simulations of the Neurothermostat using artificial occupancy data as well as occupancy data from an actual

residence, and compared the results against three conventional policies (Mozer et al., 1997). The simulation results indicate that the Neurothermostat achieves reliably lower costs (Mozer et al., 1997).

Providing effective feedback on residential electrical demand has shown the promise to reduce energy consumption. Parker et al. described a two year pilot evaluation of a low cost residential energy feedback system installed in twenty case study homes in Florida (Parker, Hoak, Cummings, & Center, 2010). Their study showed an average 7% reduction in energy use from feedback homes in the second year of monitoring after controlling for weather-related influences (Parker et al., 2010).

Ilic et al. studied the potential benefits of implementing a simple load control scheme for residential air conditioning that allows consumers to shift demand from high priced hours to low priced hours during the day (Ilic, Black, & Watz, 2002). This is another example of smart use of air conditioning that can lead to great savings for residential consumers, without sacrificing comfort. They also examined the potential for multiple consumers implementing load control to reduce wholesale prices (Ilic et al., 2002).

Herter investigated the effects of critical-peak pricing (CPP) with different usage and income levels, with the goal of informing policy makers who are considering the implementation of CPP tariffs in residential sector (Herter, 2007). She used a subset of data from the California Statewide Pricing Pilot of 2003-2004, and calculated average load change during summer events, annual percent bill change, and post-experiment satisfaction ratings across six customer segments, categorized by historical usage and income levels (Herter, 2007). She found that customers with high consumption respond significantly more in demand reduction than do the ones with low consumption, while

customers with low consumption save significantly more in percentage reduction of total electricity bills than do the ones with high consumption (Herter, 2007).

Large-scale participation in dynamic pricing programs can cause undesirable consequences that will not be monitored in small-scale programs. Black & Tyagi investigated several potential negative consequences from large-scale participation in existing dynamic programs, including the rebound effect, coincident load shifting/shedding, and limitations of fixed, uniform pricing periods (Black & Tyagi 2010).

Temperature Regulation in Commercial Buildings

It is common to have a single HVAC unit and controller to control multiple spaces or rooms in commercial buildings. The controller supplies heating or cooling to all rooms proportionally depending on the temperature reading it gets from one room, assuming that all rooms have the same load and temperature. Lin et al. developed a sensor feedback structure for multiple sensors with single HVAC system control (Lin, Federspiel, & Auslander, 2002). Their method can take advantage of all room temperature information while the traditional control method uses single sensor which can only measure one of the series rooms controlled by the same actuator (Lin et al., 2002). They developed a computer simulation program and used one year of real weather data and precise mathematical model with 48 states to verify the benefits of the method (Lin et al., 2002). Their results show that the feedback information system they developed can increase the number of comfort rooms reducing the percentage of occupancy discomfort, and save about 15% of energy at the same time (Lin et al., 2002).

Xu et al. presented a daily energy management formulation and the corresponding solution methodology for HVAC systems in facilities (e.g., hospitals, factories, malls, or schools) (Xu, Luh, Blankson, Jerdonek, & Shaikh, 2005). Their objective is to minimize the energy and demand costs through control of HVAC units while satisfying thermal comfort, system dynamics, load limit constraints, and other requirements (Xu et al., 2005). They set HVAC set-points as control variables and used a method that combines Lagrangian relaxation, neural networks, stochastic dynamic programming, and heuristics to predict system dynamics and uncontrollable load and to optimize the set-points (Xu et al., 2005). Their numerical testing and prototype implementation results show that their method can reduce total costs managing uncertainties and shedding the load in a computationally efficient manner (Xu et al., 2005).

Thermal Storage

The potential for thermal storage within the structure and furnishings of conventional commercial buildings is significant. The load requirements associated with maintaining thermal comfort may be shifted significantly through management of a building's thermal storage. Practically, this load shifting is accomplished by properly adjusting the space temperature set-points throughout the course of the day. The building is cooled during off-peak periods when electricity is inexpensive and warmed during on-peak periods in order to reduce the load on the primary air conditioning equipment. There have been a number of studies that showed significant reductions of operating costs in buildings by proper precooling and discharge of building thermal storage. The savings result from both utility rate incentives and improvements in efficient operation due to night ventilation cooling and improved chiller performance. The potential for utilizing building

thermal mass for load shifting and peak demand reduction has been demonstrated in a number of simulation, laboratory, and field studies.

Braun investigated the use of building thermal capacitance in order to reduce the operating costs associated with maintaining adequate thermal comfort conditions in buildings (Braun, 1990). His approach is to control the state of the building thermal storage through the zone temperature variations by shifting cooling loads from daytime to nighttime (Braun, 1990). Doing so, he targeted to reduce peak electrical demands, take advantage of low nighttime electrical rates, offset mechanical cooling with "free" cooling at night, and enhance equipment operation at more favorable part-load conditions (Braun, 1990). His test results indicate that optimal control of the thermal storage within building structures can significantly reduce both energy costs and peak electrical use (Braun, 1990).

Braun et al. developed a tool to evaluate the strategies of thermal mass control comparing HVAC utility costs (Braun, Montgomery, & Chaturvedi, 2001). They used inverse models to represent the behavior of the building, cooling plant, and air distribution system (Braun et al., 2001). Their models use measured data to learn system behavior and provide performance predictions (Braun et al., 2001). The evaluation tool they developed predicts the total HVAC utility cost for a specified control strategy based on weather and solar inputs, as well as occupancy and internal gains schedules and utility rates (Braun et al., 2001). They then identified intelligent thermal mass control strategies in a simulation environment using this analysis tool (Braun et al., 2001). They validated the evaluation tool using data collected from a field site located near Chicago, Illinois (Braun et al., 2001). They used this tool to predict HVAC utility costs for a summer

month billing period (Braun et al., 2001). Using various thermal mass control strategies, they performed additional studies to examine the utility savings potential for summertime operations at the field site (Braun et al., 2001). The control strategy with the best results achieved an approximately 40% reduction in total cooling costs as compared with nigh setup control (Braun et al., 2001). Figure 2-5 shows the structure of the thermal mass simulation tool that was developed in this study.

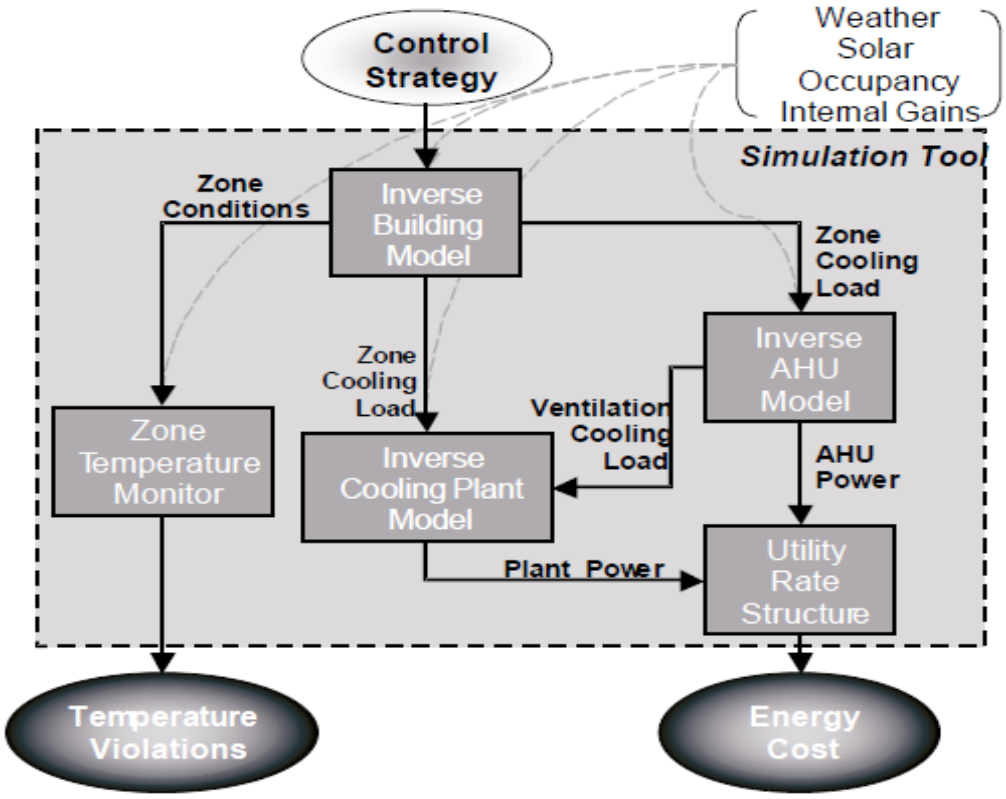

Figure 2-5 Overview of thermal mass simulation tool (Braun et al., 2001)

Xu et al. demonstrated the potential for reducing peak-period electrical demand in moderate-weight commercial buildings by modifying the control of the HVAC system (Xu, Haves, & Piette, 2004). They conducted a case study in which zone temperature set-

points were adjusted prior to and during occupancy in an 80,000 ft² office building with a medium-weight building structure and high window-to-wall ratio (Xu et al., 2004). They recorded HVAC performance data and zone temperatures using the building control system (Xu et al., 2004). They installed additional operative temperature sensors for selected zones and power meters for the chillers and AHU fans (Xu et al., 2004). They constructed an energy performance baseline from data collected during normal operation (Xu et al., 2004). They then programmed two strategies for demand shifting using the building thermal mass in the control system and implemented these strategies progressively over a period of one month (Xu et al., 2004).

Their results show that a simple demand limiting strategy performed well in the building it is implemented (Xu et al., 2004). This strategy maintained zone temperatures at the lower end of the comfort region during the occupied period up until 2 pm (Xu et al., 2004). The zone temperatures were then allowed to float to the high end of the comfort region starting at 2 pm (Xu et al., 2004). This strategy helped the chiller power be reduced by 80-100% during normal peak hours from 2-5 pm, without causing any thermal comfort complaints (Xu et al., 2004).

Liu & Henze introduced an approach to optimally control commercial building passive and active thermal storage inventory (Liu & Henze, 2006a) and (Liu & Henze, 2006b). Their simulated reinforcement learning control approach is a hybrid control scheme that combines features of model based optimal control and model-free learning control (Liu & Henze, 2006a). They conducted an experimental study to analyze the performance of a hybrid controller installed in a full-scale laboratory facility (Liu & Henze, 2006a). The results show that the proposed control approach is feasible to be

implemented in a commercial building (Liu & Henze, 2006b). Figure 2-6 illustrates the hybrid control scheme proposed by Liu & Henze.

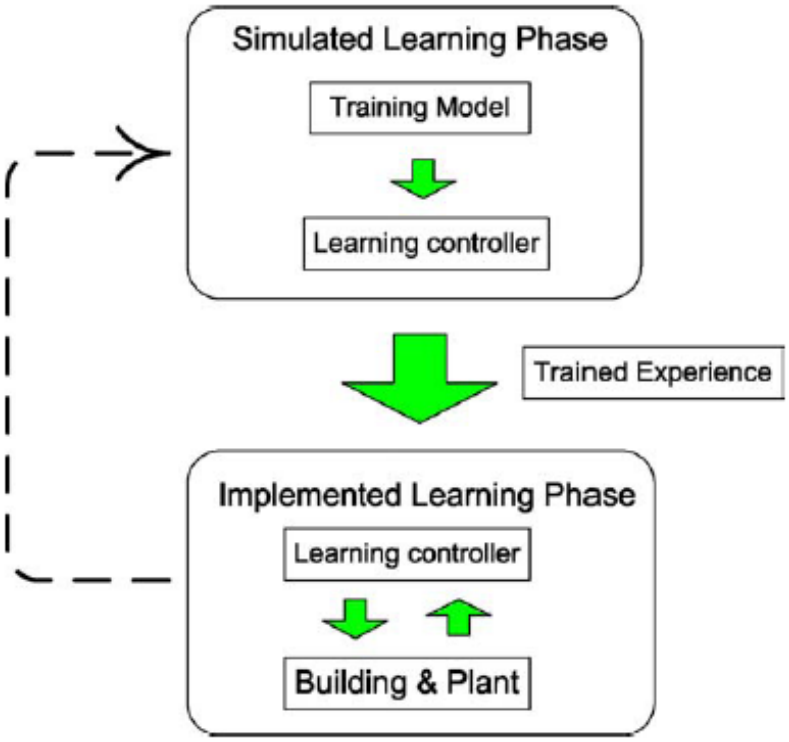

Figure 2-6 Hybrid control scheme (Liu & Henze, 2006b)

Henze et al. investigated the concurrent application of precooling and using active thermal energy storage systems such as ice storage in the context of optimal control in commercial buildings (Henze, Felsmann, & Knabe, 2004). Their objective was to minimize the total utility bill including the cost of heating and a time-of-use electricity rate without demand charges (Henze et al., 2004). Their analysis shows that the combined utilization leads to cost savings that are significantly greater than either storage (active or passive building thermal storage) but less than the sum of the individual savings (Henze et al., 2004).

Pre-cooling can be very effective if the building mass is relatively heavy. Xu & Zagreus studied the potential of pre-cooling and demand limiting in a heavy mass and a light mass commercial building in the Bay Area of California (Xu & Zagreus, 2009). They concluded that pre-cooling has the potential to improve the demand responsiveness of commercial buildings while maintaining acceptable comfort conditions (Xu & Zagreus, 2009). Their results indicated that, all other factors being equal, pre-cooling increases the depth (kW) and duration (kWh) of a given building (Xu & Zagreus, 2009).

Yin et al. discussed how to optimize pre-cooling strategies for buildings in a hot California climate zone with a building energy simulation tool, namely the Demand Response Quick Assessment Tool (DRQAT) (Yin, Xu, Piette, & Kiliccote, 2010). Figure 2-7 shows the general procedure for developing and calibrating the DRQAT simulation models for the field test buildings. They summarized the procedure used to develop and calibrate DRQAT simulation models, and applied this procedure to eleven field test buildings (Yin et al., 2010). They compared the results between the measured demand savings during the peak period and the savings predicted by the simulation model, and indicated that the predicted demand shed match well with measured data for the corresponding auto-demand response (Auto-DR) days (Yin et al., 2010). They also indicated that the accuracy of the simulation model is greatly improved after calibrating the initial models with measured data (Yin et al., 2010). They then compared the simulation results with field test data and confirmed that the optimal demand response strategies worked well for most of the buildings tested in this hot climate zone (Yin et al., 2010).

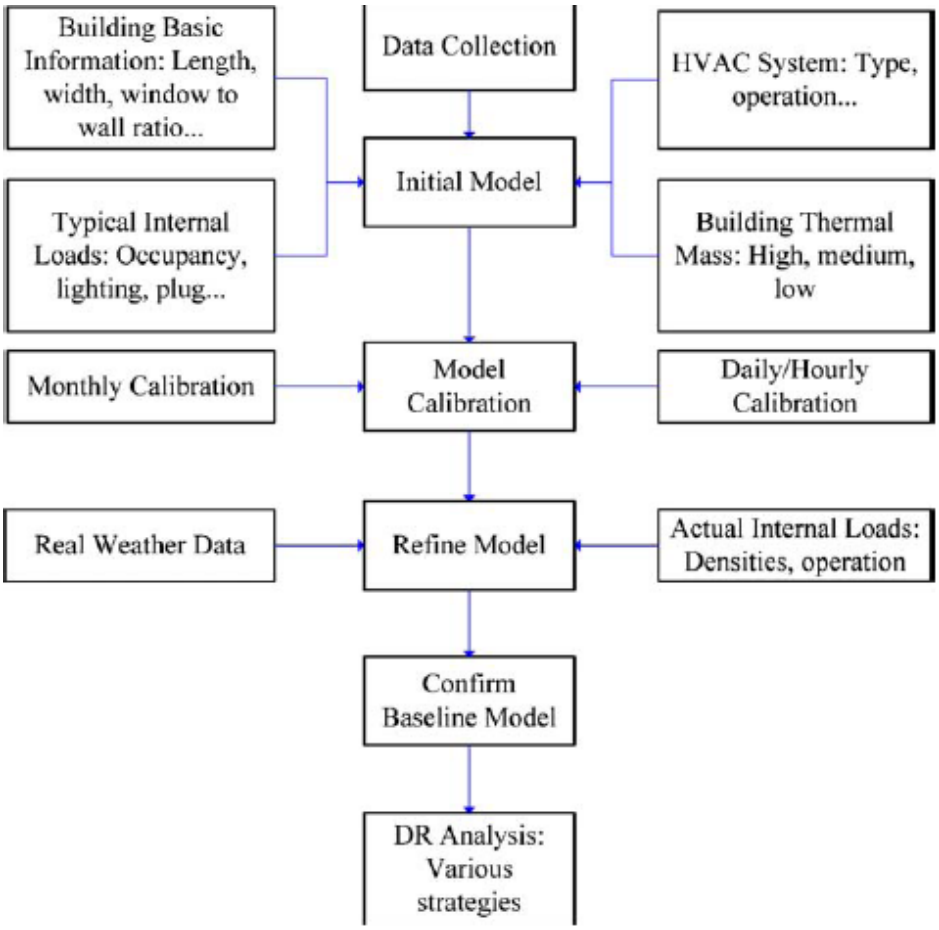

Figure 2-7 Development and calibration of the simulation model by using DRQAT (Yin et al., 2010)

Temperature Regulation using Model Predictive Control (MPC)

MPC for HVAC systems control has been investigated by several researchers in recent years. Majority of the research in this area focus on increasing energy efficiency using the advantage of time-varying constraints such as allowed room temperature variations.

Aswani et al. studied an electrical, single stage heat pump air conditioner (AC) that is common in homes and some offices (Aswani, Master, Taneja, Culler, & Tomlin, 2012a). They built a platform to actuate an AC unit that controls the room temperature of a

computer laboratory on the Berkeley campus that is actively used by students, while sensors record room temperature and AC energy consumption (Aswani et al., 2012a).

Aswani et al. used semi-parametric regression to identify models, which are amenable to analysis and control system design, of HVAC systems (Aswani, Master, Taneja, Smith, Krioukov, Culler, & Tomlin, 2012b). Two testbeds that have been built on the Berkeley campus for modeling and efficient control of HVAC systems were utilized as case studies for system identification (Aswani et al., 2012b). They used semi-parametric regression that allowed for the estimation of the heating load from occupancy, equipment and solar heating using only temperature measurements (Aswani et al., 2012b). Figure 2-8 illustrates the Berkeley Retrofitted and Inexpensive HVAC Testbed for Energy Efficiency (BRITE).

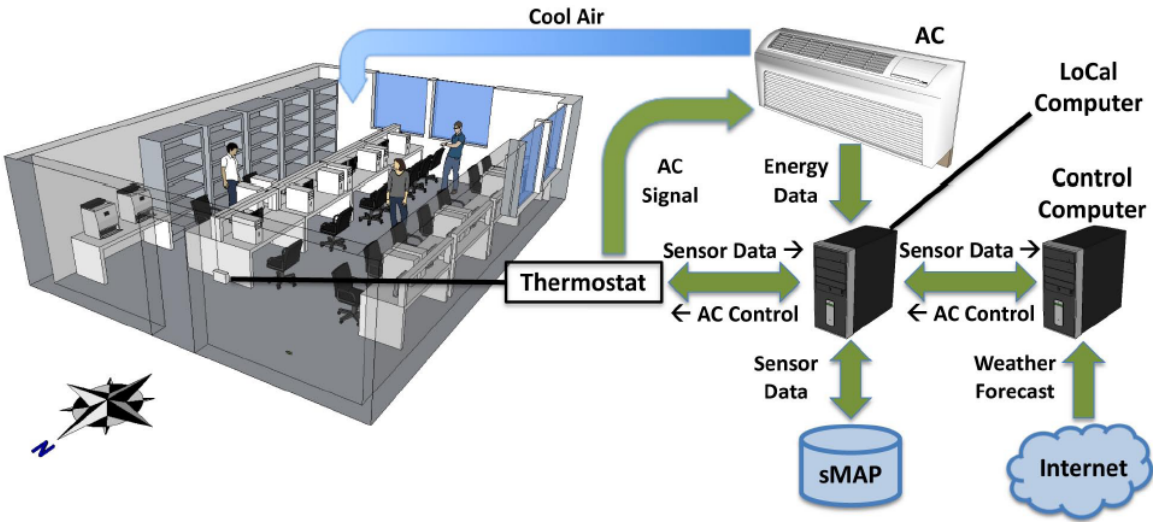

Figure 2-8 The Berkeley Retrofitted and Inexpensive HVAC Testbed for Energy Efficiency (BRITE) (Aswani et al., 2012b)

Aswani et al. implemented a control strategy that uses learning-based model predictive control (MPC) to learn and compensate for the amount of heating due to

occupancy as it varies throughout the day and year (Aswani et al., 2012a). Their techniques resulted in a 30-70% reduction in energy consumption as compared to two-position control, while still maintaining a comfortable room temperature (Aswani et al., 2012a). Their energy savings are due to their control scheme compensating for varying occupancy, while considering the transient and steady state electricity consumption of the AC (Aswani et al., 2012a).

Oldewurtel et al. developed and analyzed a Stochastic Model Predictive Control (SMPC) strategy for building climate control that takes into account weather predictions to increase energy efficiency while respecting constraints resulting from desired occupant comfort (Oldewurtel, Parisio, Jones, Morari, Gyalistras, Gwerder, Stauch, Lehmann, & Wirth, 2010a). They investigated a bilinear model under stochastic uncertainty with probabilistic, time varying constraints (Oldewurtel et al., 2010a). They conducted a large-scale simulation study to investigate the performance of the control strategy with different building variants and under different weather conditions (Oldewurtel et al., 2010a). They analyzed the SMPC approach for selected cases in detail and showed that it significantly outperformed current both rule-based control (RBC) as well as a predictive non-stochastic controller (CE) (Oldewurtel et al., 2010a). Further benefits of SMPC are reported as easy tenability with a single tuning parameter describing the level of constraint violation as well as comparatively small diurnal temperature variations (Oldewurtel et al., 2010a).

Oldewurtel et al. investigated a method to reduce peak electricity demand in building climate control by using real-time electricity pricing and applying model predictive control (Oldewurtel, Ulbig, Parisio, Andersson, & Morari, 2010b). They developed a

time-varying, hourly based electricity tariff for end-customers to use that would truly reflect marginal costs of electricity provision, based on spot market prices as well as on electricity grid load levels, and incorporated it into the MPC cost function (Oldewurtel et al., 2010b). In order to provide the MPC controller with the necessary time-varying costs for the whole prediction horizon, they forecasted the electricity tariff prices using least-squares support vector machines (Oldewurtel et al., 2010b). Results show that peak electricity demand of buildings can be significantly reduced using proposed MPC setup (Oldewurtel et al., 2010b).

Široký et al. investigated potential energy savings in a building heating system by applying MPC and using weather predictions (Široký, Oldewurtel, Cigler, & Prívara, 2011). They tested proposed MPC strategy in a two months experiment performed on a real building in Prague, Czech Republic (Široký et al., 2011). Results show that the energy savings potential for using proposed MPC strategy with weather predictions for the investigated building heating system were between 15% and 28% depending on various factors, mainly insulation and outside temperature (Široký et al., 2011).

Moroşan et al. proposed a distributed MPC method for thermal regulation in buildings which takes the advantages of both centralized and decentralized control structures (Moroşan, Bourdais, Dumur, & Buisson, 2010). The proposed MPC scheme incorporates the future occupation profile into the dynamic cost function (Moroşan et al., 2010). Simulation results indicate that proposed strategy can achieve significant consumption reductions optimizing the transitions between inoccupation and occupation phases (Moroşan et al., 2010).

Moroşan et al. then proposed another distributed model predictive control (DMPC) algorithm based on Bender's decomposition for multi-source multi-zone building temperature regulation (Moroşan, Bourdais, Dumur, & Buisson, 2011). Since the centralized computational time demand of the optimization problem grows exponentially with the number of subsystems; for large-scale buildings, the proposed DMPC strategy based on Bender's decomposition allows the decrease of the computational demand by using a network of local controllers that are coordinated by a master controller (Moroşan et al., 2011). They illustrated the effectiveness of the proposed approach compared to the PI-based control in a simulation study (Moroşan et al., 2011).

Chandan & Alleyne developed a methodology for the problem of thermal control of buildings from the perspective of partitioning them into clusters for decentralized control (Chandan & Alleyne, 2011). They presented a measure of deviation in control inputs between centralized and decentralized control in the MPC framework, referred to as the Optimality Loss Factor (OLF) (Chandan & Alleyne, 2011). They introduced another quantity called the Normalized Mean Cluster Size (NMCS) as an indicator of the robustness of any decentralized architecture to sensing and communication faults (Chandan & Alleyne, 2011). Next, they proposed an agglomerative clustering approach to determine the decentralized control architectures, which provide a satisfactory trade-off between the underlying optimality and robustness objectives (Chandan & Alleyne, 2011). They demonstrated the application of proposed partitioning methodology using simulation case studies on medium-scale buildings (Chandan & Alleyne, 2011).

Bălan et al. proposed an MPC algorithm that can be applied to nonlinear systems and uses a limited number of control sequences for on-line simulation of future behavior of

the process (Bălan, Stan, & Lăpuşan, 2009). A predicted sequence of the output signal is generated by each control sequence used in simulation (Bălan et al., 2009). Then, using a set of rules, the optimal control signal is computed (Bălan et al., 2009). A process model along with the previous sequences of the input and output signals from the process is used to simulate the future behavior of the process (Bălan et al., 2009). The proposed algorithm is used for simulation of the temperature control in a house and compared with the usual algorithms of type PI (Bălan et al., 2009).

Freire et al. studied indoor thermal comfort problem in a single-zone building equipped with an HVAC system, addressing the occupants' thermal comfort sensation by the well-known comfort index known as PMV (predicted mean vote) and by a comfort zone defined in a psychrometric chart (Freire, Oliveira, & Mendes, 2008). In this context, they proposed different MPC-based strategies for the control algorithms by using an only-one-actuator system that can be associated to a cooling and/or heating system (Freire et al., 2008). Both strategies are to optimize room air conditions, where one focused on thermal comfort and the other one energy savings while maintaining the indoor thermal comfort criterion at an adequate level (Freire et al., 2008). Simulation results show that the proposed control algorithms can simultaneously provide thermal comfort and energy consumption reduction keeping the thermal conditions of the room in the comfort zone (Freire et al., 2008).

Goyal et al. studied the use of occupancy information to reduce energy consumption while maintaining thermal comfort and indoor air quality in commercial buildings (Goyal, Ingley, & Barooah, 2012). They mainly focused on zone-level control, where the supply air flow rate and the amount of reheat are the two control inputs to be decided

(Goyal et al., 2012). They proposed three control algorithms with varying information requirements of long-horizon accurate prediction of occupancy and a model of the hydrothermal dynamics of the zone, only occupancy measurement and a dynamic model, and only occupancy measurement (Goyal et al., 2012). They used a model predictive control framework to compute the optimal control inputs on the first two strategies, and a pure feedback-based control strategy on the third one (Goyal et al., 2012). Their simulation results show that significant energy savings can be realized even with simple feedback-based algorithm with occupancy measurements (Goyal et al., 2012). Additional prediction capability (of dynamics or occupancy) results in even larger savings in energy consumption (Goyal et al., 2012).

Ma et al. proposed an MPC strategy for the control of thermal energy storage in building cooling systems, where chillers are operated each night to recharge the storage tank in order to meet the buildings demand on the following day (Ma, Borrelli, Hencey, Packard, & Bortoff, 2009). They designed an MPC for the chillers operation in order to optimally store the thermal energy in the tank by using predictive knowledge of building loads and weather conditions (Ma et al., 2009). They used periodic invariant sets, moving block strategy and dual stage optimization to tackle complexity and feasibility issues of the resulting scheme (Ma et al., 2009). Preliminary results showed that 24.5% of the daily electric bill can be saved as compared to the heuristic manual control sequence (Ma et al., 2009).

Ma et al. built on their previous work (Ma et al., 2009), improved the oversimplified building load model, and presented experimental results in (Ma, Borrelli, Hencey, Coffey, Bengea, & Haves, 2010). The experiments at University of California, Merced

show that proposed MPC can achieve a $1,205 reduction in daily electricity bill and a %11.9 improvement of the plant Coefficient of Performance (COP) (Ma et al., 2010).

In general, previous studies report that the predictive control strategies are more efficient than conventional, non-predictive ones for HVAC systems control of buildings.

CHAPTER 3: MPC-BASED HVAC LOAD CONTROL

Model Settings for Energy Efficient Control of HVAC Systems

In this section a description of the proposed model for control of HVAC systems is provided from the perspective of the consumer. The model has two conflicting goals: 1) minimizing the total energy consumption by the HVAC system and hence the associated costs for the consumer and in parallel, 2) minimizing the deviation of the indoor temperature from the consumer preference. These two goals are combined by a single objective via a weighted squared sum of energy consumption as a function of HVAC usage and the deviation between the indoor temperature and a reference temperature point. The reference temperature is set by the consumer based on his/her comfort level. Consequently, the proposed model aims to determine cost and energy efficient HVAC control policies that help consumers lower their energy costs while maintaining a comfortable building environment based on their preferences.

The optimal HVAC control policies are developed by generating AC signals based on the model objective. The AC signals are composed of control actions that determine the on/off frequency of the AC unit. $u(t)$ denotes such control action determined at time *t.* Typically, the operation of a single-state heat pump is based on two modes corresponding to the compressor being on or off. However, optimizing such hybrid system models is usually time-demanding, especially for control purposes. Therefore, a sampled control is considered in order to simplify the design of the controller. As such, a new control action is generated for each period *t* whose period length is denoted by $l(t)$ in the proposed MPC based model. It is noted that the length of a period should be no less than 10 to 15 minutes since switching more frequently than once every 10 to 15 minutes can physically

damage the heat pump. Since this constraint requires applying control actions at discrete times, a *pulse-width modulation* (PWM) based approach is used to convert the discrete time control input, $u(t)$, into a continuous signal that turns the AC on or off. For this, a similar approach presented in (Burke & Auslander, 2009) is employed. Consequently, in the proposed model $u(t)$ can also be interpreted as a duty cycle that represents the proportion of "on" time during time interval *t*.

Clearly, the energy consumption during time interval *t* is a function of $u(t)$. At the same time, these control actions determine the inside temperatures for the building across the time horizon (*e.g.,* throughout the day). Hence, the resulting objective function of the proposed model can be written as follows:

$$min_{u[\cdot],T_r[\cdot]} = \sum_{t=1}^{N} (q * l[t] * u[t])^2 + \sum_{t=1}^{N} \big(w * (T[t] - T_r[t])\big)^2 \tag{1}$$

s.t.

$$u[t] \in [0,1] \qquad \forall t \in \{1..N\}$$

$$T[t] = \boldsymbol{G}(u[t], x[t])$$

$$T[t], T_r[t] \in [T_{min}, T_{max}] \qquad \forall t \in \{1..N\}$$

The first term in the objective function computes the squared sum of energy consumption by the AC over *N* time intervals. Basically, the energy consumption is a function of the AC's energy usage per hour denoted here by *q* (usually in *kW per hour*).

As mentioned above, the control input $u[t]$ is to be calculated for intervals of 15 minutes. Since the time interval length is assumed to be 15 minutes in this study, the hourly usage is divided by 4 in the objective function. Since $u[t]$ is the proportion of "on" time for the AC, its value is constrained to be in $[0,1]$.

The temperature deviations from the identified set-points are handled by the second term in the objective function. $T[t]$ and $T_r[t]$ are the average inside temperature and the reference temperature set-point at time t respectively. At a given time period, as indicated by the second constraint above, the inside temperature is a function of the AC usage ($u[t]$) and the collection of exogenous state parameters ($x[t]$) such as the inside temperature at the beginning of period *t*, average outside temperature during period *t* and various characteristics of the building related to its thermal storage capabilities. Unfortunately, the mapping between $u[t], x[t]$ and the average inside temperature at period *t* is not straightforward in practice in that $\boldsymbol{G(\cdot)}$ is often times a nonlinear function effected by noise. For practical use of the proposed control model, an easy to use prediction process is developed and integrated into the model, which will be discussed in the next section. The last constraint incorporates minimum and maximum values for both the inside temperatures and the temperature set-points.

The subtraction given in the second part of the objective function gives the deviation between the inside and reference temperatures. By taking the square of these deviations, both positive and negative deviations from the reference set-points are penalized. The controller aims to keep inside temperature close to a reference temperature set-point by minimizing the deviation between the two. Most contemporary HVAC units function based on a reference temperature point set by the consumer. In conventional practice, the

AC unit runs based on a two-position thermostat control under a fixed thermostat set-point around which the inside temperature fluctuates. The reference temperature is usually set by the occupant and it does not change frequently (if at all) throughout the day - often times, regardless of the price fluctuations. While the above model can accommodate such cases by simply employing the reference temperature values (*i.e.*, $T_r[t]$) as fixed input parameters, it is mainly designed to deploy them as decision variables that are determined as response to the price fluctuations. Clearly, the advantages of dynamic electricity pricing from both the perspective of the consumer and the utility provider cannot be realized effectively with a fixed reference temperature set-point. The deployment of variable reference temperature set-points, on the other hand, achieves financial benefits of dynamic pricing while keeping the inside temperature within the occupants' thermal comfort limits. Therefore, a methodology is proposed to determine cost-efficient reference temperature set-points for MPC controller within a range referred to as the comfort range, which are basically captured by the lower and upper bounds specified by the last constraint.

The proposed MPC controller aims to minimize the weighted sum of the two terms in the above objective function by generating optimal AC signals $u[t]$ and hence, average inside temperatures as well as determining the reference set-points for the AC in response to fluctuations in electricity prices throughout the day. When the reference temperature set-points are control variables, typically, a higher reference temperature set-point coupling with a higher-price period will result in lower energy consumption and hence lower energy cost for the consumer. On the other hand, a lower reference temperature set-point coupling with a lower price period assures an improved cost efficient thermal

comfort for the occupant assuming that lower temperatures within a given range provides better thermal comfort. In all cases, reference temperature set-points are constrained by a comfort range specific to the occupant.

The occupant's thermal comfort preference is captured by the weight, *w,* in the objective function. Clearly, higher values of *w* represent cases where the energy cost savings and as such energy consumption are less important for the occupant. This value does not affect only the control action represented by $u[t]$ but also the selection of reference temperature set-points. In general, higher *w*, expectedly leads to higher frequency of "on" times and lower temperature set-points within a given comfort range. However, the model can still provide savings for such consumers when it can control both the AC signals and the temperature set-points. With controllable temperature set-points, the MPC controller has an additional degree for freedom to effectively manage the trade-off between the energy cost and the thermal comfort.

In the next section, an MPC based solution procedure for the proposed model is discussed. Mainly, the solution approach is built in two folds. The first stage, responding to the fluctuations in daily electricity prices, generates temperature set-points based on the occupant's attitude towards thermal comfort. The second stage develops a prediction model for the MPC controller that is eventually used to determine the control actions $u(t)$.

Model Predictive Control (MPC) Process

First, the algorithm for determining the temperature set-points for price ranges is presented. Later the MPC based prediction approach that is used to map the control action to the average inside temperatures is discussed. The outcomes of both stages are

then used as inputs for the MPC controller, which generates the vector of control actions over the planning time horizon.

Algorithm for Determining Variable Reference Temperature Set-Points

A simple yet effective algorithm is used to assign reference temperature set-points for each hour of the day based on the real-time price of electricity for that hour over a time horizon for which the price schedule is already announced and known. Since day ahead pricing (DAP) – a form of RTP where upcoming hourly energy prices are announced to the users one day ahead – is assumed in the proposed strategy, the reference temperature set-points for the next 24-hour period can be determined in advance of the day. As such, effectively, the algorithm generates price ranges based on the scheduled price fluctuations for a given day and assigns them to temperature set-points. It is assumed that within the predefined temperature range, the lower temperature provides a better thermal comfort for the consumers. Since the objective function in the model introduced in the first section of this chapter attempts to minimize the weighted squared summation of the total cost and the indoor temperature in hot climates, the AC is operated at lower bounds of the temperature range when the price of electricity is at lower values. On the other hand, the operation temperature of the AC is raised as the price of electricity increases. Consequently, the algorithm is designed to assign lower temperature set-points for lower price ranges and higher set-points for higher price ranges.

The proposed algorithm first determines the maximum ($max(p_h)$) and minimum ($min(p_h)$) electricity pricing values for the next 24-hour period and from these it identifies a number of price ranges depending on the number of temperature set-point candidates. The temperature set-point candidates are the temperature values between any

given maximum and minimum allowed temperature set-points which can be pre-determined by the users. In the end, each price range is coupled with a temperature set-point. The temperature set-points are then assigned to each hour of the day based on the range in which the price of corresponding hour falls in.

To model consumer choice on thermal comfort, a *discomfort tolerance index*, *a*, is defined which is used to capture the trade-off between thermal comfort and energy cost for the occupant. The value of *a,* in general, varies across individuals. Clearly, this value is a mapping from the weight *w* in the objective function given in (1) and inversely correlated with *w*. A high discomfort tolerance (i.e., $\alpha > 0$) represents a consumer who has higher tolerance for higher indoor temperatures in return for cost savings. Such customers prefer that wider price ranges are assigned to higher temperatures. Whereas, low tolerance ($\alpha < 0$) customers prefer the opposite as they are less willing to compromise comfort for savings. It is referred to the consumer with $\alpha = 0$ as the neutral consumer who has a balanced preference between comfort and savings leading to uniform price ranges allocated to temperature set-points. Clearly, this value is a mapping from the weight *w* in the objective function given in (1) and inversely correlated with *w*. That is, higher values of *a* correspond to lower values of *w* in (1).

The reference temperature set-points are subject to maximum ($T_{\max}$) and minimum ($T_{\min}$) allowable levels and the physical limits of the air conditioner. Maximum and minimum allowable reference temperature set-points can be determined by the users. In order to keep the thermal comfort level of the users at a reasonable range, it can be assumed that the AC is operated within the American Society of Heating, Refrigerating and Air-Conditioning Engineers (ASHRAE) zone (Standart, A. S. H. R. A. E., 1992).

Algorithm for Temperature Set-Point Assignment (TSA)

Step 0: *Initialize* α

Step 1:

$$n \leftarrow \frac{T_{max} - T_{min}}{k} + 1$$

$$RANGE \leftarrow max(p_h) - min(p_h)$$

Set $r_0 \leftarrow min(p_h)$

If $\alpha = 0$ *Go to Step 2*

Else Go to Step 3

Step 2: *For each set-point* $j (j = 1 \; to \; n)$

Set $r_j \leftarrow r_{j-1} + \frac{RANGE}{n}$

Go to Step 4

Step 3: *For each set-point* $j (j = 1 \; to \; n)$

Set $r_j \leftarrow r_{j-1} + RANGE * \frac{2^{a(j-1)}(1-2^a)}{(1-2^{an})}$

Step 4: *For each hour* $h = 1 \; to \; 24$

$$T_h^{set} \leftarrow k\left[argmin\{j : p_h \leq r_j\} - 1\right] + T_{min}$$

Figure 3-1 Algorithm to assign reference temperature set-points

The temperature set-point assignment (TSA) algorithm is shown in Figure 3-1, where k is the temperature set-point interval used to calculate the total number of set-points, n, and r_j denotes the price range for the jth set-point. The proposed TSA algorithm assigns temperature set-points to price ranges based on consumer's discomfort tolerance index (i.e., α).

As illustrated in Figure 3-2, the algorithm assigns lower temperature set-points to wider price ranges when the occupant's discomfort tolerance index is low. The opposite is true when the index value is high. A neutral consumer (*i.e.,* $\alpha = 0$) generates equally sized price ranges for all temperature set-points.

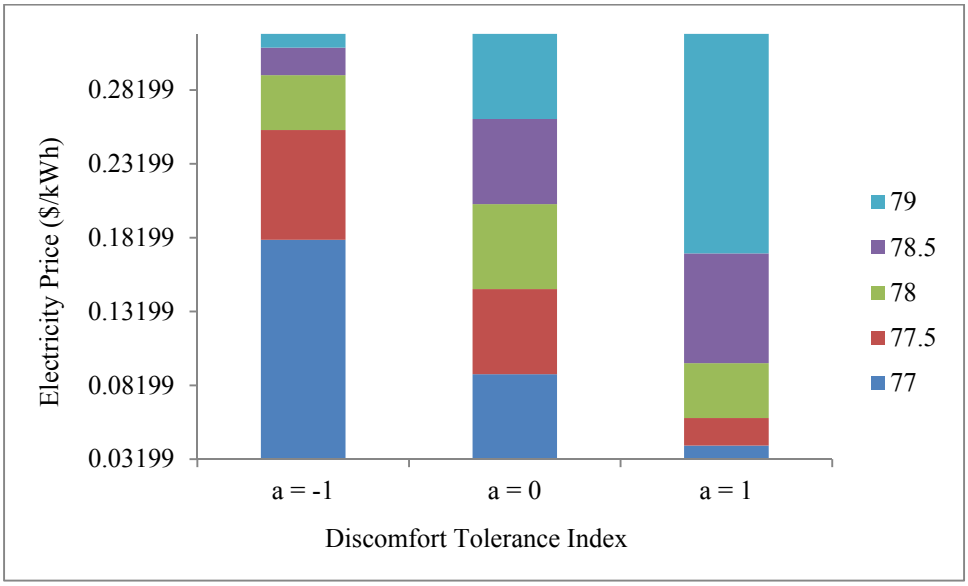

Figure 3-2 Assignment of temperature set-points to price intervals as a function of comfort intolerance.

Prediction Model for the Inside Temperature

Mathematical model identification is an important step towards implementing efficient predictive control schemes for dynamic systems. All MPC schemes inherently

require a nominal model for system optimization. In the case of building HVAC load control, it is essential to provide MPC controller with a model that describes the impact of inputs (outside temperature, AC operation, *etc*.) on the output (inside temperature of the building) at each control interval.

Although the building thermal system is nonlinear in nature, it can be approximated by a linear model since the main physical effect is convective heat transfer and is described by Newton's law of cooling which is a linear ordinary differential equation (ODE). Moreover, a nonlinear dynamic model used in an MPC controller will generally lead to a non-convex optimization which can be extremely difficult to solve. Consequently, to ensure usability and practical implementation of the proposed system, a linear model that accurately represents system dynamics with the least number of variables possible is developed. The approximation enables efficient optimization in terms of time and cost for the MPC controller. Consequently, the controlled variable (average inside temperature, $T[t]$) is defined as a function of a manipulated variable (AC signal, $u[t]$) and a measured disturbance (outside temperature, $\hat{u}[t]$). The advantage is that all variables can be easily measured via sensors and loggers and effectively transferred to the MPC controller in real-life application. The cooling process can be described by a linear model, represented in a discrete state space (with the sampling time τ) where state variables are used to describe the system by a set of first-order differential or difference equations, rather than by one or more nth-order differential or difference equations.

The discrete-time state-space model structure is often written in the following form:

$$\begin{cases} x(t+\tau) = Ax(t) + Bv(t) + Ke(t) \\ T(t) = Cx(t) + Dv(t) + e(t) \end{cases} \quad (2)$$

where $x(t)$ is the state vector at time t, $v(t)$is the input vector composed of $\{u[t], \hat{u}[t]\}$ and $T(t)$denotes the inside temperature at time t. Random component $e(t)$ represents the white-noise disturbance. The state-space matrices, A, B, C, D and K, are to be estimated from the physical data with respect to T_s. State variables $x(t)$ can be reconstructed from the measured input-output data, but are not themselves measured during an experiment.

The state-space model structure is a good choice for quick estimation because it requires only one user input, the *model order*. The *model order* is an integer equal to the dimension of $x(t)$ and relates to, but is not necessarily equal to, the number of delayed inputs and outputs used in the corresponding linear difference equation. In order to identify the AC control signal input, $u(t)$, for each sampling interval τ, the concept of pulse width modulation is employed as described in the first section of this chapter.

Based on collected measurements, a purely statistical approach based on multiple-input single-output (MISO) discrete-time state-space model can be used for parameter identification. Several common tools similar to the System Identification Toolbox of MATLAB can be used for this purpose and embedded into the MPC controller. Such applications estimate model parameters by minimizing the error between the model output and the measured response.

The output y_{model} of the linear model is given by:

$$y_{model}(t) = \theta z(t),$$

where θ is a transfer function and $z(t)$ is the input vector. To determine θ, the toolbox minimizes the difference between the model output $y_{model}(t)$ and the measured output $y_{meas}(t)$. The minimization criterion is a weighted norm of the error $\lambda(t)$, where

$$\lambda(t) = y_{meas}(t) - y_{model}(t) = y_{meas}(t) - \theta z(t)$$

Here, $y_{model}(t)$ is one of the following:

- Simulated response of the model for a given input $z(t)$.
- Predicted response of the model for a given input $z(t)$ and past measurements of output $(y_{meas}(t-1), y_{meas}(t-2), \dots)$.

Accordingly, the error $\lambda(t)$ is called simulation error or prediction error. The estimation algorithms adjust parameters in the model structure θ such that the norm of this error is as small as possible.

Experiment for Parameter Identification

To illustrate the use of the prediction model, an experimental validation that utilizes the above procedure is carried out. In the experiment, data needed for parameter identification is collected from a typical house in Coral Gables, Florida displayed in Figure 3-3. The house is around 2,000 square feet, and equipped with a single-stage heat pump air conditioner. Figure 3-4 shows the rear of the house and the air conditioner unit.

Figure 3-3 Experiment house in Coral Gables, Florida

Figure 3-4 Rear of the experiment house and the air conditioner unit

Three outside temperature loggers are installed on different sides of the house, and averaged out the data for a better set of outside temperature data. Outside temperature loggers that are installed on the west side of the house are displayed in Figure 3-6. An inside temperature logger is also installed next to the current thermostat shown in Figure 3-7. To capture the AC consumption data, a pair of data loggers is installed along with the current transformers for both phases of the electric disconnect. Figure 3-5 shows data loggers and current transformers installed in the air conditioner unit (details of data collection strategy can be found in Appendix A). This data is then converted to duty cycle (PWM) over 15 minute periods. To estimate and validate the model, data sets from two consecutive weekdays (June 25 and June 26, 2012) are used.

Figure 3-5 Data loggers and current transformers installed in the AC unit

Figure 3-6 Outside temperature loggers installed on the west side of the house

Figure 3-7 Inside temperature logger installed next to the current thermostat

It is important to note that the AC continues to cool the building for a few minutes even after it is turned off because of the dynamics of the heat pump. Specifically, it takes a while for the evaporator that cools the air to warm up, and so it keeps cooling the air for some time after the heat pump is turned off (Vargas & Parise, 1995). Therefore, there exists a "delay" in the system model. A discrete time model where each time period (τ) is 15 minutes is considered. Thus, this delay can be included and realized in each time period where the AC is on and turned off but still cooling.

The corresponding state-space matrices for the third-order discrete-time state-space model using real-life data from the first day with sampling time of 15 minutes are identified as

$$A = \begin{bmatrix} 0.9759 & -0.02625 & 0.002302 \\ -0.1922 & 0.4219 & 0.3488 \\ 0.06496 & -0.08368 & 0.231 \end{bmatrix} \quad B = \begin{bmatrix} 0.0009866 & -0.03179 \\ 0.05506 & -0.2371 \\ -0.125 & -0.08221 \end{bmatrix}$$

$$C = [26.13 \quad 1.775 \quad -0.004073] \quad D = [0 \quad 0] \quad K = \begin{bmatrix} 0.01643 \\ 0.0312 \\ 0.0936 \end{bmatrix}$$

Typically, the quality of a model is evaluated by comparing the model response to the measured output for the same input signal. Figure 3-8 shows that the third order state space model with the parameters above fits reasonably well (Model Fit: %86.47) to the measured temperature data used to identify these parameters.

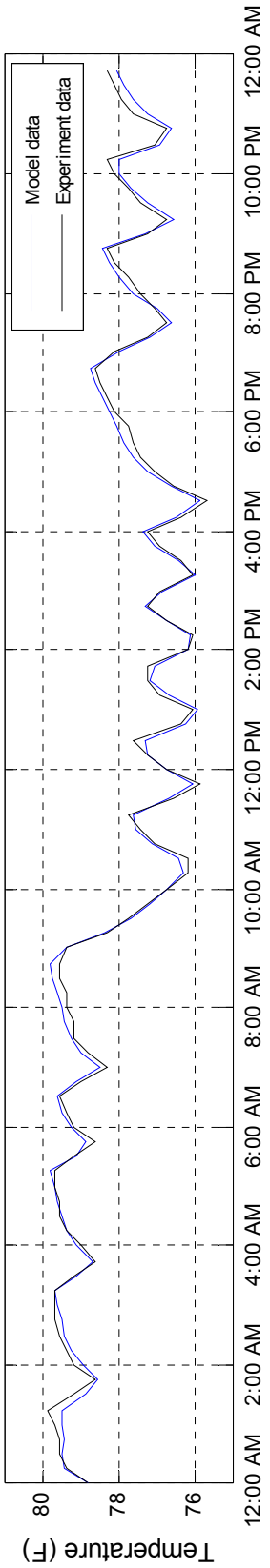

Figure 3-8 Experimental and simulated temperature (Model Fit: %86.47)

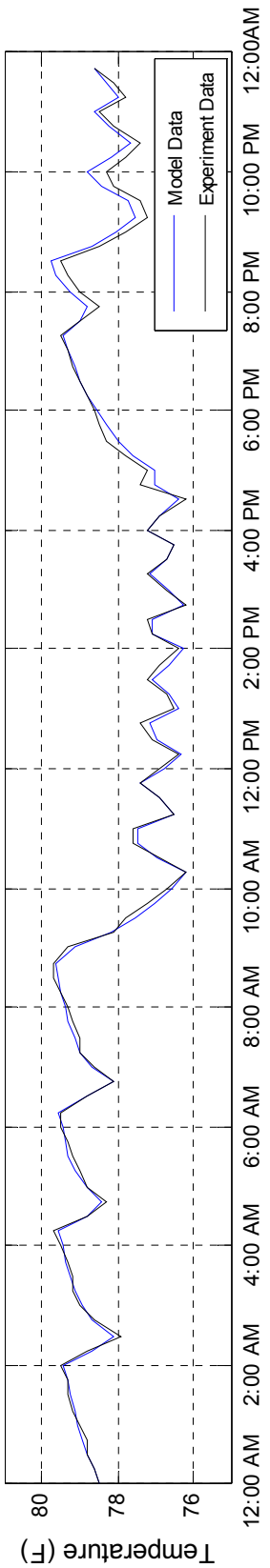

Figure 3-9 Experimental and simulated temperature (Model Fit: %84.16)

To further validate acquired model, a different set of experimental data from day 2 is employed to check if the model could reproduce the same system behavior (cross-validation). This avoids the risk of over-fitting the data and assures that the identified model can be generalized for a reasonable time horizon. Therefore, the computed parameters were applied to the identified model with the physical output data measured on day 2 using the Simulink/MATLAB environment. The simulation procedure is as follows: The input data set (outside temperature and AC duty cycle) measured on day 2 was employed in the identified model and the model response (inside temperature) was compared with measured inside temperature. The results presented in Figure 3-9 show a considerably good agreement (Model Fit: %84.16) between the identified model and the measured validation data.

It is noted that due to changes in seasonal temperatures and possible modifications in the building settings the state vector may vary in time. As such the parameter values derived at certain point in time may not provide good fits in the long run. As such, the MPC controller should be able to rerun the parameter identification process periodically or on a condition-based fashion. Since the computational process is simplified thanks to the linear approximation, the parameters can be updated in reasonably short periods. Alternatively, the parameters can be updated when the model fit drops below a pre-set threshold (*e.g.,* 80%).

Experimental Analysis of the Proposed MPC Process

A simulation based experimental analysis is carried out to investigate the impact of the proposed model and MPC based solution procedure on energy cost savings, peak time energy consumption and the occupant's thermal comfort. The analysis is carried out in

two folds. First, the proposed MPC process is tested under a fixed temperature set-point. In this case, the temperature set-point is treated as an exogenous input parameter in the model given in (1). The MPC controller's performance is compared to the conventional two-position control of the AC unit. Next, the case with endogenous temperature set-points is considered, where the temperature set-points are determined by the procedure described in the first sub-section of the previous section. The TSA algorithm is applied to both the two-position control and the MPC process, and the results are compared.

In order to set up the experiment under the simulation environment, a controller imitating the real-life interactions between the input and output parameters is identified and integrated into the simulation framework. The simulated controller is needed to generate feedback for the proposed MPC process. In real-life application, the actual inside temperature is to be measured through sensors and utilized by the MPC controller at each control interval. Subsequently, the collected data is fed back to the MPC controller for dynamic update. Without such a feedback from the system, the model predictive thermal control of the building may not be fully implemented. However, in a simulation study such data will not be available. On the other hand, the output data cannot be generated by the prediction model itself in the simulation study since the system output will be the same as the previously predicted one, which will make the comparisons pointless. To overcome this obstacle and to have an accurate assessment of the proposed approach, a more precise nonlinear model that is due to Hammerstein-Wiener is employed for simulating the output generation. The nonlinear Hammerstein-Wiener plant model is used to represent the real system in the simulation framework and

to update the MPC controller with the system output data (inside temperature) in each control step.

The simulation based analysis for MPC implementation is developed and implemented using Simulink/MATLAB. The MPC controller block is built under the Model Predictive Control Toolbox of MATLAB and added to Simulink framework along with the nonlinear plant model block. Figure 3-10 depicts the simulation framework for the MPC control scheme. The experiment input data for outside temperature is sent to the MPC controller block. The MPC controller then generates the AC control input minimizing the objective function with respect to the reference temperature set-points, which are previously determined using the TSA algorithm presented in the previous section. Accordingly, the controller also produces the nonlinear plant model output, namely the inside temperature. The AC control input and the outside temperature data for the next time period are then sent to the nonlinear plant model to generate the inside temperature for the next time frame. To further discuss the process and relevant results, it first needs to be explained how the nonlinear plant operates in the simulation model.

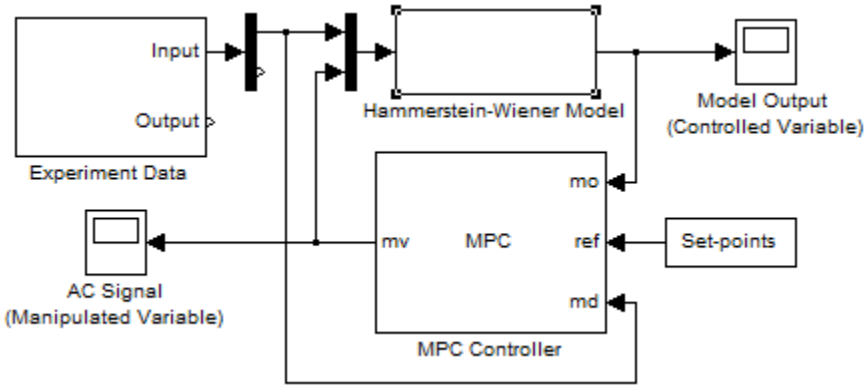

Figure 3-10 Simulink/MATLAB simulation framework for the MPC scheme

Plant Model

In order to describe the dynamic building system accurately, a Hammerstein-Wiener model that decomposes the input-output relationship into two or more interconnected elements is employed. In this case, the dynamics are represented by a linear transfer function and the nonlinearities are captured using nonlinear functions of inputs and outputs of the linear system. The Hammerstein-Wiener model achieves this configuration as a serial connection of static nonlinear blocks with a dynamic block. These models are popular because they have a convenient block representation, transparent relationship to linear systems, and are easier to implement than heavy-duty nonlinear models (such as neural networks and Volterra models).

Below is a block diagram that represents the structure of a Hammerstein-Wiener model:

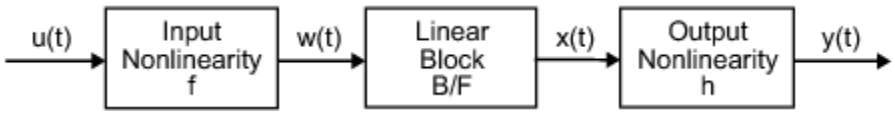

where:

- $w(t) = F(v(t))$ is a nonlinear function transforming input data $u(t)$. Typically, $w(t)$ has the same dimension as $u(t)$.
- $x(t) = (B/F)w(t)$ is a linear transfer function. $x(t)$ has the same dimension as $y(t)$, and B and F are similar to polynomials in the linear Output-Error model.

- For ny outputs and nv inputs, the linear block is a transfer function matrix containing entries:

$$\frac{B_{j,i}(q)}{F_{j,i}(q)}$$

  where $j = 1,2,\dots,ny$ and $i = 1,2,\dots,nv$.

- $y(t) = h(x(t))$ is a nonlinear function that maps the output of the linear block to the system output.

Basically, $w(t)$ and $x(t)$ are internal variables that define the input and output of the linear block, respectively.

Since f performs on the input port of the linear block, this function is called the input nonlinearity. Similarly, since h performs on the output port of the linear block, this function is called the output nonlinearity. If system contains several inputs and outputs, the functions f and h must be defined for each input and output signal. It should also be noted that both the input and output nonlinearity do not have to be included in the model structure.

Using System Identification Toolbox of MATLAB, the nonlinear Hammerstein-Wiener model for the plant is identified and validated in a similar way used in the experiment presented in the previous section. As expected, Figure 3-11 shows that the nonlinear Hammerstein-Wiener model fits very well (Model Fit: %93.57) to the measured temperature data.

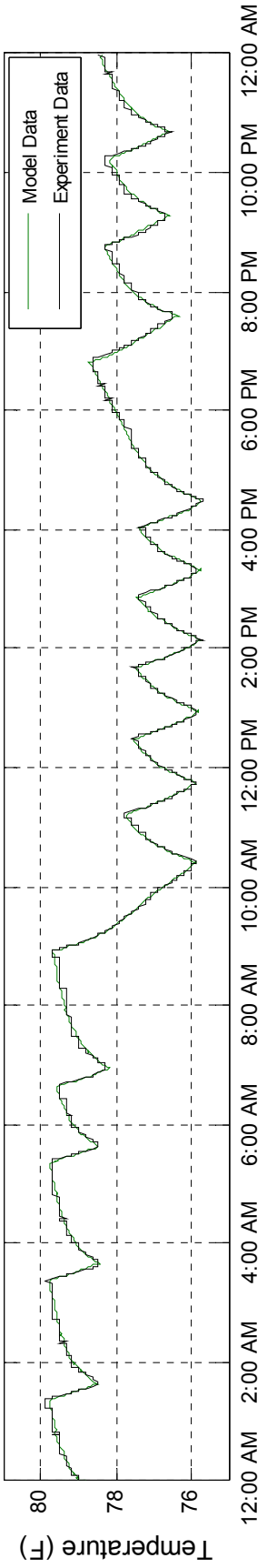

Figure 3-11 Experimental and simulated temperature (Model Fit: %93.57) with the nonlinear plant model

Modeling the Two-Position Thermostat Control

Most thermostats currently employ two-position control for the HVAC equipment in the buildings. For the purpose of comparing the energy consumption and the energy cost of different control strategies, it is useful to identify a simulation model of the two-position control of the thermostat. In two-position control, the AC turns on when the inside temperature exceeds $T_{on}(T + k)$ and turns off when the temperature reaches $T_{off}(T - k)$. Figure 3-12 shows the model of two-position control of thermostat with a fixed thermostat set-point, T, in Simulink/MATLAB environment. It should be noted that the nonlinear plant model is also used to generate outputs in the simulation study.

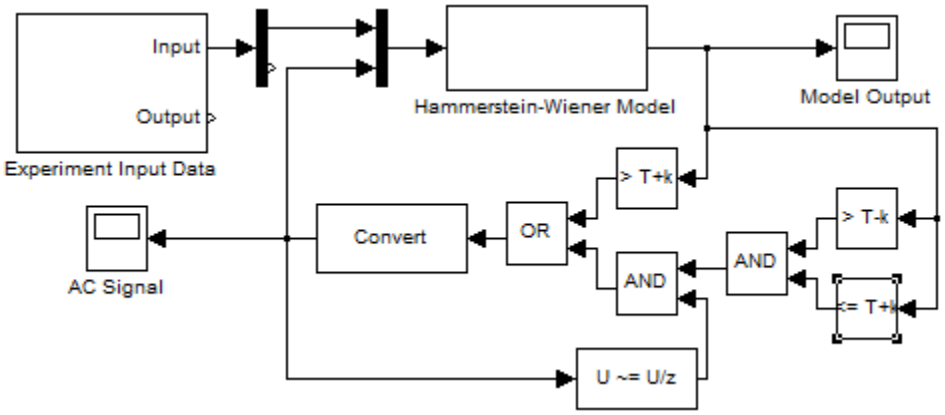

Figure 3-12 The simulation framework for the two-position thermostat control

Pricing and Outside Temperature Data

Real-time electricity pricing data for the simulation study is acquired from a major utility company (PJM, 2012). The publicly available DAP (day ahead pricing) rates for selected days are used. In DAP, the electricity pricing data for the next 24-hour period is released ahead of time. Figure 3-13 illustrates the DAP on a hot summer day. Moreover, the outside temperature data given in Figure 3-14 is applied to the simulation study.

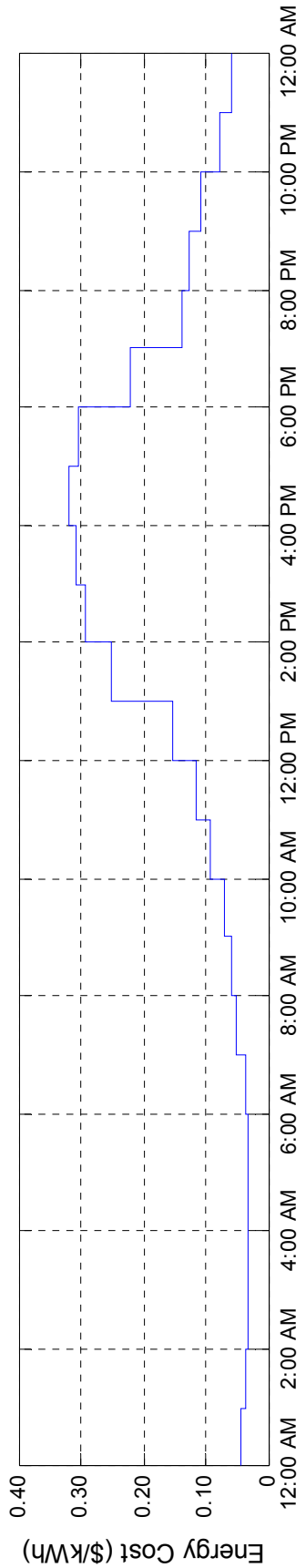

Figure 3-13 PJM DAP fluctuations on a summer day with high temperatures

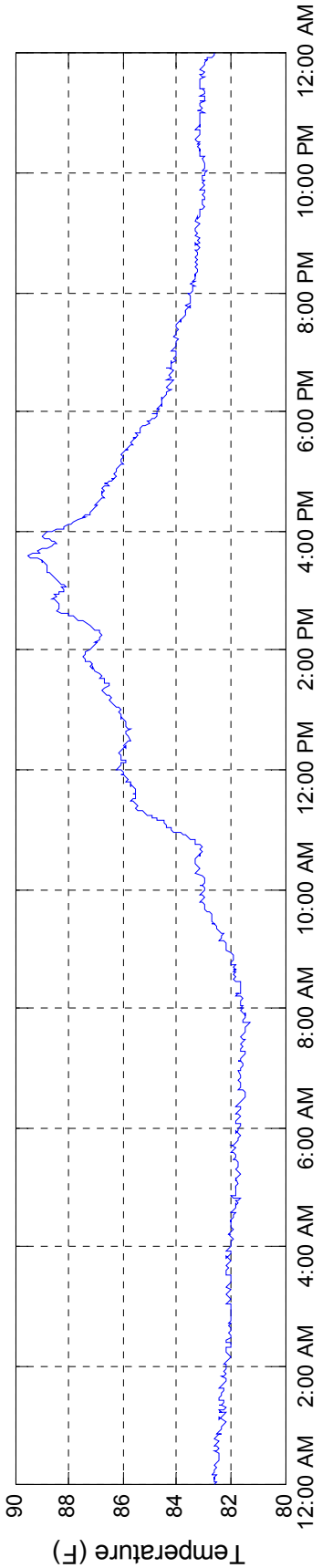

Figure 3-14 Outside temperature data

Experiment Results

As mentioned earlier, the experiment is first run under a fixed temperature set-point. In this case, the set-point is fixed at a certain value throughout the day. In the implementation the case where the temperature set-point is fixed at 78°F is considered. In the second part, the temperature set-points are treated as decision variables and determined using the TSA algorithm. The algorithm is employed to assign reference temperature set-points for each hour of the day, and these variable reference temperature set-points are utilized in the proposed MPC controller. In this case, a temperature range of 77°F-79°F is used for the temperature set-points. The performance of MPC controller is compared with two-position control in each case. Reference temperature set-points employed in MPC controller are used as thermostat set-points in two-position control. For both cases, a ± 0.5°F hysteresis band ($k = 0.5$°F) is considered in the two-position control scheme, and the inside temperature is constrained between 75°F and 80°F for the MPC controller.

In all computations, q is assumed to be 3.95kW since a typical residential AC unit consumes on average 3.95kW per hour. Moreover, in the objective function given in (1) it is assumed that $w = 0.8$. In what follows, results are displayed and discussed for each case.

Comparison with Fixed Temperature Set-Points

To analyze the performance of the proposed MPC controller with a fixed reference temperature set-point, the reference temperature set-point is fixed at 78°F in the MPC controller and the results are compared with those of two position control with a thermostat setting of the same value. In this case, since the reference temperature is fixed

to a certain value, the objective function for the MPC is to minimize the total energy consumption while keeping the inside temperature as close to the fixed reference temperature as possible. Basically, the energy consumption, thereby the energy cost of the two control strategies are compared. Figure 3-15 shows the inside temperature fluctuation and the AC status for both cases.

Simulation results show that MPC process leads to a non-uniform temperature fluctuation with more frequent AC operation compared to the two position control. In the experiment, it is observed that the two position control with a fixed thermostat setting of 78°F leads to a total energy consumption of 26.94 kWh with a total cost of $3.78. On the other hand, MPC control with a similar fixed reference temperature set-point consumes 25.69 kWh with a cost of $3.61. According to the results, the MPC process yields 4.6% reduction in energy consumption and 4.5% savings in related costs. The energy consumption and energy cost during peak hours (2:00 – 6:00 PM) for the two-position control are 6.85 kWh and $2.01 respectively, whereas the MPC control strategy results with 6.45 kWh and $1.90. This implies a 5.8% and 5.5% reduction in energy consumption and cost respectively with the MPC process. In this case while the MPC controller reduces the energy usage, it ends with a somewhat higher inside temperature (78.31°F vs. 78.05°F). It is noted that lower inside temperatures can be obtained by increasing the weight (*i.e.,* the value of w) of the temperature potentially in return for diminishing savings. Overall, the analysis indicates that with fixed temperature set-points the use of the MPC is in general more advantageous providing in the long run, however, the benefits due to reduction in energy consumption and cost savings may not be significant. Based on this result, it is conjectured that the real-time pricing does not

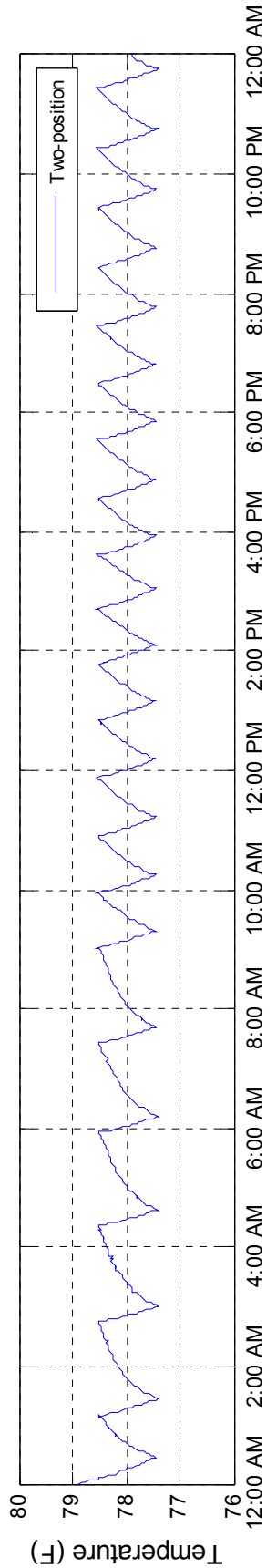

Figure 3-15a Inside temperature with two-position control

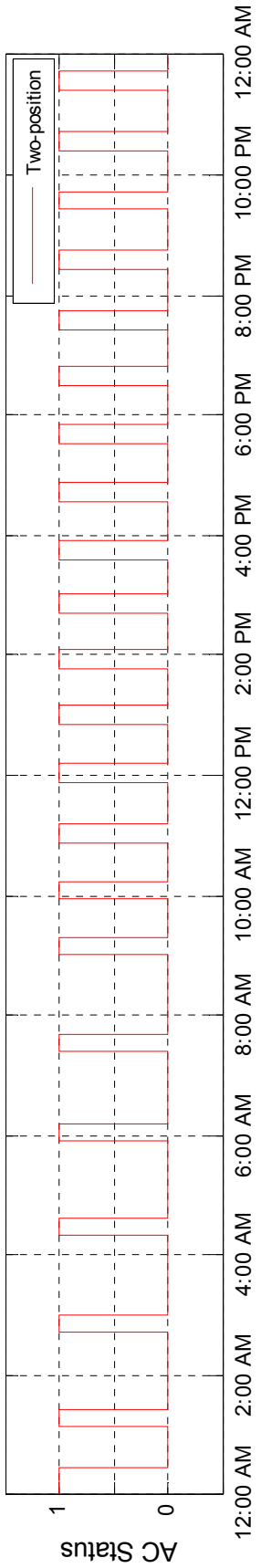

Figure 3-15b AC status with two-position control

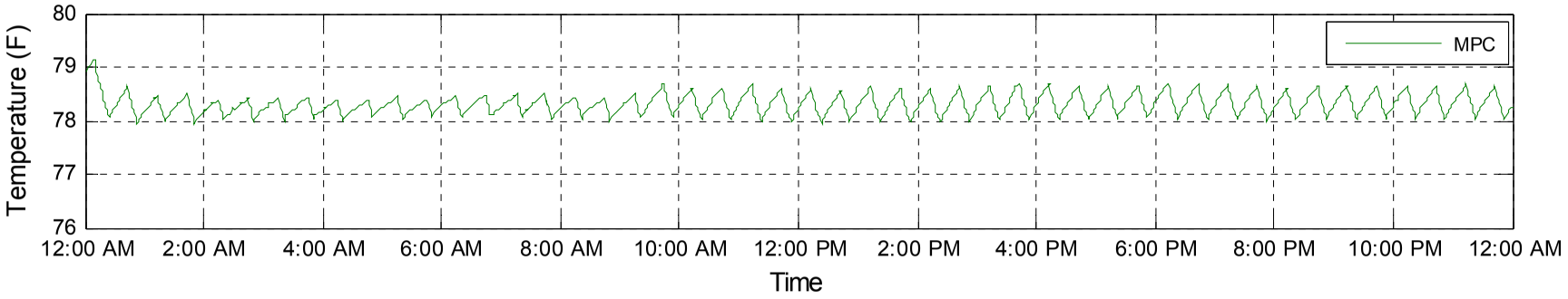

Figure 3-15c Inside temperature with the MPC process

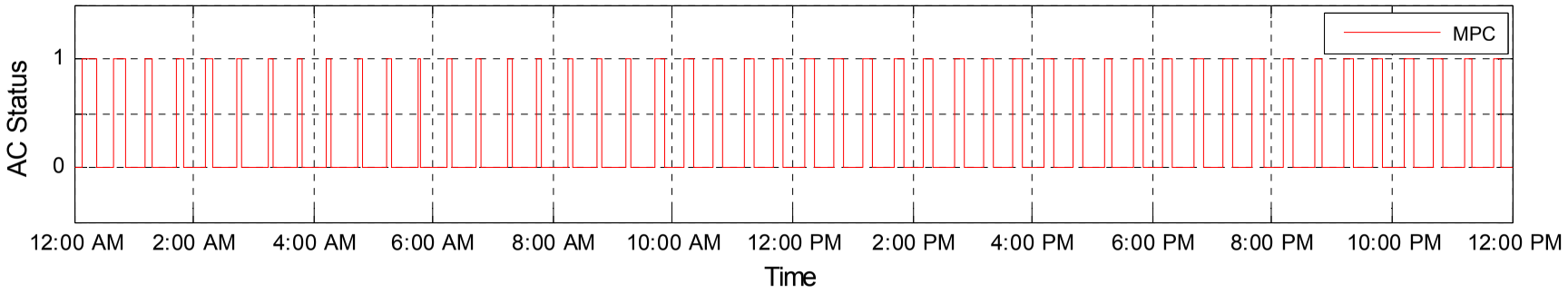

Figure 3-15d AC status with the MPC process

Figure 3-15 Inside temperature and AC status for both control strategies with the fixed temperature set-point of 78°F

necessarily lead to significant reduction in energy cost savings through only load shifting under fixed temperature set-points. In order for the consumers and as well as the utility providers to enjoy the promising benefits of the real-time pricing, it is suspected that the determination of the temperature set-points should be the part of the control process. As such, the experimental analysis is extended to the case where the temperature set-points are treated as endogenous parameters by the control strategies. This case is discussed next.

Comparison with Assigned Temperature Set-Points

In this stage of the experiments the temperature set-points are determined by the proposed TSA algorithm based on given lower and upper temperature bounds. As in the previous case, the temperature set-point interval is set to 0.5°F ($k = 0.5$°F) and the minimum and maximum allowable temperature set-points are assumed to be 77°F and 79°F, respectively. Therefore, the reference temperature set-point candidates are 77°F, 77.5°F, 78°F, 78.5°F, and 79°F. The experiment is carried out for three types of consumers with respect to their discomfort tolerance levels: low tolerance ($a = -1$), neutral ($a = 0$), and high tolerance ($a = 1$). Figure 3-16 shows the assigned reference temperature set-points for all three discomfort tolerance indices generated by the TSA algorithm based on the pricing data of Figure 3-13. It is recalled that a consumer with low discomfort tolerance index is reluctant to accept higher temperature set-points in return for cost savings. As expected, the consumer with high discomfort tolerance index is willing to live with relatively higher set-points during the high price periods of the day.

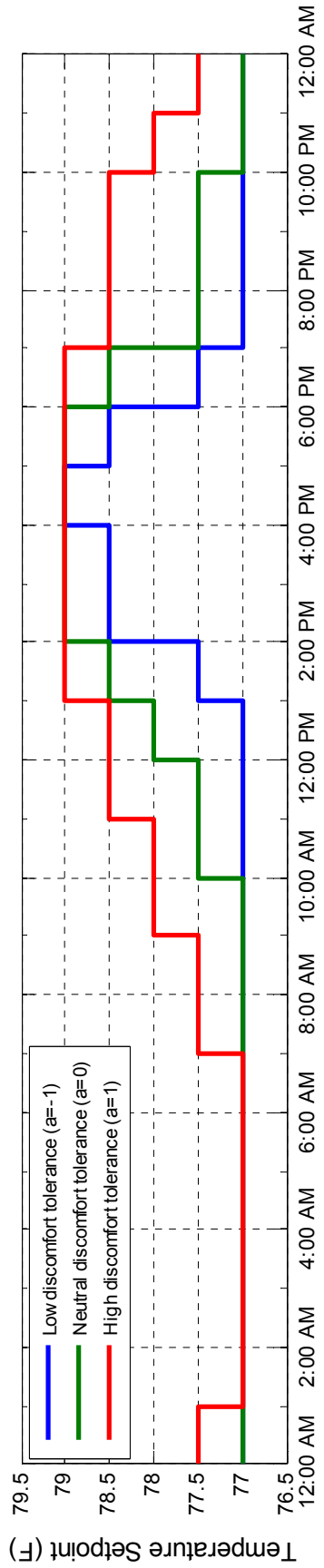

Figure 3-16 Discomfort tolerance index based reference temperature set-points

To enhance the comparison analysis, the reference temperature assignments generated by the TSA algorithm are employed not only for the MPC process but also in the two-position control strategy. Similar to the previous case, the performance of MPC is compared with the two-position control strategy under similar conditions. Figure 3-17 depicts the change of inside temperature and the AC status for both control strategies for the neutral consumer ($a = 0$).

Simulation results show that, with a neutral discomfort tolerance index, two-position control with variable assigned temperature set-points consumes 29.71 kWh with a cost of $3.59, whereas the MPC control strategy results in 27.33 kWh and $3.12 in cost. In this case, the MPC strategy provides an 8% reduction in energy consumption with 13.1% savings in related costs. Two-position control strategy consumes 5.00 kWh with a cost of $1.50 during peak hours, while MPC control strategy results in 3.82 kWh with a cost of $1.14. This means 23.6% and 24% reduction in peak time energy consumption and cost respectively. The average daily temperatures for two position and MPC control strategies were recorded as 77.68°F and 77.96°F respectively. The results indicate that with a negligible compromise in average inside temperature, the consumer can enjoy significant cost savings under the MPC process with endogenous temperature set-points. Interestingly, it is observed that with the MPC process similar average temperatures can be achieved with considerably lower energy consumption.

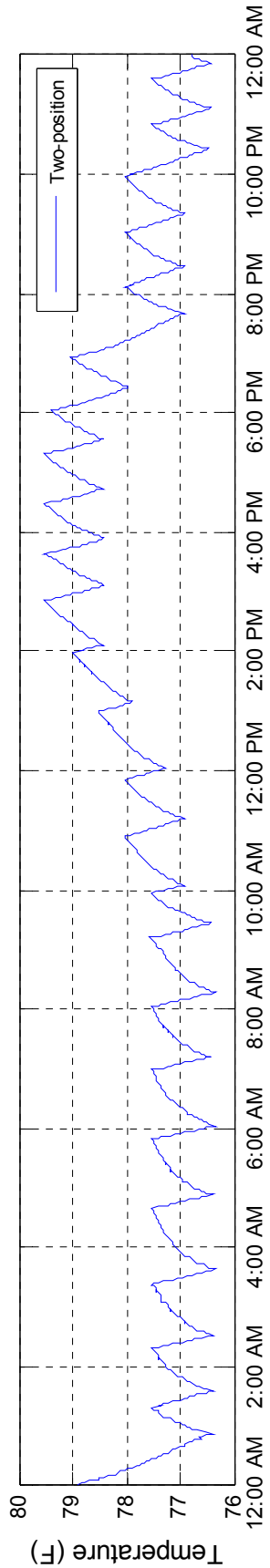

Figure 3-17a Inside temperature with two-position control

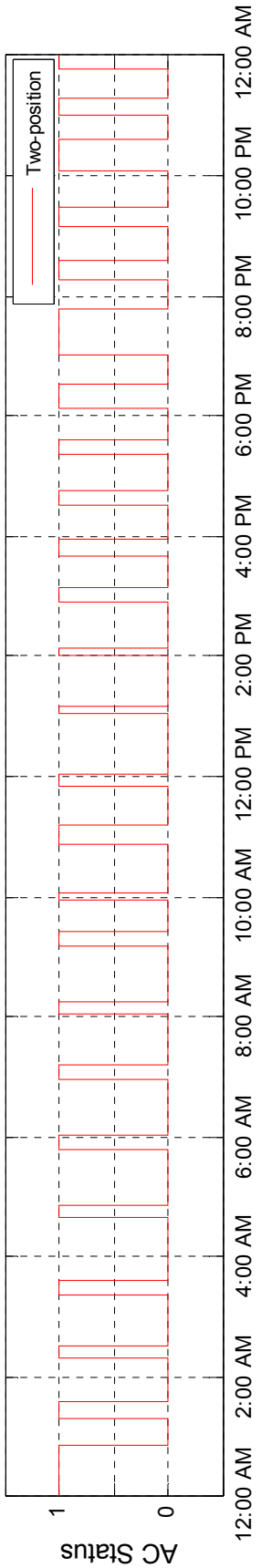

Figure 3-17b AC status with two-position control

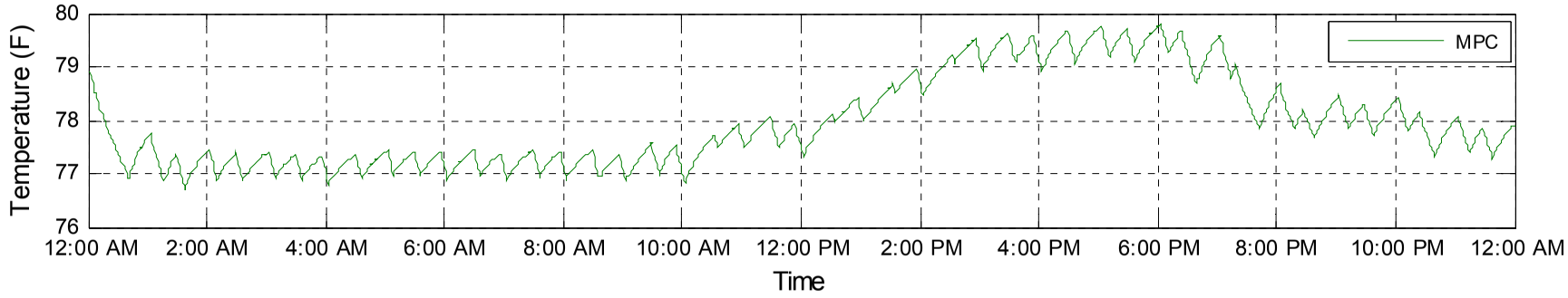

Figure 3-17c Inside temperature with the MPC process

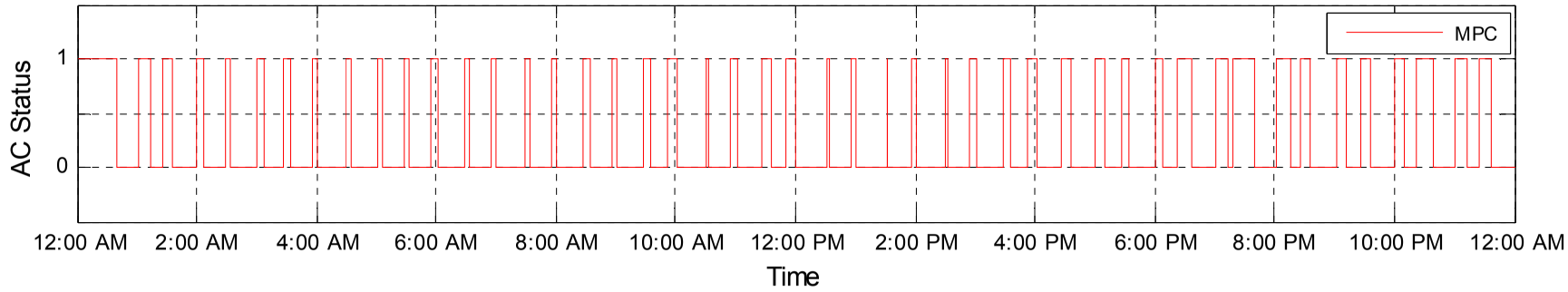

Figure 3-17d AC status with the MPC process

Figure 3-17 Inside temperature and AC status for both control strategies with the variable temperature set-points

Overall Comparison

Table 3-1 presents the overall comparison between two-position and MPC control strategies for both fixed and variable temperature set-points. Based on the results given in the table, the MPC process can be compared with variable temperature set-points to the two-position control with fixed set-points. This comparison is insightful given the fact that the latter control strategy is common practice for AC control. It is interesting to observe that compared to the two-position control with fixed temperature set-points, while the MPC process with variable set-points results in a 1.4% increase in total energy consumption, it offers a 17.5% reduction in total energy cost due to AC usage. Furthermore, the MPC process with variable set-points is superior to the two-position control with fixed temperature set-points in both energy consumption and energy costs during the peak hours, resulting in 44.2% and 43.3% reductions respectively. These results suggest that the proposed MPC strategy would allow the consumers effectively take advantage of the dynamic pricing while facilitating an efficient demand response setting which enables the utility providers adopt effective demand management policies.

Table 3-1 Summary of the results for both control strategies

		Energy (kWh)		Cost ($)		Average Temp (°F)
	Method	**Peak-hours**	**Total**	**Peak-hours**	**Total**	
Fixed Temperature Set-Point (78°F)	Two-position control	6.85	26.94	2.01	3.78	78.05
	MPC	6.45	25.69	1.90	3.61	78.31
Variable Temperature Set-Point (a=0)	Two-position control	5.00	29.71	1.50	3.59	77.68
	MPC	3.82	27.33	1.14	3.12	77.96

Table 3-2 illustrates the results for MPC process with variable reference set-points under all three discomfort tolerance indices considered in the analysis. As pointed out by the results, it can be concluded that the total energy consumption and costs increase as discomfort tolerance index decreases, whereas average daily temperatures increase as expected. However, interestingly, energy consumption and costs during peak-hours in fact increase with discomfort tolerance index. At first look, this is a counter intuitive conclusion. To explain this result, it is first noted that for a consumer with low discomfort tolerance the inside temperature during any given period is no higher than that of a higher tolerance consumer. As such, cooler inside temperatures during the periods preceding the peak hours create a thermal storage for the building, which reduces the need for energy consumption for the low-index consumer during the peak hours.

Table 3-2 Summary of results for the MPC process with variable temperature set-points across different discomfort tolerance indices

	Discomfort Tolerance Index	Energy (kWh)		Cost ($)		Average Temp (°F)
		Peak-hours	Total	Peak-hours	Total	
Model Predictive Control	a= -1	3.29	28.32	0.97	3.23	77.64
	a= 0	3.82	27.33	1.14	3.12	77.96
	a= 1	4.68	25.03	1.39	3.03	78.46

CHAPTER 4: MPC CONTROLLER PROTOTYPE

In this chapter, a prototype for the proposed HVAC load control strategy is developed to validate the simulation results through prototype experiments. A cost-benefit analysis is also conducted to identify the payback period considering cost of prototype development and cost savings.

Although the performance of the proposed control strategy is confirmed through simulation studies in the previous chapter, building an actual prototype would not only further validate the simulation results but would also help in assessing the economic feasibility of introducing such a controller as part of a building energy management system. The low cost of build and ease of operation for the controller shown in this chapter will allow the adoption of this controller in the building HVAC control industry.

The prototype development starts with the introduction of the necessary equipment followed by the stages of prototype assembly. Once the prototype build is complete, a series of prototype experiments is performed in order to validate its performance. The results of these experiments are then compared to the simulation results discussed in the previous chapter. It is expected that the results from the prototype experiments will be parallel with the simulation results. A cost-benefit analysis is then performed for the prototype build and the payback period is calculated using the experimental results.

Prototype Equipment

There is a certain number of equipment needed to develop the proposed controller. A microcontroller, Arduino Uno, is used as the main controller unit. A relay kit to adjust control inputs, four temperature sensors (two for indoor, two for outdoor), a breadboard, and several jumper cables are also utilized in the prototype. These specific pieces of

equipment are selected to build the prototype because of the following key considerations:

- MATLAB Support Package for Arduino which makes it possible to use MATLAB or Simulink to communicate with the Arduino board over a USB cable. This package is based on a server program running on the board, which listens to commands arriving via serial port, executes the commands, and, if needed, returns a result.
- Ease of use and reliability of the Arduino controller.
- The cost and availability of these equipment in industry.

Microcontroller (Arduino Uno)

Arduino Uno is a microcontroller board based on the ATmega328. It has 14 digital input/output pins (of which 6 can be used as PWM outputs), 6 analog inputs, a 16 MHz ceramic resonator, a USB connection, a power jack, an ICSP header, and a reset button shown in Figure 4-1. Figure 4-2 shows the back side of Arduino Uno.

The Arduino Uno can be powered via the USB connection or with an external power supply. External (non-USB) power can come either from an AC-to-DC adapter (wall-wart) or battery. The board can operate on an external supply of 6 to 20 volts. If supplied with less than 7V, however, the 5V pin may supply less than five volts and the board may be unstable. If using more than 12V, the voltage regulator may overheat and damage the board. The recommended range is 7 to 12 volts.

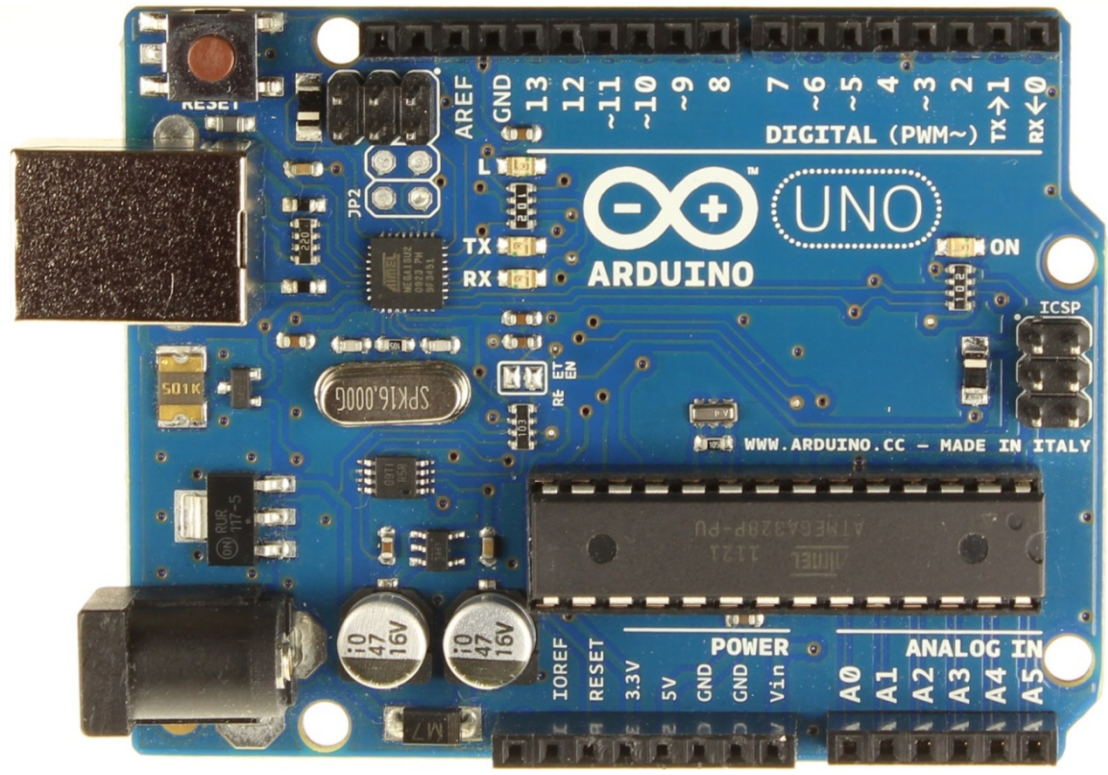

Figure 4-1 Arduino Uno front side

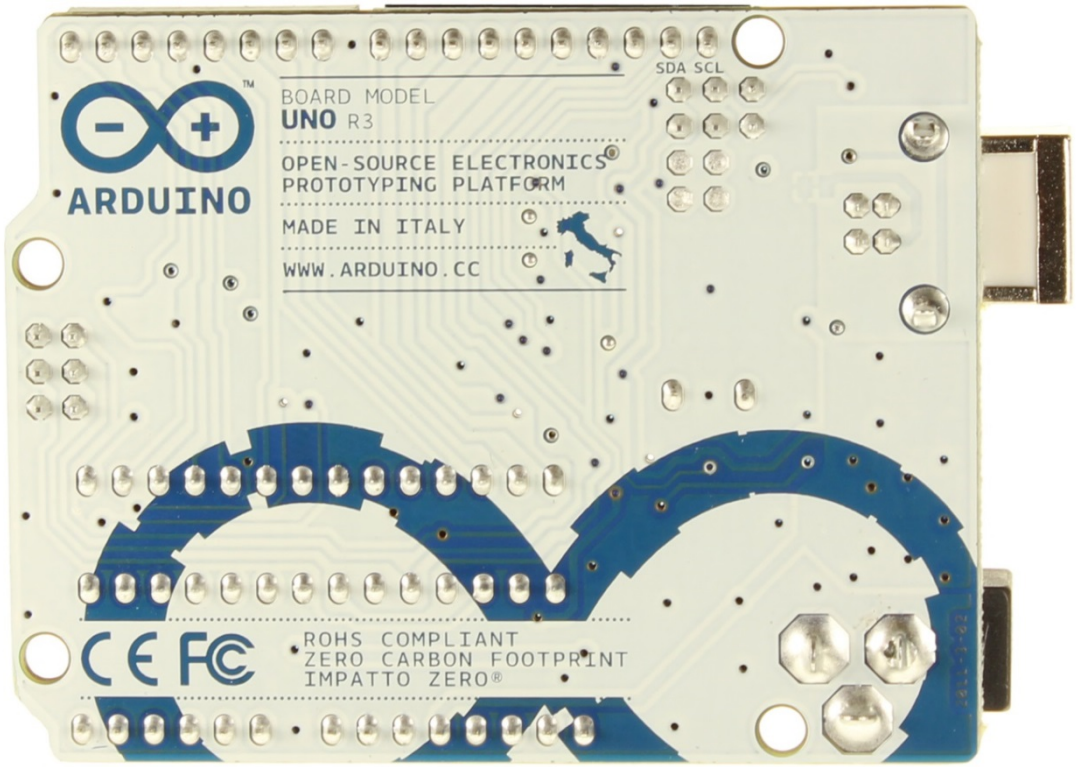

Figure 4-2 Arduino Uno back side

Summary

Microcontroller	Atmega328
Operating Voltage	5V
Input Voltage (recommended)	7-12V
Input Voltage (limits)	6-20V
Digital I/O Pins	14 (of which 6 provide PWM output)
Analog Input Pins	6
DC Current per I/O Pin	40 mA
DC Current for 3.3V Pin	50 mA
Flash Memory	32 KB (Atmega328) of which 0.5 KB used by bootloader
SRAM	2 KB (Atmega328)
EEPROM	1 KB (Atmega328)
Clock Speed	16 MHz

Beefcake Relay Control Kit

A relay must be used to switch the HVAC unit on and off. Microcontrollers are capable of this process, but only for very small devices such as mini LED lamps. Therefore, a beefcake relay control kit that enables to control the circuit by a low-power signal is selected to be utilized. The relay is controlled by 5V logic through a transistor, and an LED tells you when the relay is closed. The other elements of beefcake relay control kit include two 1k Ohm resistors, a 10k Ohm resistor, a diode small signal, a transistor, an LED, two screw terminals, and a relay control board. Figure 4-3 and Figure 4-4 display the disassembled and assembled elements of the beefcake relay control kit respectively. Also displayed is the relay board schematic in Figure 4-5.

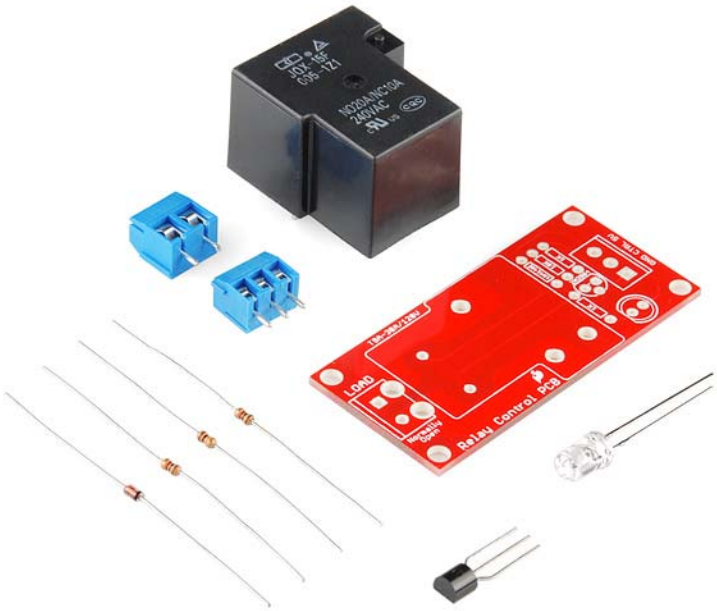

Figure 4-3 Disassembled beefcake relay control kit

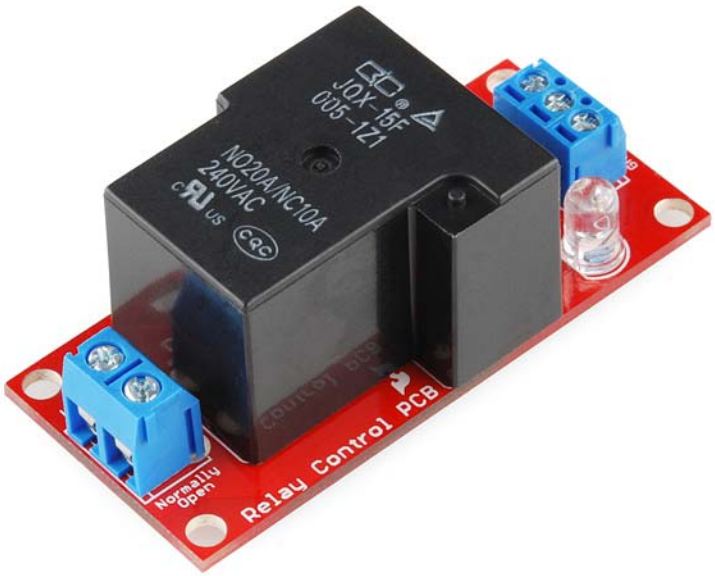

Figure 4-4 Assembled beefcake relay control kit

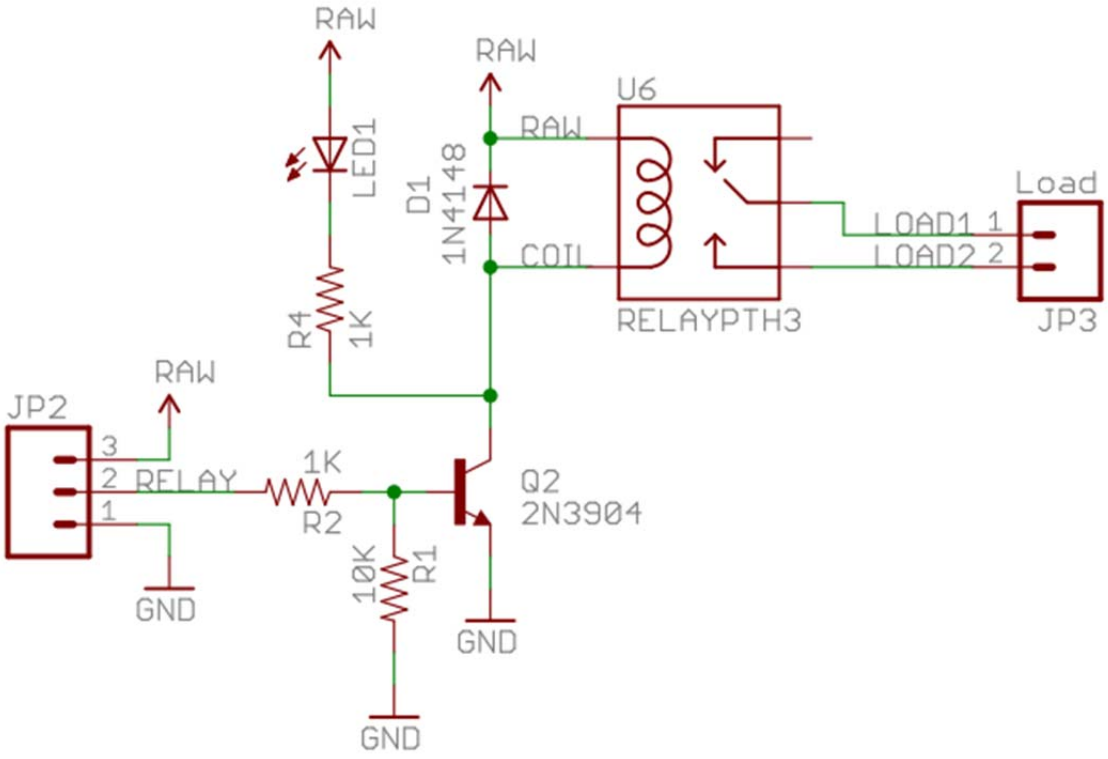

Figure 4-5 Relay board schematic

Temperature Sensor

Temperature sensors are employed to capture both indoor and outdoor temperatures which are then transferred to the controller. A total of four sensors are positioned for temperature feedback, two for indoor and two for outdoor environment. Figure 4-6 shows the temperature sensors used in the prototype. These temperature sensors require a ground and a 2.7 to 5.5 VDC. The sensors provide a voltage output that is linearly proportional to the Celsius temperature. The output voltage is read on the Vout pin and can be converted to temperature easily using the scale factor of 10 mV/°C. They also don't require any external calibration to provide typical accuracies of ±1°C at +25°C and ±2°C over the −40°C to +125°C temperature range.

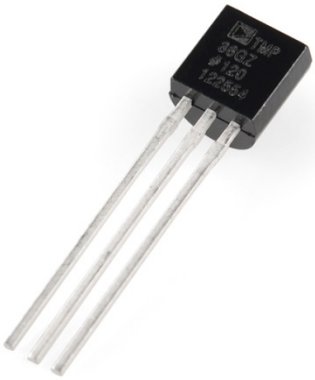

Figure 4-6 Temperature sensor

Breadbord

A breadboard is the perfect base for electronics prototyping. It is solderless which makes it easy to create temporary prototypes and experiments with circuit design. It also simplifies the circuit design by reducing the number of jumper wires required. The breadboard selected is displayed in Figure 4-7. It has 2 power buses, 30 columns, and 10 rows – a total of 400 tie in points.

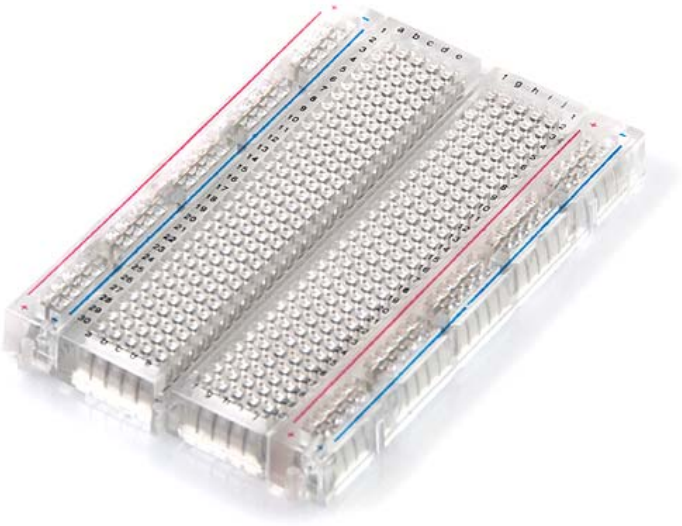

Figure 4-7 Breadboard

Jumper Wires

Two types of jumper wires are used in the circuit design. These are 155mm long male to male and male to female jumpers. The left side of Figure 4-8 displays the male to male jumpers whereas the right side displays the male to female ones used.

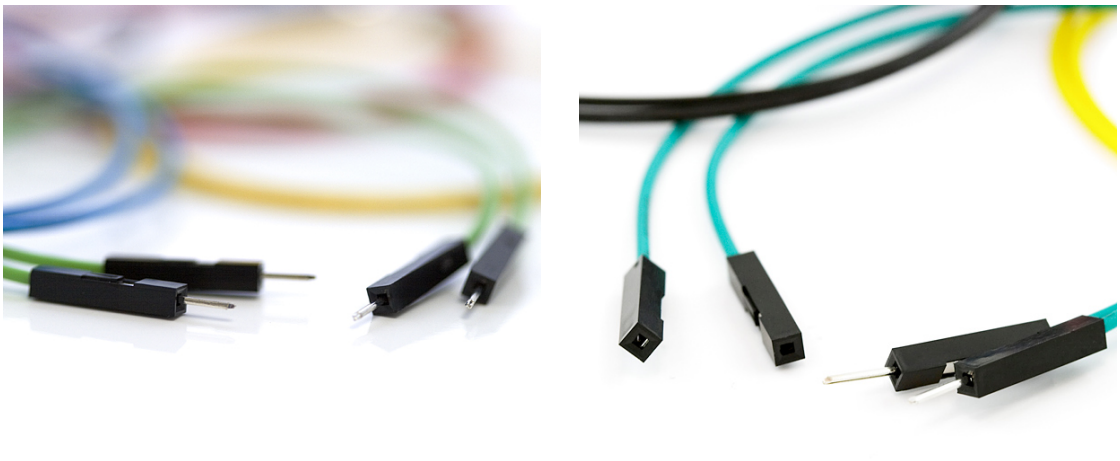

Figure 4-8 Male to male and male to female jumper wires

Stages of Prototype Assembly

1. Firstly all elements that go into developing the prototype are laid out as seen in Figure 4-9. These include a microcontroller (Arduino Uno), two 1k Ohm resistors, a 10k Ohm resistor, a diode small signal, a transistor, an LED, two screw terminals, a relay control board, a breadboard, a number of male to male and male to female jumpers, and four temperature sensors.

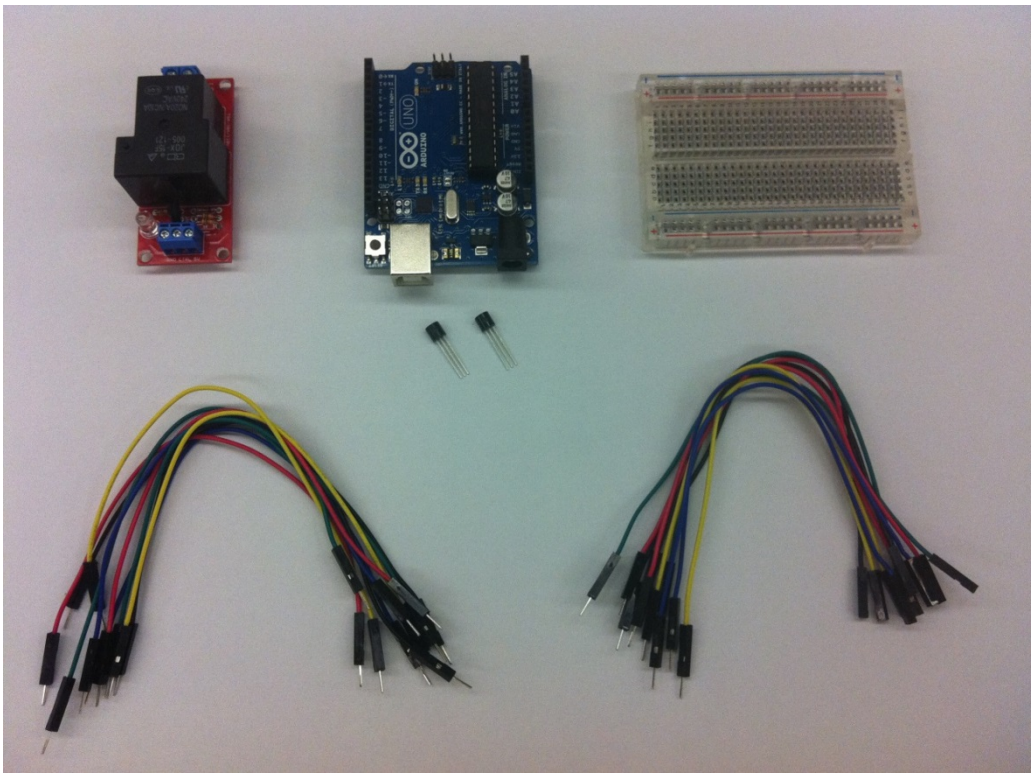

Figure 4-9 Prototype elements

2. The beefcake relay control kit comes disassembled and the elements of the kit must be soldered to the relay control board. This assembly can be seen in Figure 4-4. Once the beefcake relay kit has been assembled, it is then ready to be used in the prototype.
3. The next step is to connect the Arduino microcontroller to the breadboard. The Arduino has a limited amount of digital and analog input/outputs. Therefore, the Arduino is connected to the breadboard in order to extend the capability of the microcontroller while simplifying the design by reducing the number of jumper wires needed. The breadboard is activated by connecting the 5V positive and the ground from the Arduino to the breadboard with two jumper wires. Figure 4-10 displays the connection as well as the red and the blue wires that connect the 5V positive and the ground respectively.

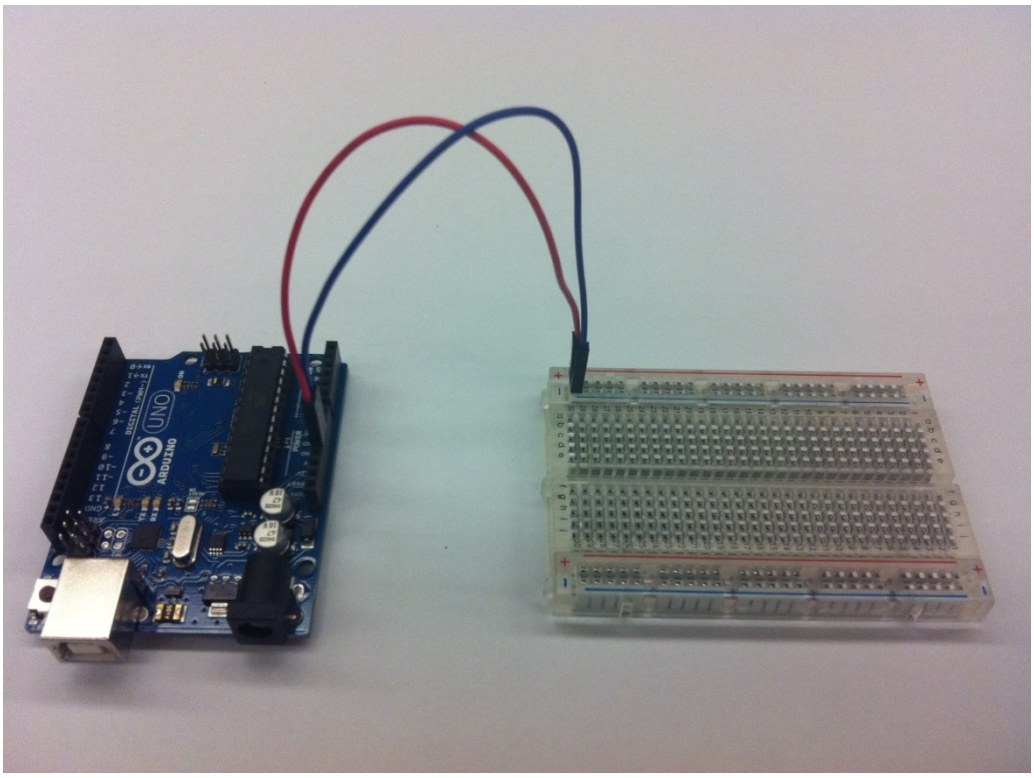

Figure 4-10 Arduino-breadboard connection

4. Once this step is done, the temperature sensors can now be connected to the breadboard. In this case, four temperature sensors are employed in the system. Two of these temperature sensors will be placed on the inside of the test facility and two on the outside. Temperature sensors have three legs: one positive leg, one negative leg, and the middle leg that goes to an input port on the analog side of the Arduino. In Figure 4-11 below one can see that for each temperature sensor a yellow jumper wire is used to connect the positive side to the breadboard, a green jumper wire is used to connect the negative side to the breadboard, and a black jumper wire is used to connect the temperature sensor to the Arduino. In order to display this clearly the jumper wires connecting the temperature sensors are kept short, but in reality these cables can be extended as far as needed to capture temperatures in different locations.

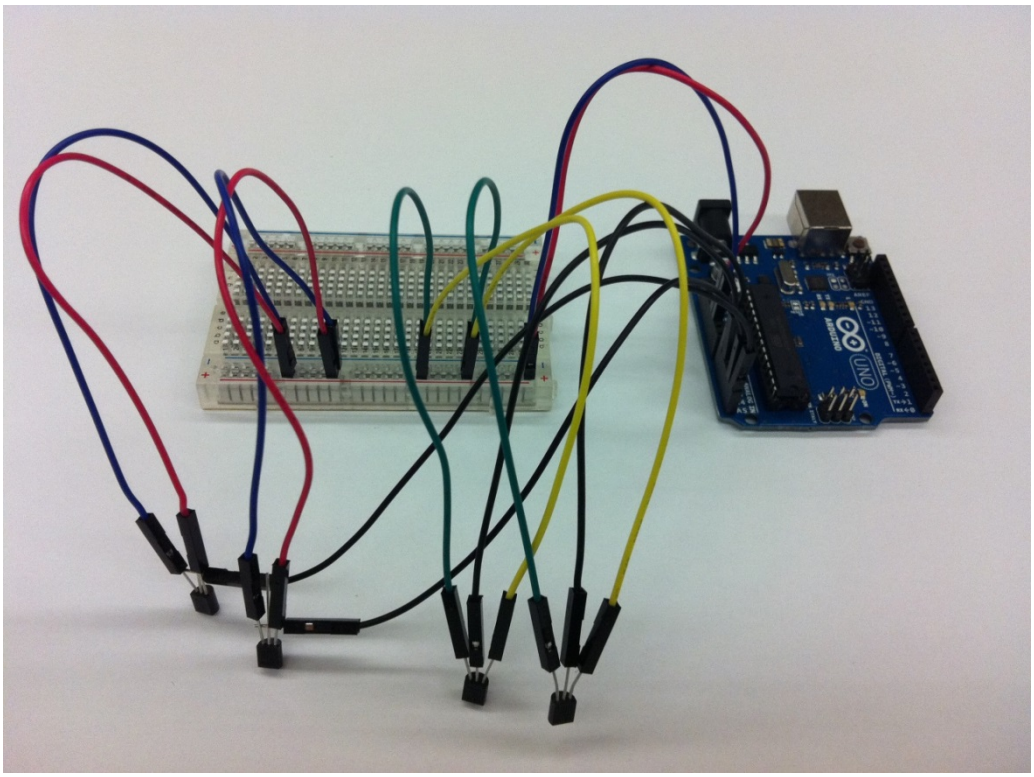

Figure 4-11 Temperature sensor connection

5. The next step in the process is to connect the beefcake relay to the breadboard and the Arduino. Through the three port terminal on the relay, the positive and the ground are connected to the breadboard using red and blue jumper wires respectively. A black jumper wire is then used to connect the controller terminal to the Arduino. In this case the relay must be connected to the output side of the Arduino. This whole process is shown in Figure 4-12 below.

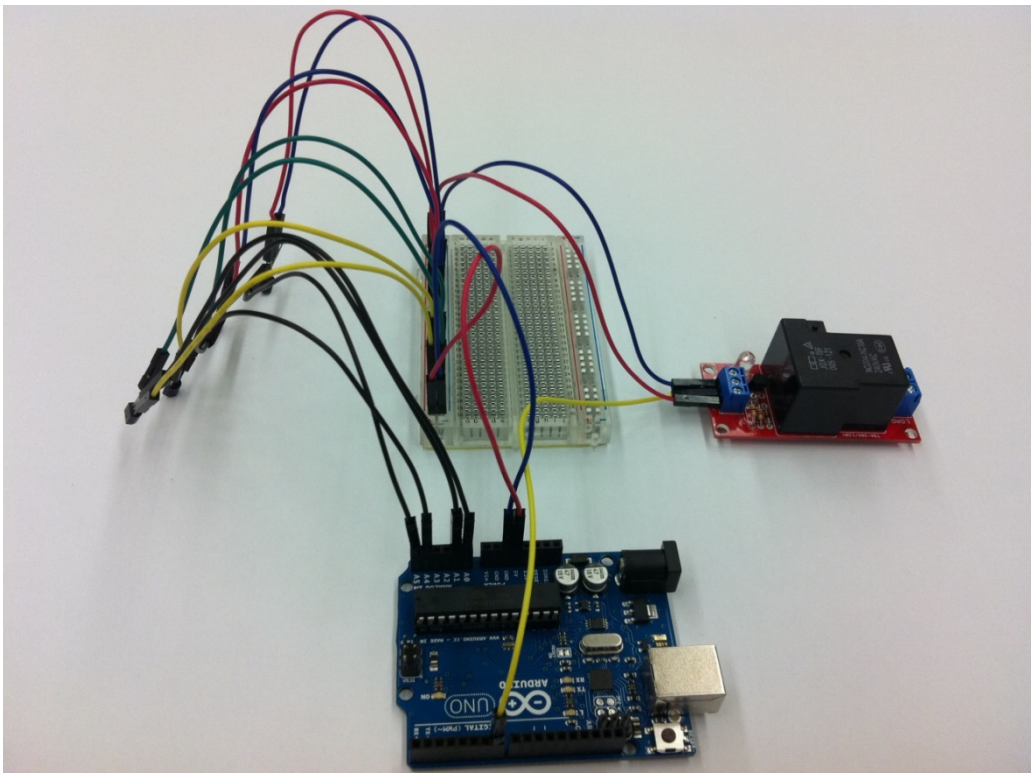

Figure 4-12 Beefcake relay connection

6. Once this is done, the circuit is completed by connecting the load terminal on the beefcake relay to the negative side of the power source (in this case a 5V battery) and the normally open terminal port to the HVAC unit to be controlled. The positive side of the battery is then connected to the HVAC unit to complete the circuits. Figure 4-13 shows the final prototype.

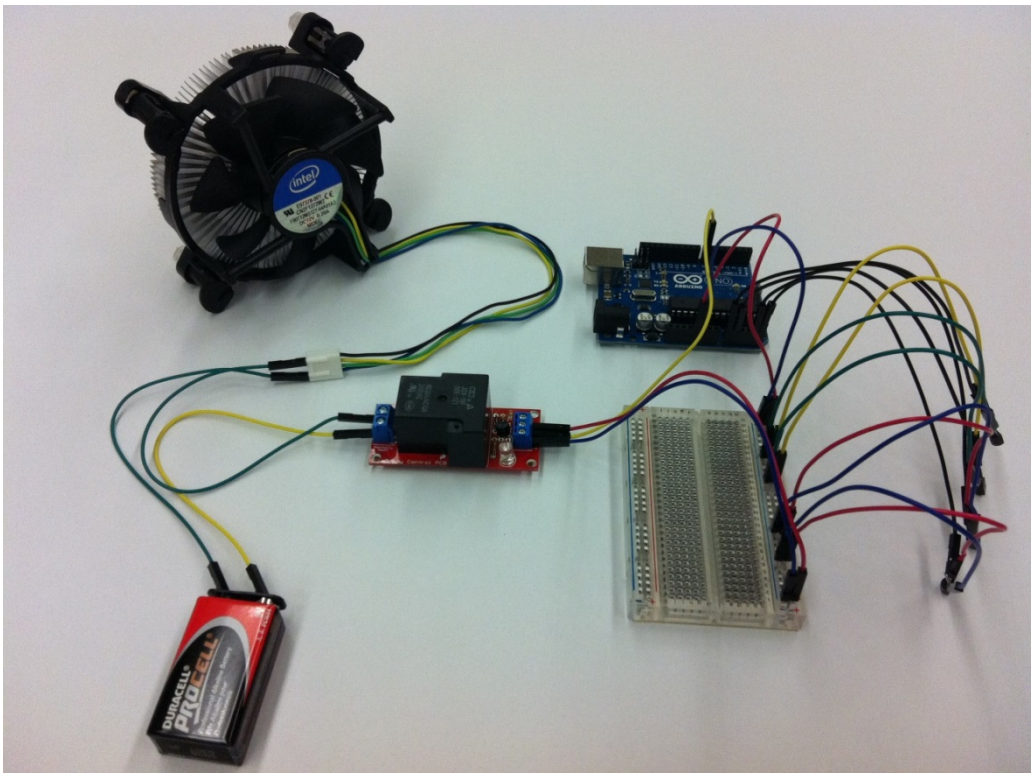

Figure 4-13 Final prototype

It should be noted that the goal of the prototype developed is to validate the simulation results of the proposed control strategy in a laboratory environment. A more compact and secure structure that combines the power source, relay, and controller should be introduced to perform the proposed control strategy in a building energy management system. In the next section, a series of prototype experiments is performed and the experimental results are compared with the ones acquired from the simulation studies in the previous chapter.

Prototype Experiments

A microcontroller is normally designed to take control actions by implementing the control algorithm that is embedded into the processor core. MATLAB Support Package for Arduino, however, enables to run any control algorithm developed in MATLAB or

Simulink on a desktop/laptop while communicating with the Arduino board over a USB cable to execute the commands and to receive feedback for control input decisions. In other words, the Arduino is used as a stepping stone (secondary relay) to transfer information back and forth from a desktop/laptop. One advantage of using this package is that it allows to skip uploading the control algorithm developed in MATLAB onto the Arduino board which first requires converting and transferring the MATLAB code to the compatible software, Arduino Software. Uploading large code files may also create memory issues depending on the memory capacity of the Arduino board. Furthermore, it is much more convenient and easy to troubleshoot any issue while controlling on the desktop/laptop as opposed to the Arduino board. Although a desktop/laptop is employed to run the control algorithms by communicating with the Arduino board in the prototype experiments, it should be noted that in real-life environment the microcontroller is expected to control the entire setup without the use of the desktop/laptop.

In the experiments, a 10 gallon glass tank with a plastic lid on the top is utilized for the control environment. This does not only simplify the utilization of the HVAC unit to be controlled, but also makes it possible to use the short-wired temperature sensors for both indoor and outdoor environments on the same control board. For the HVAC unit, a typical desktop computer fan is employed. To place the HVAC unit (fan) on the setup, a portion of the glass is cut out on the top of the tank. Indoor temperature sensors are also extended into the tank from the controller setup. Figure 4-14 and Figure 4-15 display the entire prototype control setup.

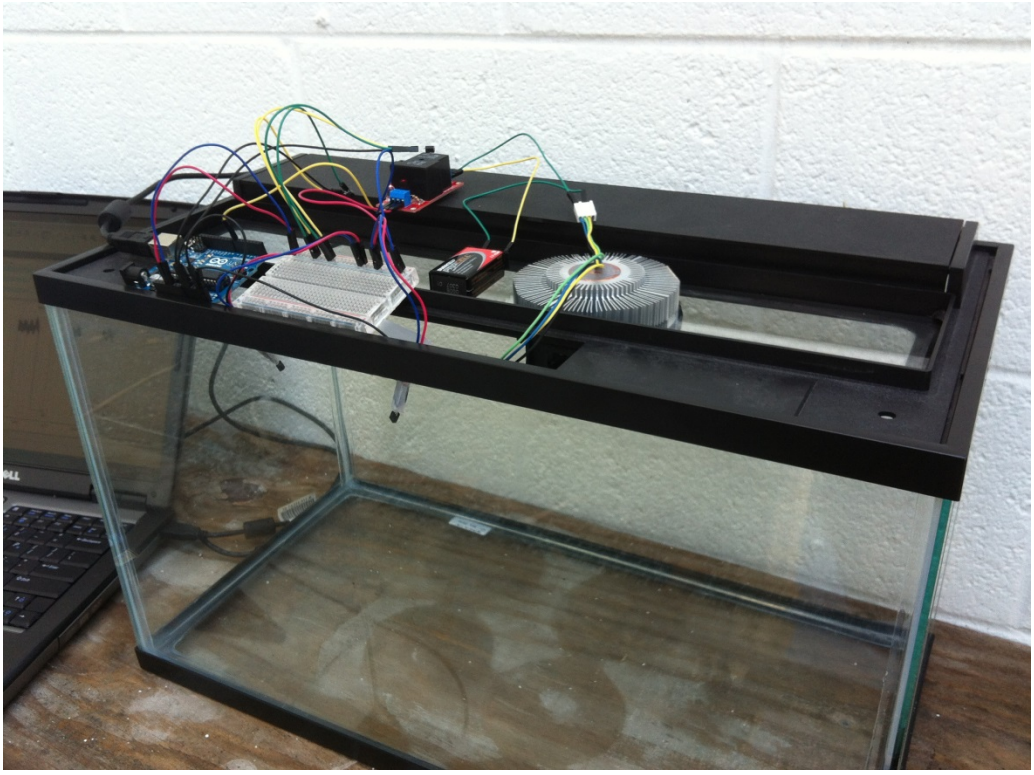

Figure 4-14 Prototype control setup top view

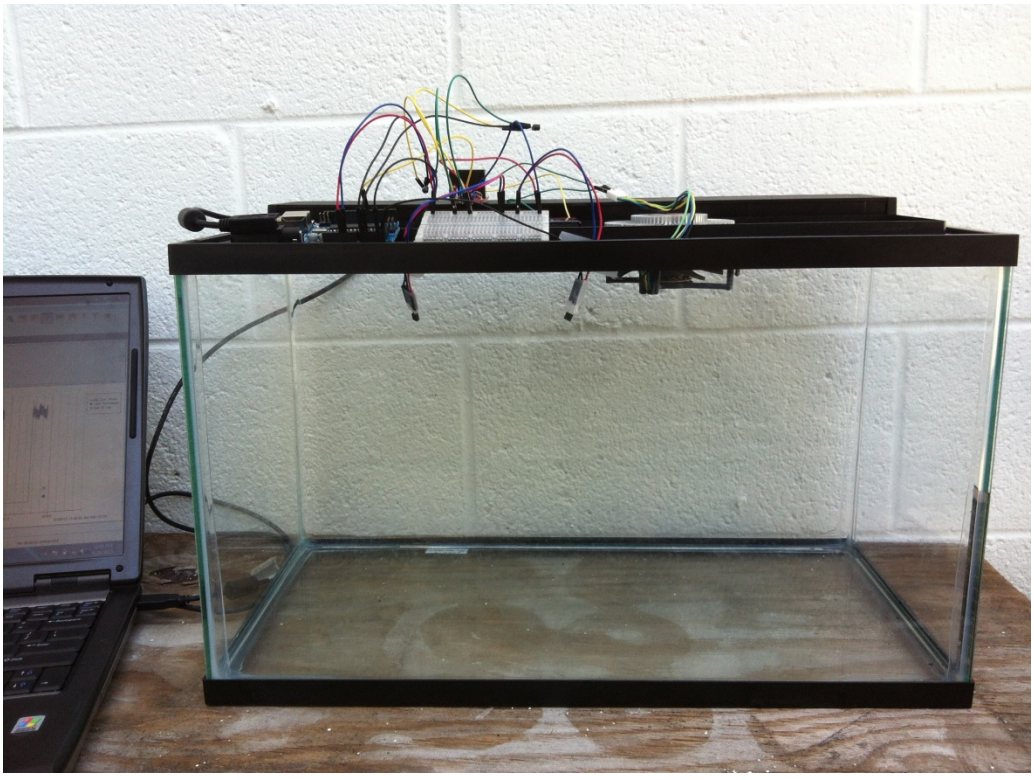

Figure 4-15 Prototype control setup side view

In order to compare the proposed MPC control strategy to the two-position control in the prototype setup, four separate experiments are performed: two experiments for MPC control (one for each fixed and variable temperature set-points) and two experiments for two-position control (one for each fixed and variable temperature set-points). For this purpose, four cool summer days with similar outside temperatures are selected and the control setup is set in a shaded outside area. Since the HVAC unit is just a computer fan for ventilation only (not an actual cooling unit), cooler days are chosen so that the HVAC unit would be able to make a considerable impact on indoor temperature in a shorter time span. This is more representative of an air conditioner operation in a real house less dependent of outside temperature. On a hot day, the HVAC unit would constantly be running but still not be able to cool down the glass tank. Also the controlled environment is placed in a shaded area in order to avoid direct sunlight which will have a much greater impact on indoor temperature compared to the case of a house because of the transparency of glass tank.

The thermal dynamics of the prototype control environment under the given HVAC unit (fan), outside temperatures, and the insulation of the setup are different than the ones in the simulation studies. In order to identify the parameters of the discrete-time state-space model to be utilized in the MPC controller during the prototype experiments, data on the fan energy consumption in PWM format and indoor and outdoor temperatures is first collected by manually operating the fan at various levels. Extra attention was paid to conduct both data collection and experiments under similar outdoor temperature conditions. This data collection took two days prior to the four-day experiment. The data collected in the first day was used to identify the parameters of the discrete-time state-

space model to be utilized in the MPC controller. The second day data was used to validate these parameters. The same procedure further discussed in the previous chapter is followed for both parameter identification and validation. The results show a considerably good agreement between the identified model and the measured validation data. One should also note that there is no need to utilize a nonlinear model in the prototype experiments, and hence there is no need to identify the parameters of this model, because actual feedback can already be received from the real control environment through temperature sensors.

Once the parameters of the discrete-time state-space model to be utilized in the MPC controller were identified, the four-day prototype experiments can be initiated. During experiments for both MPC and two-position control strategies, a laptop with MATLAB software installed is employed to run control algorithms communicating with the prototype developed. Figure 4-16 illustrates the outside temperature data on the four days chosen for the experiments: the two-position control with fixed temperature set-point, the MPC control with fixed temperature set-point, the two-position control with variable temperature set-points, and the MPC control with variable temperature set-points. The same real-time electricity pricing data used in the simulation studies in the previous chapter is also used for the each of the four prototype experiment days as illustrated in Figure 3-13.

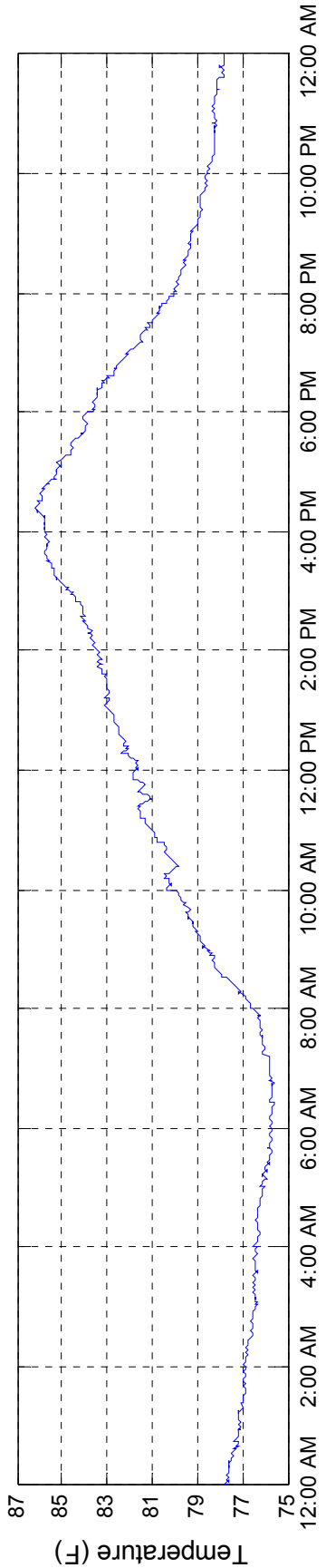

Figure 4-16a Outside temperature for the experiment of the two-position control with fixed temperature set-point

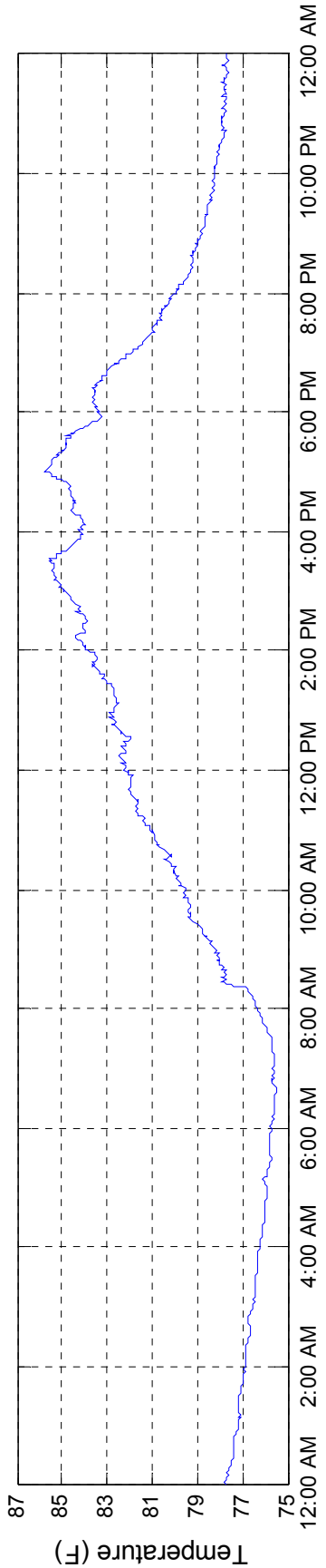

Figure 4-16b Outside temperature for the experiment of the MPC control with fixed temperature set-point

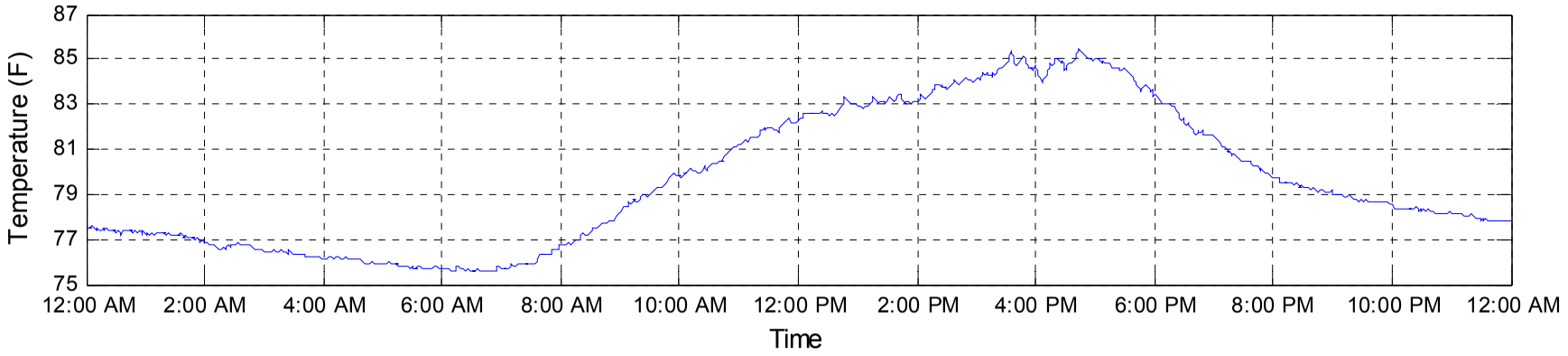

Figure 4-16c Outside temperature for the experiment of the two-position control with variable temperature set-points

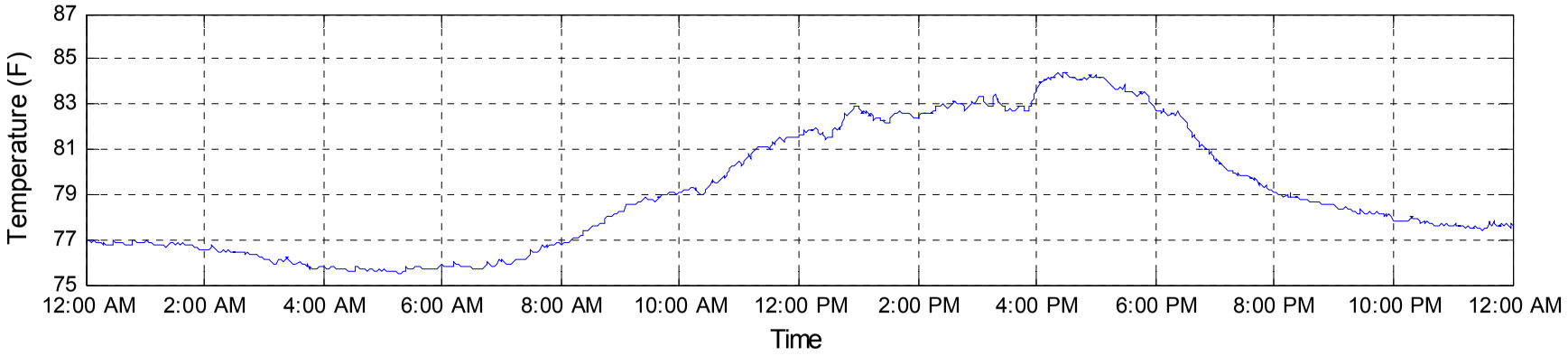

Figure 4-16d Outside temperature for the experiment of the MPC control with variable temperature set-points

Figure 4-16 Outside temperature data for the prototype experiment days

Experiment Results

The experiments are first performed under a fixed reference (thermostat for two-position control case) temperature set-point of 78°F. The experiments are then performed under variable temperature set-points where the TSA algorithm is employed to assign reference temperature set-points for each hour of the day. The performance of the MPC controller is compared with the two-position control in each case. Finally, an overall comparison is used to show the benefits of the MPC control strategy with variable temperature set-points over the conventional two-position control with fixed temperature set-point.

Furthermore, a ± 0.5°F hysteresis band ($k = 0.5$°F) is considered in the two-position control scheme, and the inside temperature is constrained between 75°F and 80°F for the MPC controller as it is done for the simulation studies. Although a computer fan is used in the prototype experiments, q is assumed to be 3.95kWh for calculation purposes since a typical residential AC unit consumes on average 3.95kW per hour. This is also used for a more representative cost-benefit analysis. Moreover, w is assumed to be 0.8 in the MPC controller similar to the simulation studies.

Comparison with Fixed Temperature Set-Points

In the first two days, the experiments are performed by fixing the reference temperature set-point in the MPC controller and the thermostat settings in the two-position control at 78°F. Figure 4-17 shows the inside temperature fluctuation and the AC status for both cases.

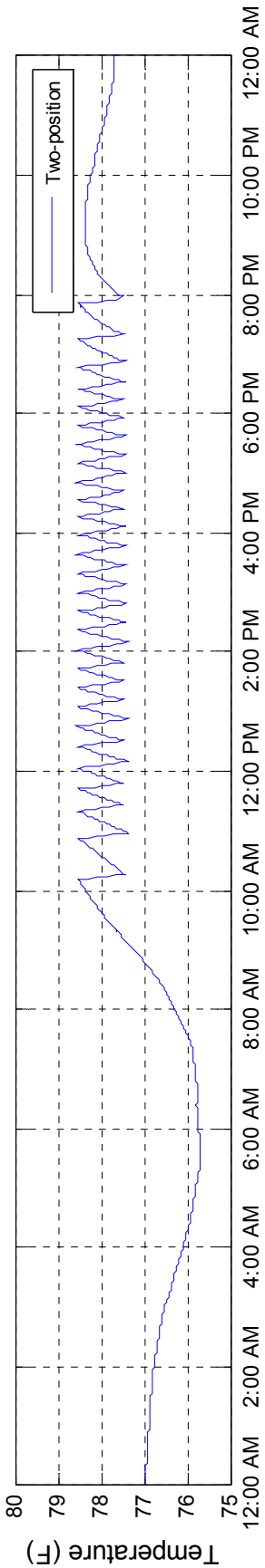

Figure 4-17a Inside temperature with two-position control

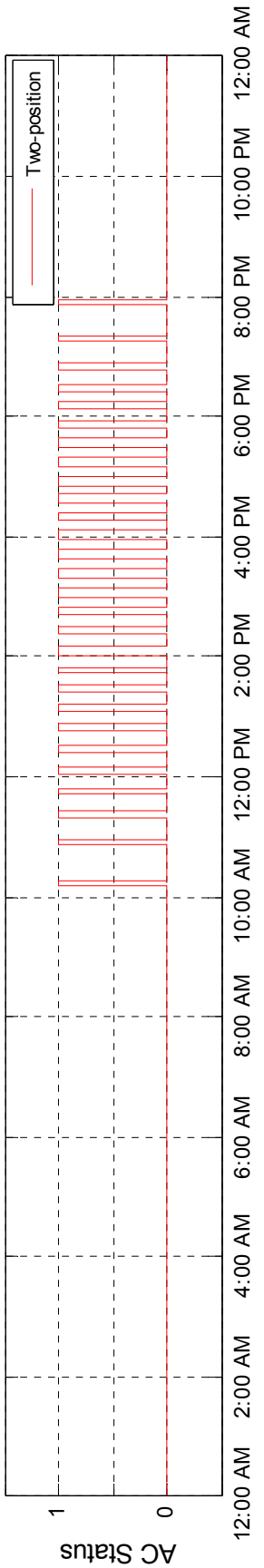

Figure 4-17b AC status with two-position control

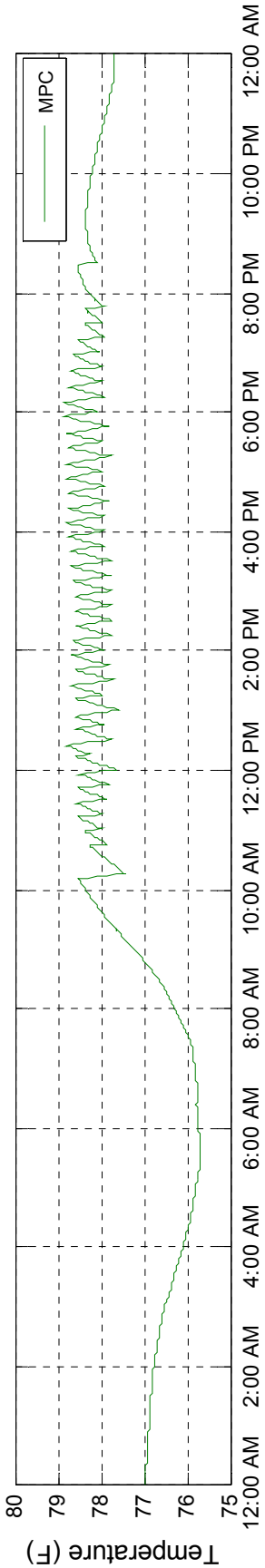

Figure 4-17c Inside temperature with the MPC process

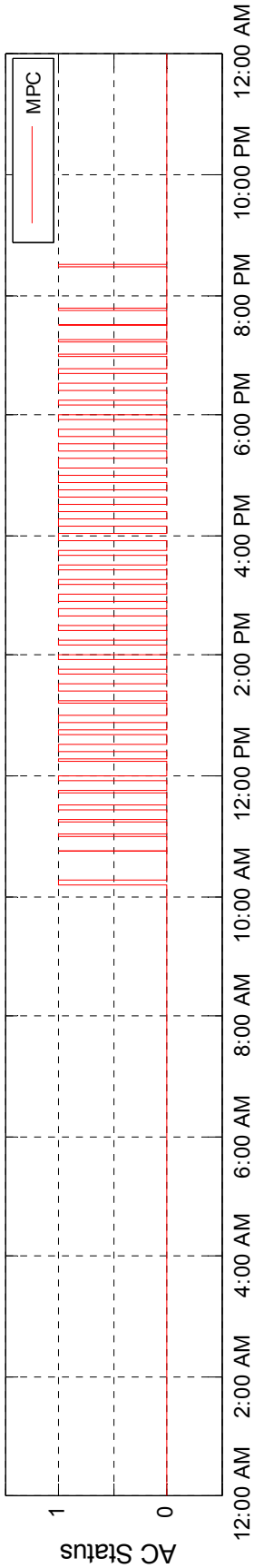

Figure 4-17d AC status with the MPC process

Figure 4-17 Inside temperature and AC status for both control strategies with the fixed temperature set-point of 78°F

Similar to the simulation studies, the prototype experiment results show that the two position control with a fixed thermostat setting of 78°F leads to a total energy consumption of 12.36 kWh with a total cost of $3.04. On the other hand, MPC control with a similar fixed reference temperature set-point consumes 11.58 kWh with a cost of $2.82. This means that the MPC process provides 6.3% reduction in energy consumption and 7.2% savings in related costs over the two-position control. The energy consumption and energy cost during peak hours (2:00 – 6:00 PM) for the two-position control are 6.66 kWh and $2.05 respectively, whereas the MPC control strategy results with 6.12 kWh and $1.88. This implies a 8.1% and 8.3% reduction in energy consumption and cost respectively with the MPC process. Average indoor temperature values for two-position and MPC control strategies are 77.37°F and 77.48°F respectively. Overall, the experimental analysis indicates that, with fixed temperature set-points, the MPC control strategy is in general more advantageous, but does not yield to significant benefits. This is strictly parallel to the results acquired from the simulation studies. Next, the case where variable temperature set-points are incorporated into the control strategies is analyzed.

Comparison with Assigned Temperature Set-Points

In the next two days of the prototype experiments, the reference/thermostat temperature set-points generated by the TSA algorithm are employed in the MPC and the two-position control strategies. Since the same real-time electricity pricing data used in the simulation studies is used, the reference temperature set-points to be used in the prototype experiments are also the same, and could be seen in Figure 3-16. One should note that the same temperature range, 77°F-79°F, and the same temperature set-point interval, 0.5°F ($k = 0.5$°F), are also used for temperature set-point assignment in the

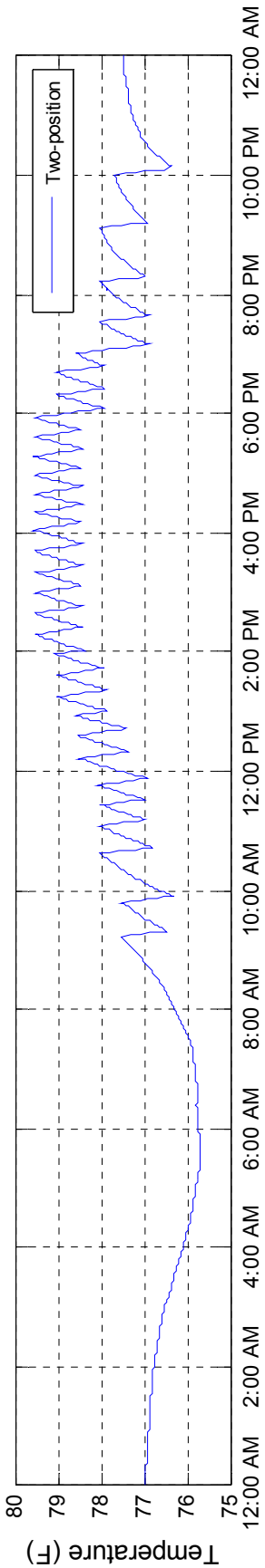

Figure 4-18a Inside temperature with two-position control

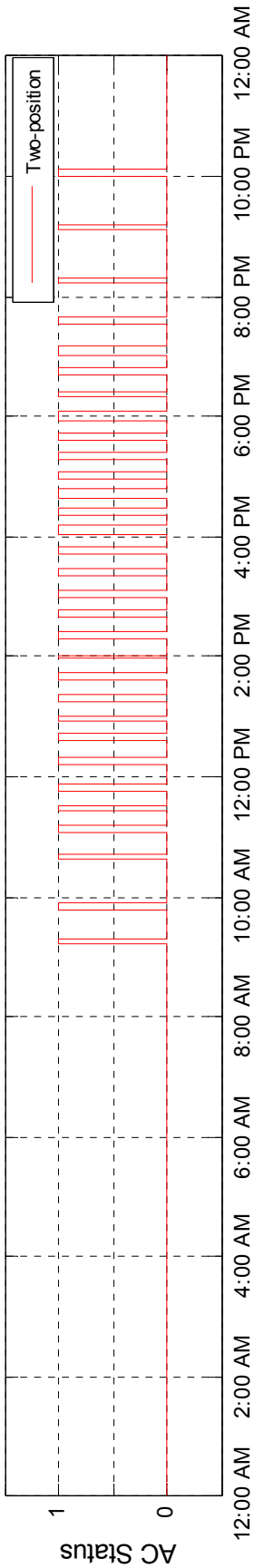

Figure 4-18b AC status with two-position control

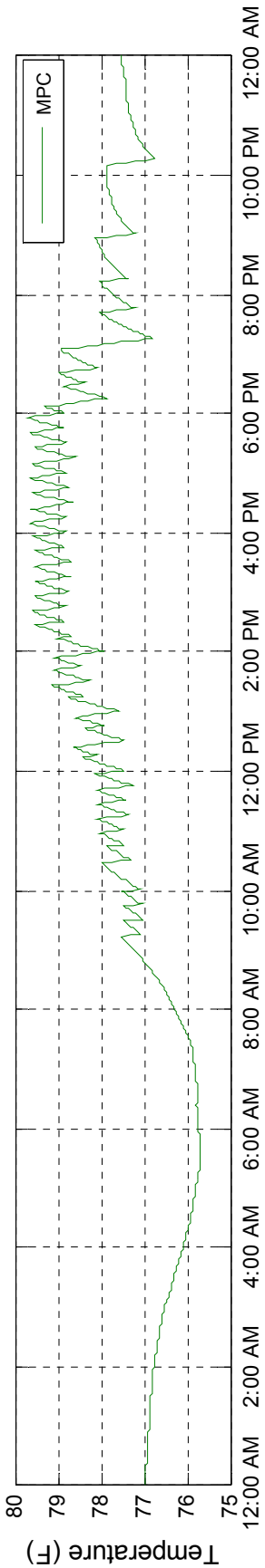

Figure 4-18c Inside temperature with the MPC process

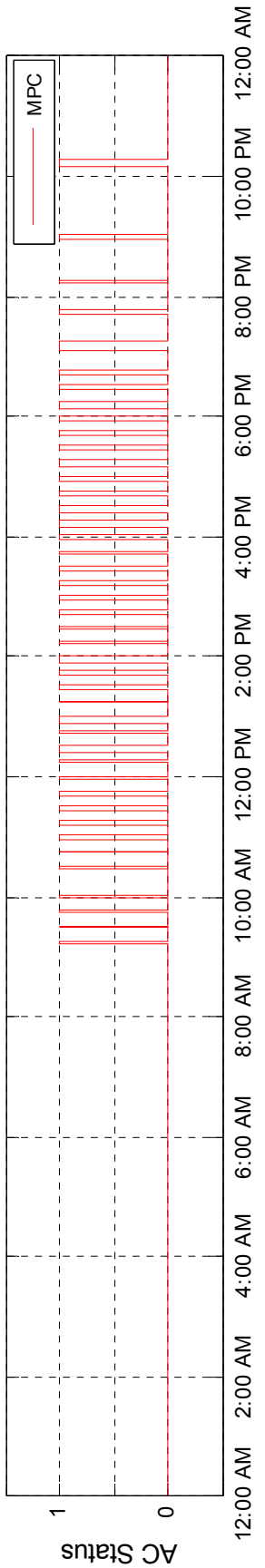

Figure 4-18d AC status with the MPC process

Figure 4-18 Inside temperature and AC status for both control strategies with the variable temperature set-points

prototype experiments. For general comparison purposes, the assigned temperature set-points with the neutral discomfort tolerance index are used in the experiments. Figure 4-18 shows the change of inside temperature and the AC status for both control strategies for the neutral consumer ($a = 0$).

The results of the prototype experiments show that, with a neutral discomfort tolerance index, two-position control with variable assigned temperature set-points consumes 12.54 kWh with a cost of $2.72, whereas the MPC control strategy results in 11.76 kWh and $2.58 in cost. In this case, the MPC strategy provides an 6.2% reduction in energy consumption with 5.1% savings in related costs. Two-position control strategy consumes 5.28 kWh with a cost of $1.62 during peak hours, while MPC control strategy results in 4.92 kWh with a cost of $1.51. This means 6.8% and 6.8% reduction in peak time energy consumption and cost respectively. The average daily temperatures for two position and MPC control strategies were recorded as 77.35°F and 77.46°F respectively. The experiment results draw a parallel conclusion to the simulation results discussed in the previous chapter. It is observed that, under the MPC control strategy with variable temperature set-points, significant cost savings could be achieved with a negligible compromise in average inside temperature. Similarly, the MPC process results in considerably lower energy consumption compared to the two position control with similar average temperatures realized.

Overall Comparison

Table 4-1 summarizes the overall comparison between two-position and MPC control strategies for both fixed and variable temperature set-points. As it can be seen in Table 4-1, the MPC process with variable set-points offers a 4.9% and 15.1% reductions in total energy consumption and energy costs respectively compared to the two-position control. The reductions in total energy consumption and energy costs during peak hours improve to 26.1% and 26.3% respectively. These results validate the performance of the proposed MPC controller, and are in line with the simulation results discussed in the previous chapter.

Table 4-1 Summary of the results for both control strategies

	Method	Energy (kWh)		Cost ($)		Average Temp (°F)
		Peak-hours	Total	Peak-hours	Total	
Fixed Temperature Set-Point (78°F)	Two-position control	6.66	12.36	2.05	3.04	77.37
	MPC	6.12	11.58	1.88	2.82	77.48
Variable Temperature Set-Point (a=0)	Two-position control	5.28	12.54	1.62	2.72	77.35
	MPC	4.92	11.76	1.51	2.58	77.46

Cost-Benefit Analysis

After validating the advantages of the proposed MPC control strategy through a series of prototype experiments, a cost-benefit analysis is conducted to display the economic feasibility of implementing such a controller as part of a building energy management system. For this purpose, the average cost savings achieved by implementing the proposed MPC control strategy compared to the two-position control strategy were first quantified. Next, the total implementation cost of the proposed MPC controller is quantified. This includes the total cost of equipment utilized in the controller build as

well as the cost of labor to assemble the controller. To conclude this section, the payback period is calculated considering cost of prototype build and cost savings.

Cost Savings

To quantify the average cost savings, the cost of the HVAC unit consumption acquired from the prototype experiment results for the following cases are compared: 1) the MPC control strategy under the variable temperature set-points 2) the two-position control strategy under the fixed temperature set-point. One should note that the two-position control strategy under the fixed temperature set-point is the most common control strategy currently employed in the thermostats in the United States. According to the prototype experiments, the daily cost of the HVAC unit consumption under both control strategies are \$2.58/day and \$3.04/day respectively. Therefore, the daily cost savings that could be achieved by implementing the proposed MPC controller would be:

$$\$3.04 - \$2.58 = \$0.46/day$$

This corresponds to an average annual savings of:

$$\$0.46 * 365 \approx \$168/year$$

Implementation Cost

There are two separate costs that need to be considered while quantifying the total cost of implementing the proposed MPC controller. The first cost that needs to be calculated is the total cost of equipment utilized in the MPC controller build. To do so, the purchase price of each piece of equipment that was used in building the prototype is listed, as shown in Table 4-2. It is very conservative to consider the individual purchase price of each piece of equipment in the cost-benefit analysis, since it will cost much less to purchase this equipment in bulk for mass production.

Table 4-2 Cost of prototype equipment

	Cost/unit	Quantity	Cost
Arduino Uno	$29.95	1	$29.95
Beefcake Relay Control Kit	$7.95	1	$7.95
Breadboard	$5.95	1	$5.95
Jumper Wires	$3.95	2	$7.90
Temperature Sensor	$1.50	4	$6.00
		TOTAL	**$57.75**

Secondly, the labor cost for the assembly of the proposed controller is quantified. The labor cost is conservatively estimated to be $40 for building the controller. Similar to the equipment cost, the labor will actually cost much less for mass production.

The overall cost of implementing the proposed MPC controller in the actual building environment is the summation of the equipment cost and the labor cost, and is estimated to be approximately $100.

Payback Period

Finally, the period of time required for the return on the investment of developing the proposed MPC controller to repay the sum of the original investment is calculated. Using the average annual cost savings and the cost of implementation quantified above, the simple payback period is calculated as follows:

$$Payback\ period = \frac{Implementation\ Cost}{Cost\ Savings} = \frac{\$100}{\$168/year} \cong 0.6\ year \cong 7months$$

One should note that the payback period calculated above is for reference purposes. It is quantified considering a decent size residential house with average HVAC load consumption behavior. In larger buildings where there is higher HVAC consumption, the

savings will increase and the payback period will decrease accordingly. Also as mentioned earlier, it will cost much less to implement the proposed MPC controller when produced in large quantities.

CHAPTER 5: CONCLUSION AND FUTURE RESEARCH

Conclusion

In this research, a practical cost and energy efficient model predictive HVAC load control (MPC) strategy is proposed for buildings facing dynamic real-time electricity pricing. The proposed MPC strategy aims to reduce the total energy consumption and hence, cost of electricity for the user, while considering the thermal comfort of the consumers by concurrently minimizing the deviation of the inside temperatures from the consumer's choice of reference temperatures. To achieve this, the model assigns temperature set-points (reference temperatures) to price ranges based on the consumer's discomfort tolerance index and accordingly generates efficient signal actions for each time period for the AC unit.

The signal action is composed of a duty cycle that represents the proportion of "on" time for the AC during any given time period. A parameter prediction model is developed for the mapping between the signal action and the inside temperature. To ensure practical use of the overall strategy, the prediction model is tailored for a linear approximation of the mapping. To determine the reference temperatures for the planning horizon (usually a day), an algorithm is developed for temperature set-point assignment (TSA). A discomfort tolerance index is defined to capture the consumer's attitude towards thermal comfort in reference to cost of comfort. The TSA algorithm assigns temperature set-points to price ranges according to this index. Both the input/output mapping and the produced temperature set-points serve as inputs for the proposed MPC controller, which is used to generate signal actions for the AC unit.

To investigate and demonstrate the effectiveness of the proposed approach a simulation based experimental analysis is first carried out using real-life pricing data. Then, an actual prototype is built for the proposed HVAC load control strategy and a series of prototype experiments is conducted similar to the simulation studies to validate the simulation results. In both cases, the MPC process is first compared to the conventional two-position control approach under fixed temperature set-point. The latter strategy represents the common practice in real life where the reference temperature is usually kept at a fixed level throughout the planning horizon. The experimental results indicate that while the MPC process leads to energy reduction and cost savings for the consumer, in general, with only load shifting under fixed temperature set-points, the benefits are not too promising. In the second part of the analysis, the controller employs the TSA algorithm to control the temperature set-points. In this case, the experiments reveal that with the MPC strategy, reduction in energy consumption (both for total electricity use and for peak time consumption) and cost savings significantly improve. The obtained results suggest that the proposed MPC strategy, when controlling both the load and the temperature set-points, allows the consumers effectively take advantage of the dynamic pricing and enjoy significant cost savings in electricity usage. On the other hand this strategy can be instrumental in facilitating an effective demand response framework, which enables the utility providers adopt efficient demand management policies using real-time pricing.

The key findings of the simulation studies and prototype experiments can be summarized as follows:

- Under a fixed temperature set-point;
  - Simulation studies show that compared to the two-position control the proposed MPC strategy results in 4.6% and 4.5% savings in energy consumption and energy cost respectively. Furthermore, the savings in energy consumption and energy cost with the proposed MPC strategy are 5.8% and 5.5% respectively during peak hours.
  - Prototype experiments show that compared to the two-position control the proposed MPC strategy results in 6.3% and 7.2% savings in energy consumption and energy cost respectively. Furthermore, the savings in energy consumption and energy cost with the proposed MPC strategy are 8.1% and 8.3% respectively during peak hours.
- Under variable temperature set-points with a neutral discomfort tolerance index;
  - Simulation studies show that compared to the two-position control the proposed MPC strategy results in 8% and 13.1% savings in energy consumption and energy cost respectively. Furthermore, the savings in energy consumption and energy cost with the proposed MPC strategy are 23.6% and 24% respectively during peak hours.
  - Prototype experiments show that compared to the two-position control the proposed MPC strategy results in 6.2% and 5.1% savings in energy consumption and energy cost respectively. Furthermore, the savings in energy consumption and

energy cost with the proposed MPC strategy are 6.8% and 6.8% respectively during peak hours.

- When compared the two-position control with a fixed temperature set-point to the proposed MPC strategy with variable temperature set-points;
  - Simulation studies show that the proposed MPC strategy results in a 1.4% increase in energy consumption and a 17.5% savings in energy cost. Furthermore, the proposed MPC strategy results in 44.2% and 43.3% savings in energy consumption and energy cost respectively during peak hours.
  - Prototype experiments show that the proposed MPC strategy results in 4.9% and 15.1% savings in energy consumption and energy cost respectively. Furthermore, the savings in energy consumption and energy cost with the proposed MPC strategy are 26.1% and 26.3% respectively during peak hours.

A cost-benefit analysis is also performed to display the economic feasibility of implementing such a controller as part of a building energy management system and the payback period is identified considering cost of prototype build and cost savings. This analysis also helps the adoption of the proposed controller in the building HVAC control industry.

This research has also been recently published in (Avci, Erkoc, & Asfour, 2012) and (Avci, Erkoc, Rahmani, & Asfour, 2013). The proposed TSA algorithm is introduced and discussed in (Avci et al., 2012). The MPC strategy is proposed, and the findings are discussed in (Avci et al., 2013).

Future Research

Since the proposed MPC strategy is tailored for the energy user, its benefits could be best realized when a component that can effectively capture the consumer's discomfort tolerance index is introduced and integrated into the controller. Such a component would be able to deduce the tolerance index via direct input, past usage behavior or both for a particular user. An interesting research extension is to develop an effective and practical component that can accomplish this task.

One should also note that the control strategy discussed in this research considers the problem from the perspective of a single user. Another interesting future extension is the macro analysis of demand response of multiple users and the impact of increasing number of "smart energy users", who employ the MPC mechanism, on the peak-energy consumption and the utility companies' pricing strategies.

The fact that the user preference is incorporated into the proposed control strategy in the form of discomfort tolerance index provides some flexibility in the duration when the actual consumption occurs in a large scale implementation. However, the effect of utilizing different discomfort tolerance indices by multiple customers on the peak-demand reduction needs to be further studied. More specifically, by utilizing various combinations of discomfort tolerance indices in a community, a methodology should be developed to regulate and/or limit the utilization of unique discomfort tolerance index for an effective demand response implementation.

Another direction of future research is through further analysis for the effect of higher discomfort tolerance indices on the participation on the peak-demand as compared to utilizing lower discomfort tolerance indices by over-cooling/over-heating the building to

achieve financial benefits. In other words, customers with higher tolerance indices who are willing to benefit from low energy prices may excessively consume energy during low-price period, which may shift the peak-demand to the low-price period and eventually lead to higher peaks as compared to the customers with lower tolerance indices.

Finally, parameter identification of linear state-space model proposed for MPC implementation needs to be repeated as the parameters lead to less accuracy in the model for the following days. The frequency of parameter identification will depend on many variables including temperature changes in the weather, occupancy pattern in the building, and unexpected thermal activities. The optimal thresholds for re-calculating the parameters of the dynamic model of the building thermal plant to employ in the MPC controller need to be determined.

REFERENCES

Arnold, M., & Andersson, G. (2011). Model predictive control of energy storage including uncertain forecasts. In *Power Systems Computation Conference (PSCC), Stockholm, Sweden*.

Aswani, A., Master, N., Taneja, J., Culler, D., & Tomlin, C. (2012a). Reducing transient and steady state electricity consumption in HVAC using learning-based model-predictive control. *Proceedings of the IEEE*, *100*(1), 240-253.

Aswani, A., Master, N., Taneja, J., Smith, V., Krioukov, A., Culler, D., & Tomlin, C. (2012b). Identifying models of HVAC systems using semiparametric regression. In *Proceedings of the American Control Conference*.

Avci, M., Erkoc, M., & Asfour, S. S. (2012). Residential HVAC load control strategy in real-time electricity pricing environment. In *Energytech, 2012 IEEE* (pp. 1-6). IEEE.

Avci, M., Erkoc, M., Rahmani, A., & Asfour, S. (2013). Model predictive HVAC load control in buildings using real-time electricity pricing. *Energy and Buildings*.

Balan, R., Stan, S. D., & Lapusan, C. (2009). A model based predictive control algorithm for building temperature control. In *Digital Ecosystems and Technologies, 2009. DEST'09. 3rd IEEE International Conference on* (pp. 540-545). IEEE.

Black, J. W., & Tyagi, R. (2010). Potential problems with large scale differential pricing programs. In *Transmission and Distribution Conference and Exposition, 2010 IEEE PES* (pp. 1-5). IEEE.

Boait, P. J., & Rylatt, R. M. (2010). A method for fully automatic operation of domestic heating. *Energy and Buildings*, *42*(1), 11-16.

Braun, J. E. (1990). Reducing energy costs and peak electrical demand through optimal control of building thermal storage. *ASHRAE transactions*, *96*(2), 876-888.

Braun, J. E., Montgomery, K. W., & Chaturvedi, N. (2001). Evaluating the performance of building thermal mass control strategies. *HVAC&R Research*, *7*(4), 403-428.

Burke, W., & Auslander, D. (2009). Low-frequency pulse width modulation design for hvac compressors. In *The ASME*.

California Energy Commission. (2000). California Energy Demand: 2000-2010. *California Energy Commission, Sacramento*.

California Energy Commission. (2002). 2002-2012 Electricity Outlook Report (commission final-p700-01-004f). *California Energy Commission, Tech. Rep.*

Chandan, V., & Alleyne, A. (2011). Optimal Partitioning for the Decentralized Thermal Control of Buildings. *Submitted to the IEEE transactions on control systems technology*.

Chen, X., Jang, J., Auslander, D. M., Peffer, T., & Arens, E. A. (2008). Demand response-enabled residential thermostat controls. CooKE, D. (2011). *Empowering Customer Choice in Electricity Markets* (No. 2011/13). OECD Publishing.

Dawson-Haggerty, S., Ortiz, J., Jiang, X., Hsu, J., Shankar, S., & Culler, D. (2010). Enabling green building applications. In *Proceedings of the 6th Workshop on Hot Topics in Embedded Networked Sensors* (p. 4). ACM.

Energy, E. P. B. E. S. (1997). Forecasting Division. Canada's energy outlook, 1996-2020. *Natural Resources Canada*.

Energy Information Administration. (2009). Residential Energy Consumption Survey (RECS). Available from: http://www.eia.gov/consumption/residential/data/2009/.

Federal Energy Regulatory Commission. (2009). A national assessment of demand response potential. *Government Printing Office, Washington, DC*. Available from: https://www.ferc.gov/legal/staff-reports/06-09-demand-response.pdf

Federal Energy Regulatory Commission. (2012). Assessment of demand response and advanced metering: 2012 staff report. Available from: https://www.ferc.gov/legal/staff-reports/12-20-12-demand-response.pdf

Fernandez-Camacho, E., & Bordons-Alba, C. (1995). *Model predictive control in the process industry*. Springer.

Freire, R. Z., Oliveira, G. H., & Mendes, N. (2008). Predictive controllers for thermal comfort optimization and energy savings. *Energy and buildings*, *40*(7), 1353-1365.

Goyal, S., Ingley, H., & Barooah, P. (2012). Zone-level control algorithms based on occupancy information for energy efficient buildings. In *American Control Conference*.

Henze, G. P., Felsmann, C., & Knabe, G. (2004). Evaluation of optimal control for active and passive building thermal storage. *International Journal of Thermal Sciences*, *43*(2), 173-183.

Herter, K. (2007). Residential implementation of critical-peak pricing of electricity. *Energy Policy*, *35*(4), 2121-2130.

Ilic, M., Black, J. W., & Watz, J. L. (2002). Potential benefits of implementing load control. In *Power Engineering Society Winter Meeting, 2002. IEEE* (Vol. 1, pp. 177-182). IEEE.

International Energy Agency. (2003). The Power to Choose – Demand Response in Liberalized Electricity Markets. Available from: http://www.schneider-electric.us/documents/solutions1/demand-response-solutions/powertochoose_2003.pdf.

Kulkarni, M. R., & Hong, F. (2004). Energy optimal control of a residential space-conditioning system based on sensible heat transfer modeling. *Building and environment*, *39*(1), 31-38.

Lin, C., Federspiel, C., & Auslander, D. (2002). Multiple sensors with single HVAC system control.

Liu, S., & Henze, G. P. (2006a). Experimental analysis of simulated reinforcement learning control for active and passive building thermal storage inventory: Part 1: Theoretical foundation. *Energy and buildings*, *38*(2), 142-147.

Liu, S., & Henze, G. P. (2006b). Experimental analysis of simulated reinforcement learning control for active and passive building thermal storage inventory: Part 2: Results and analysis. *Energy and buildings*, *38*(2), 148-161.

Lu, J., Sookoor, T., Srinivasan, V., Gao, G., Holben, B., Stankovic, J., Field, E., & Whitehouse, K. (2010). The smart thermostat: using occupancy sensors to save energy in homes. In *Proceedings of the 8th ACM Conference on Embedded Networked Sensor Systems* (pp. 211-224). ACM.

Ma, Y., Borrelli, F., Hencey, B., Packard, A., & Bortoff, S. (2009). Model predictive control of thermal energy storage in building cooling systems. In *Decision and Control, 2009 held jointly with the 2009 28th Chinese Control Conference. CDC/CCC 2009. Proceedings of the 48th IEEE Conference on* (pp. 392-397). IEEE.

Ma, Y., Borrelli, F., Hencey, B., Coffey, B., Bengea, S., & Haves, P. (2010). Model predictive control for the operation of building cooling systems. In *American Control Conference (ACC), 2010* (pp. 5106-5111). IEEE.

Maciejowski, J. M. (2002). *Predictive control: with constraints*. Pearson education.

Mayne, D. Q., & Rawlings, J. B. (2009). *Model Predictive Control: theory and design.* Nob Hill Publishing.

Mohsenian-Rad, A. H., & Leon-Garcia, A. (2010). Optimal residential load control with price prediction in real-time electricity pricing environments. *Smart Grid, IEEE Transactions on*, *1*(2), 120-133.

Morari, M., & H Lee, J. (1999). Model predictive control: past, present and future. *Computers & Chemical Engineering*, *23*(4), 667-682.

Moroşan, P. D., Bourdais, R., Dumur, D., & Buisson, J. (2010). Building temperature regulation using a distributed model predictive control. *Energy and Buildings*, *42*(9), 1445-1452.

Moroşan, P. D., Bourdais, R., Dumur, D., & Buisson, J. (2011). A distributed MPC strategy based on Benders' decomposition applied to multi-source multi-zone temperature regulation. *Journal of Process Control*, *21*(5), 729-737.

Mozer, M. C., Vidmar, L., & Dodier, R. H. (1997). The neurothermostat: Predictive optimal control of residential heating systems. *Advances in Neural Information Processing Systems*, 953-959.

Oldewurtel, F., Parisio, A., Jones, C. N., Morari, M., Gyalistras, D., Gwerder, M., Stauch, V., Lehmann, B., & Wirth, K. (2010a). Energy efficient building climate control using stochastic model predictive control and weather predictions. In *American Control Conference (ACC), 2010* (pp. 5100-5105). IEEE.

Oldewurtel, F., Ulbig, A., Parisio, A., Andersson, G., & Morari, M. (2010b). Reducing peak electricity demand in building climate control using real-time pricing and model predictive control. In *Decision and Control (CDC), 2010 49th IEEE Conference on* (pp. 1927-1932). IEEE.

Parker, D., Hoak, D., Cummings, J., & Center, F. S. E. (2010). Pilot Evaluation of Energy Savings and Persistence from Residential Energy Demand Feedback Devices in a Hot Climate. *Proc of the ACEEE Summer Study on Energy Efficiency in Buildings (ACEEE 2010)*, 245-259.

Piette, M. A. (2009). Linking continuous energy management and open automated demand response.

PJM. (2012). Day-Ahead Energy Market. Available from: http://www.pjm.com/markets-and-operations/energy/day-ahead.aspx.

Rathouse, K., & Young, B. (2004). *Domestic heating: Use of controls*. Technical Report RPDH 15, Building Research Establishment, UK.

Scott, J., Brush, A. B., Krumm, J., Meyers, B., Hazas, M., Hodges, S., & Villar, N. (2011). PreHeat: controlling home heating using occupancy prediction. In *Proceedings of the 13th international conference on Ubiquitous computing* (pp. 281-290). ACM.

Široký, J., Oldewurtel, F., Cigler, J., & Prívara, S. (2011). Experimental analysis of model predictive control for an energy efficient building heating system. *Applied Energy*, *88*(9), 3079-3087.

Standard, A. S. H. R. A. E. (1992). 55, Thermal environmental conditions for human occupancy. *American Society of Heating, Refrigerating and Air conditioning Engineers*.

Tiptipakorn, S., & Lee, W. J. (2007). A residential consumer-centered load control strategy in real-time electricity pricing environment. In *Power Symposium, 2007. NAPS'07. 39th North American* (pp. 505-510). IEEE.

Tiptipakorn, S., Lee, W. J., & Wang, L. (2009). Enabling customer demand and budget management in the real-time pricing environment. In *Industrial & Commercial Power Systems Technical Conference-Conference Record 2009 IEEE* (pp. 1-6). IEEE.

Tiptipakorn, S., Lee, W. J., Mao, C., & Lu, J. (2010). Price naming on home appliance load controls in real-time pricing environment. In *Power and Energy Society General Meeting, 2010 IEEE* (pp. 1-6). IEEE.

U. S. DOE. (2011). Buildings Energy Data Book. Available from: http://buildingsdatabook.eren.doe.gov/.

Xu, J., Luh, P. B., Blankson, W. E., Jerdonek, R., & Shaikh, K. (2005). An optimization-based approach for facility energy management with uncertainties. *HVAC&R Research*, *11*(2), 215-237.

Xu, P., Haves, P., Braun, J. E., & Hope, L. T. (2004). Peak demand reduction from pre-cooling with zone temperature reset in an office building. In *Proceedings of the ACEEE*.

Xu, P., & Zagreus, L. (2006). Demand shifting with thermal mass in light and heavy mass commercial buildings. *Info:*.

Vargas, J. V. C., & Parise, J. A. R. (1995). Simulation in transient regime of a heat pump with closed-loop and on-off control. *International journal of refrigeration*, *18*(4), 235-243.

Wang, W., Katipamula, S., Huang, Y., & Brambley, M. R. (2011). *Energy Savings and Economics of Advanced Control Strategies for Packaged Air-Conditioning Units with Gas Heat* (No. PNNL-20955). Pacific Northwest National Laboratory (PNNL), Richland, WA (US).

Yin, R., Xu, P., Piette, M. A., & Kiliccote, S. (2010). Study on Auto-DR and pre-cooling of commercial buildings with thermal mass in California. *Energy and Buildings*, *42*(7), 967-975.

APPENDIX A

Data Collection and Analysis

Data Logger Software (HOBOware)

HOBOware software is used for launching, reading out, and plotting data, making it easy to analyze environmental conditions recorded with HOBO data loggers and wireless HOBO data nodes. HOBOware can be utilized to view data, create graphs, perform analysis, save projects for future use, among others. The data can also be exported to Microsoft Excel or other ASCII-compatible programs for additional analysis.

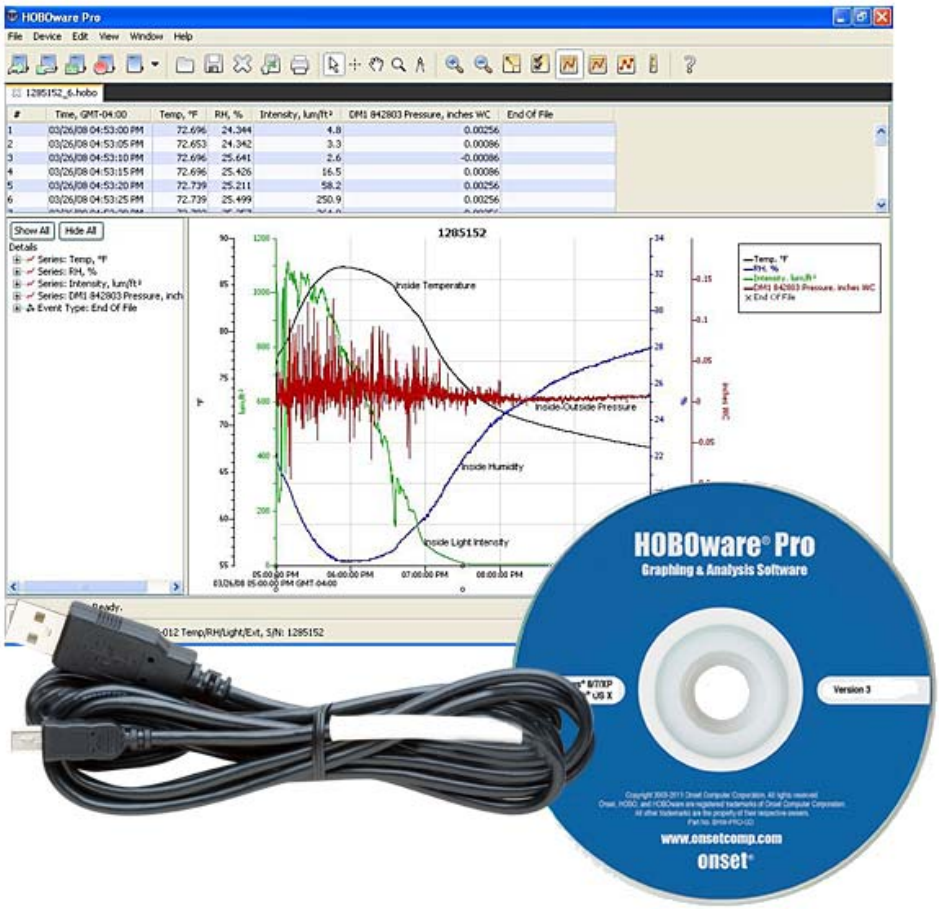

HOBOware software CD, USB cable, and user interface

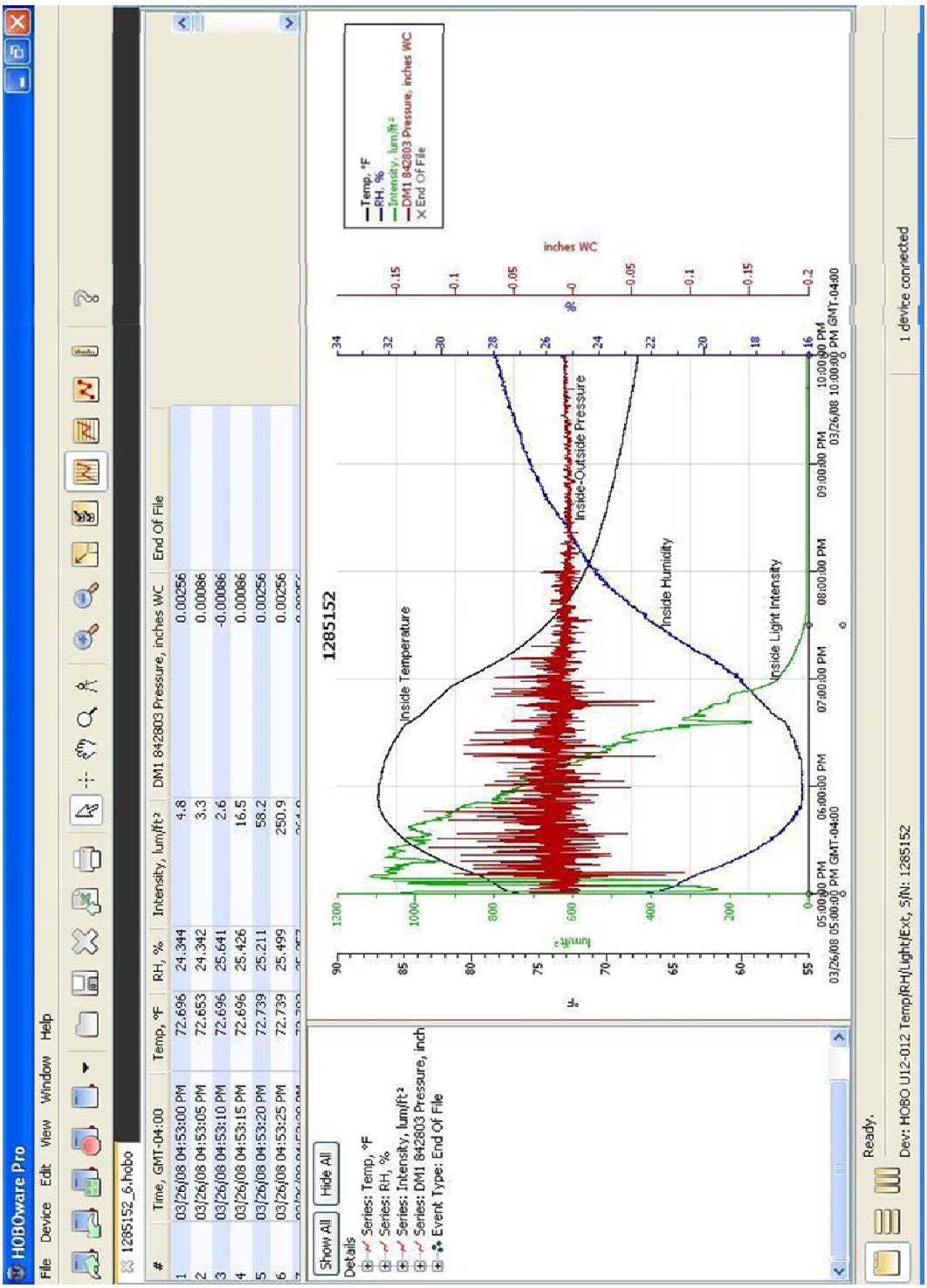

HOBOware software user interface with data and its graph

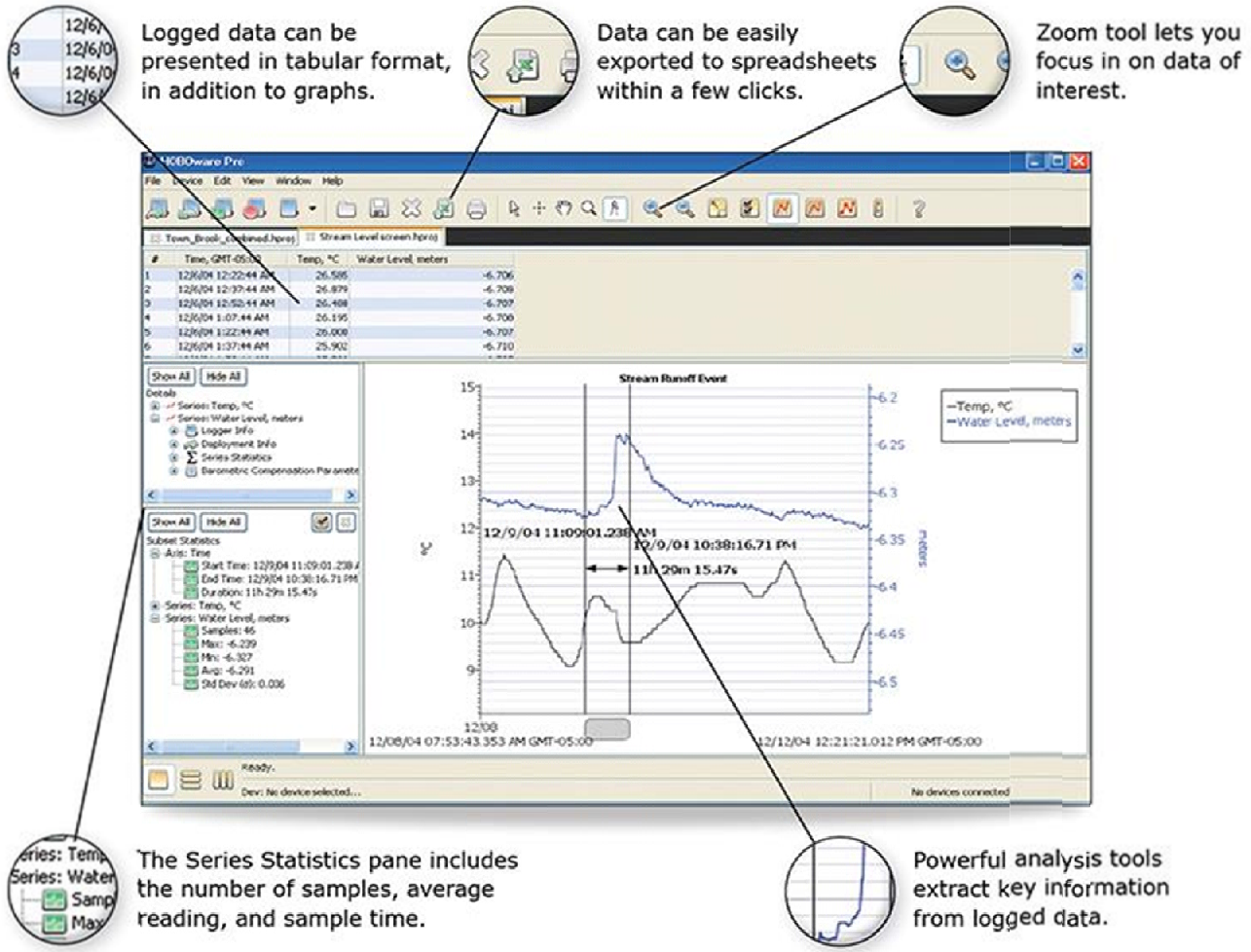

HOBOware software user interface details

Temperature/Relative Humidity Data Logger (HOBO U10-003)

The HOBO U10-003 is a two-channel data logger that records temperature and relative humidity with its integrated sensors. It has a 10-bit resolution and capacity for 52,000 measurements. The logger uses a direct USB interface for launching and data readout by a computer. HOBOware software is required for logger operation.

HOBO U10 Temp/RH data logger

External Data Logger (HOBO U12-006)

The HOBO U12 is a data logger with four-external channels that that accept a wide range of onset and third-party sensors/transducers with a 0-2.5 VDC output, including external temperature, AC current, pressure, air velocity, and kW sensors. It has a 12-bit resolution and can record up to 43,000 measurements or events. The logger uses a direct USB interface for launching and data readout by a computer. HOBOware software is required for logger operation.

HOBO U12 External data logger

AC Current Sensor (Onset CTV-C)

The split-core AC current sensor is responsive over the range of 0 to 100 amps AC for use with HOBO U12 data loggers with external input channels. With an input current of AC current, sine wave, single phase 50 Hz or 60 Hz, load power factor 0.5 to 1.0 lead or lag.

Onset CTV-C AC Current Sensor

APPENDIX B

System Identification Data and Graphs

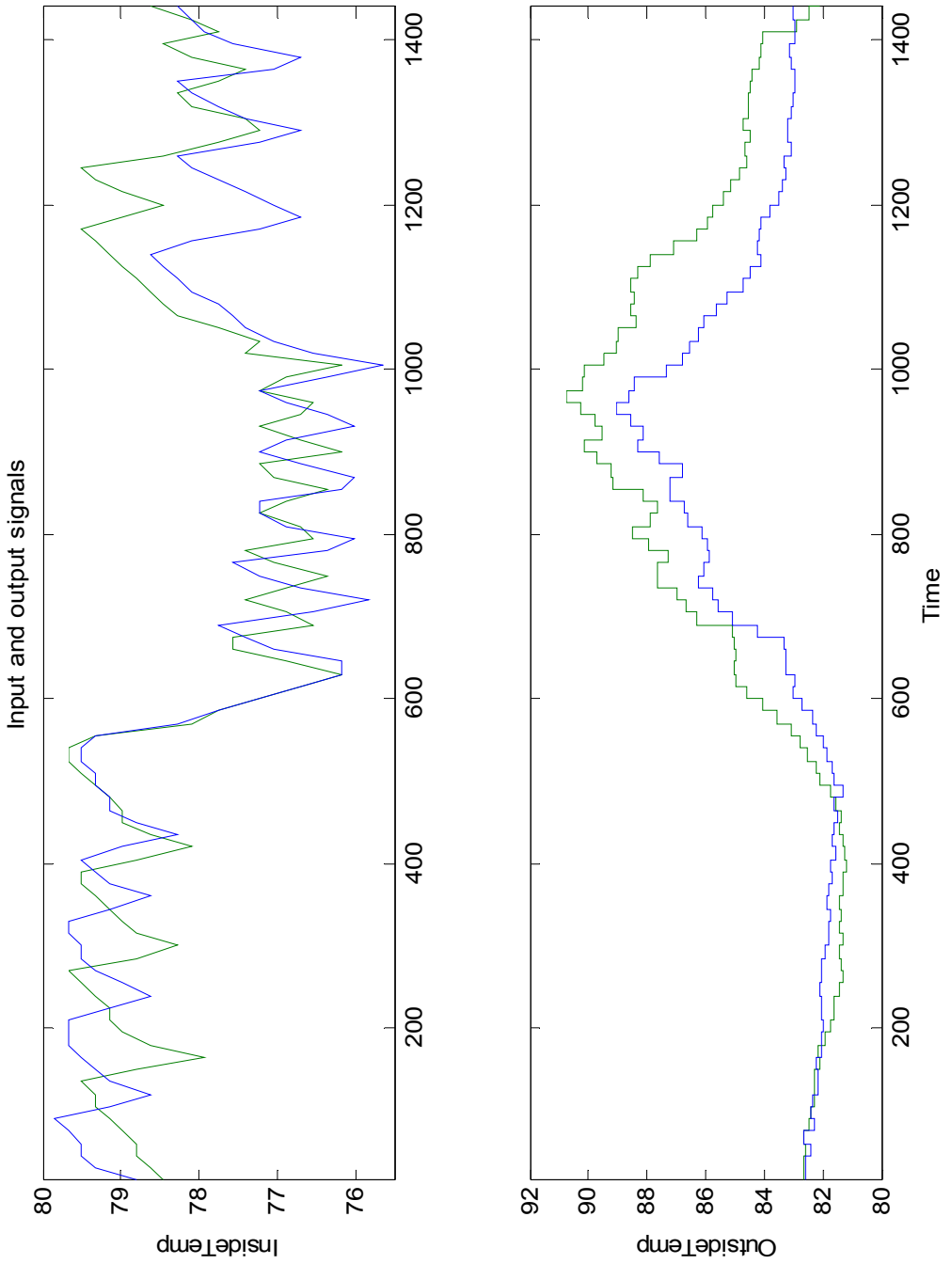

Time Plot – Inside Temperature vs. Outside Temperature

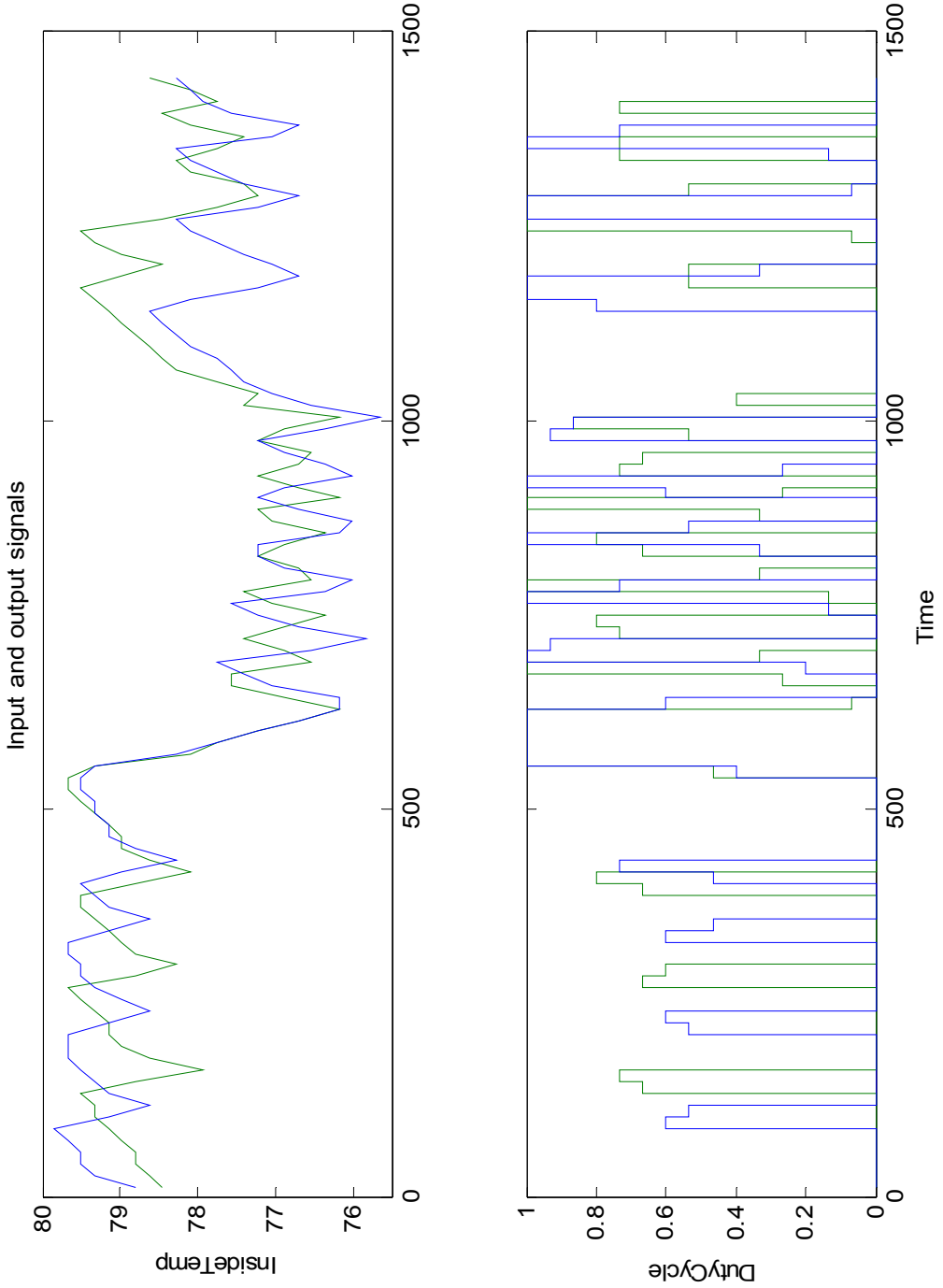

Time Plot – Inside Temperature vs. AC Duty Cycle

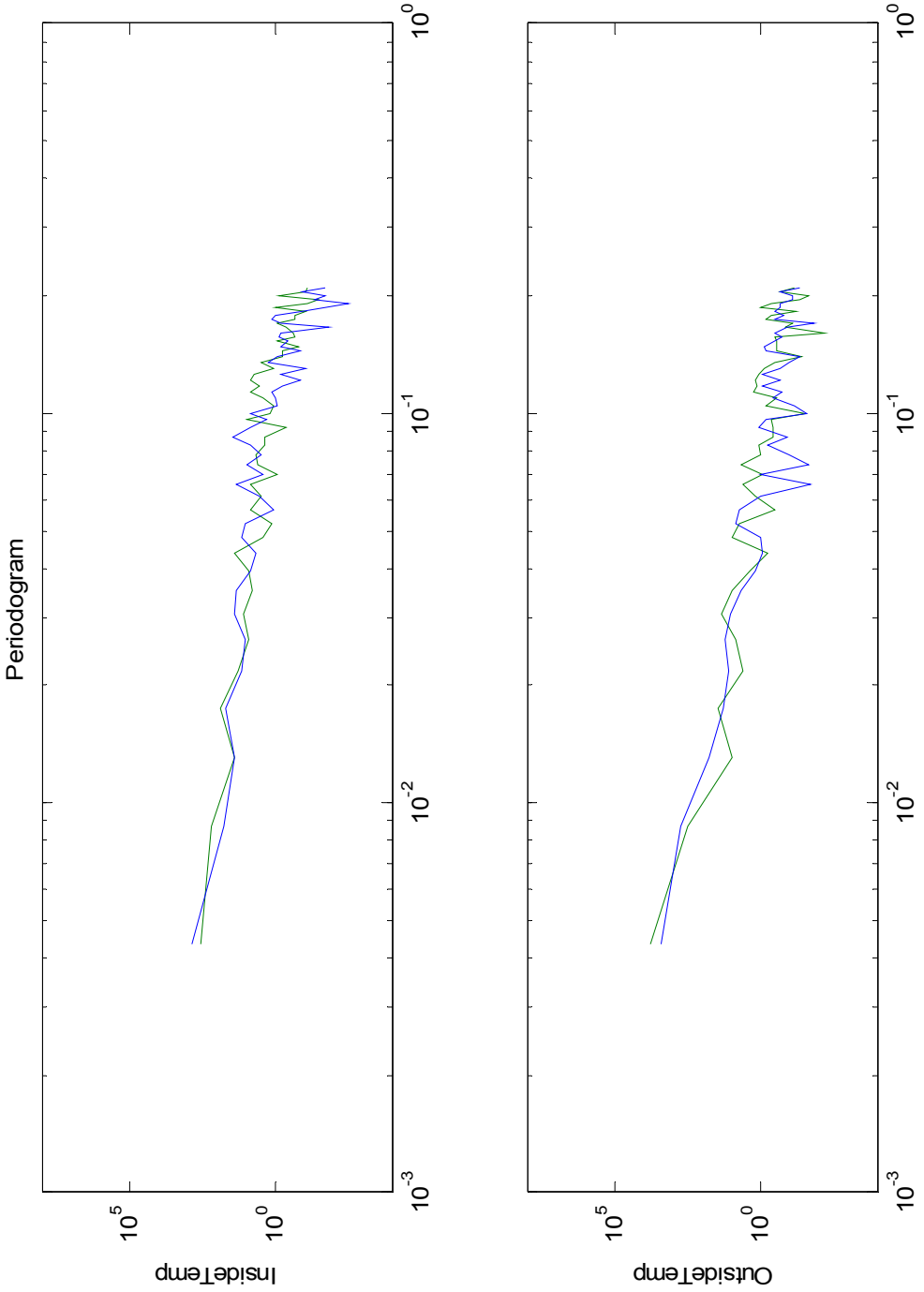

Data Spectra – Inside Temperature vs. Outside Temperature

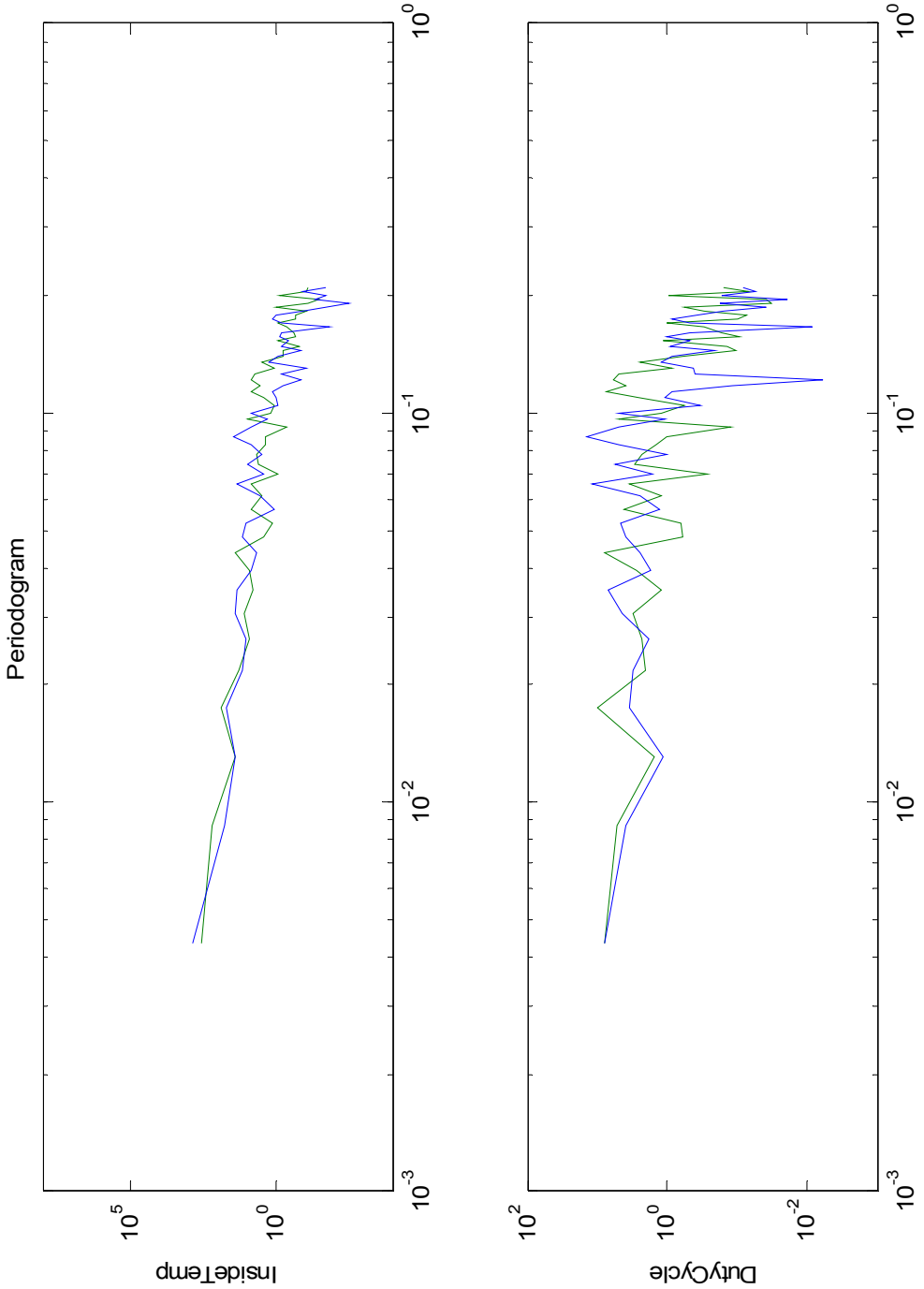

Data Spectra – Inside Temperature vs. AC Duty Cycle

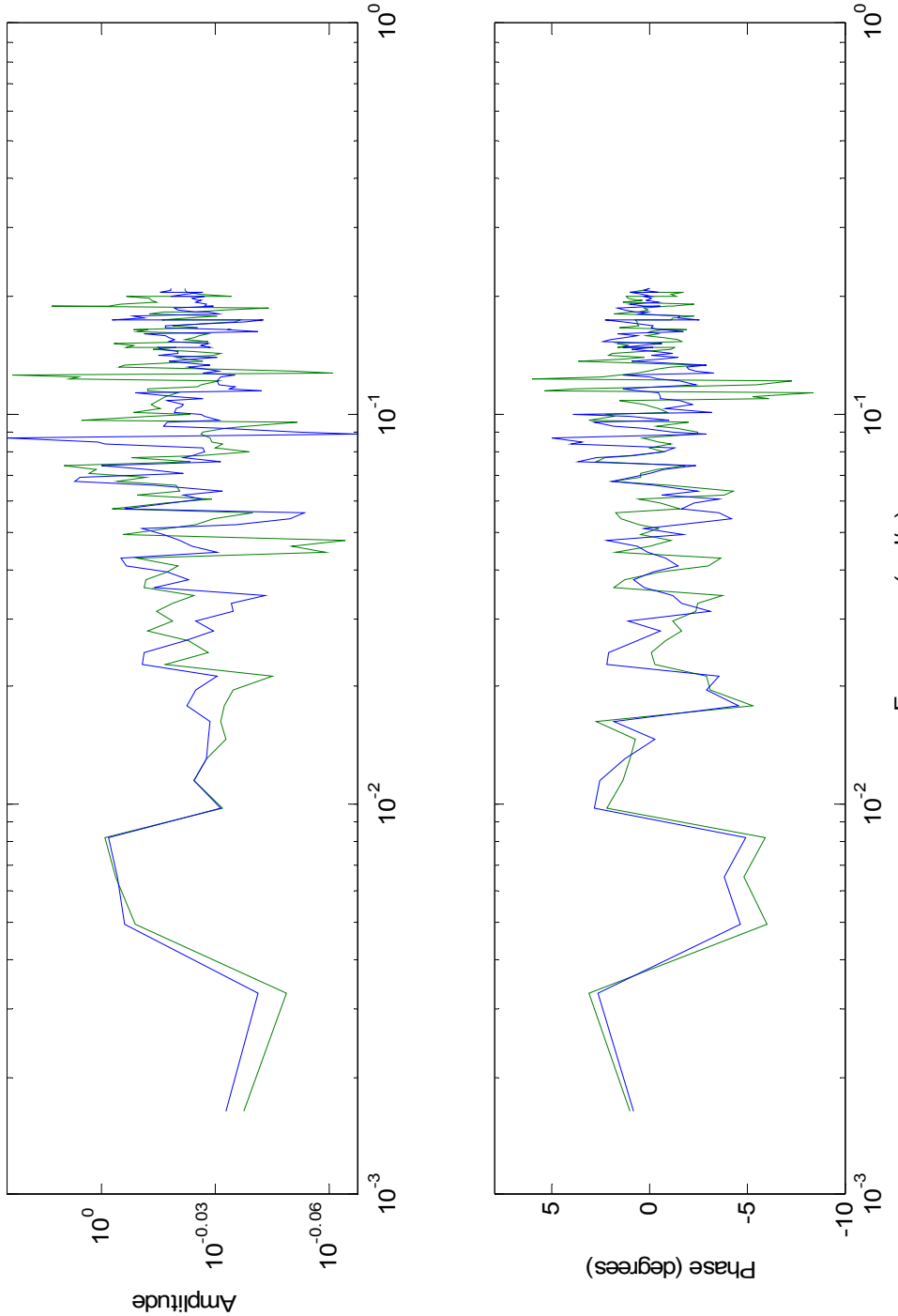

Frequency Function – Inside Temperature vs. Outside Temperature

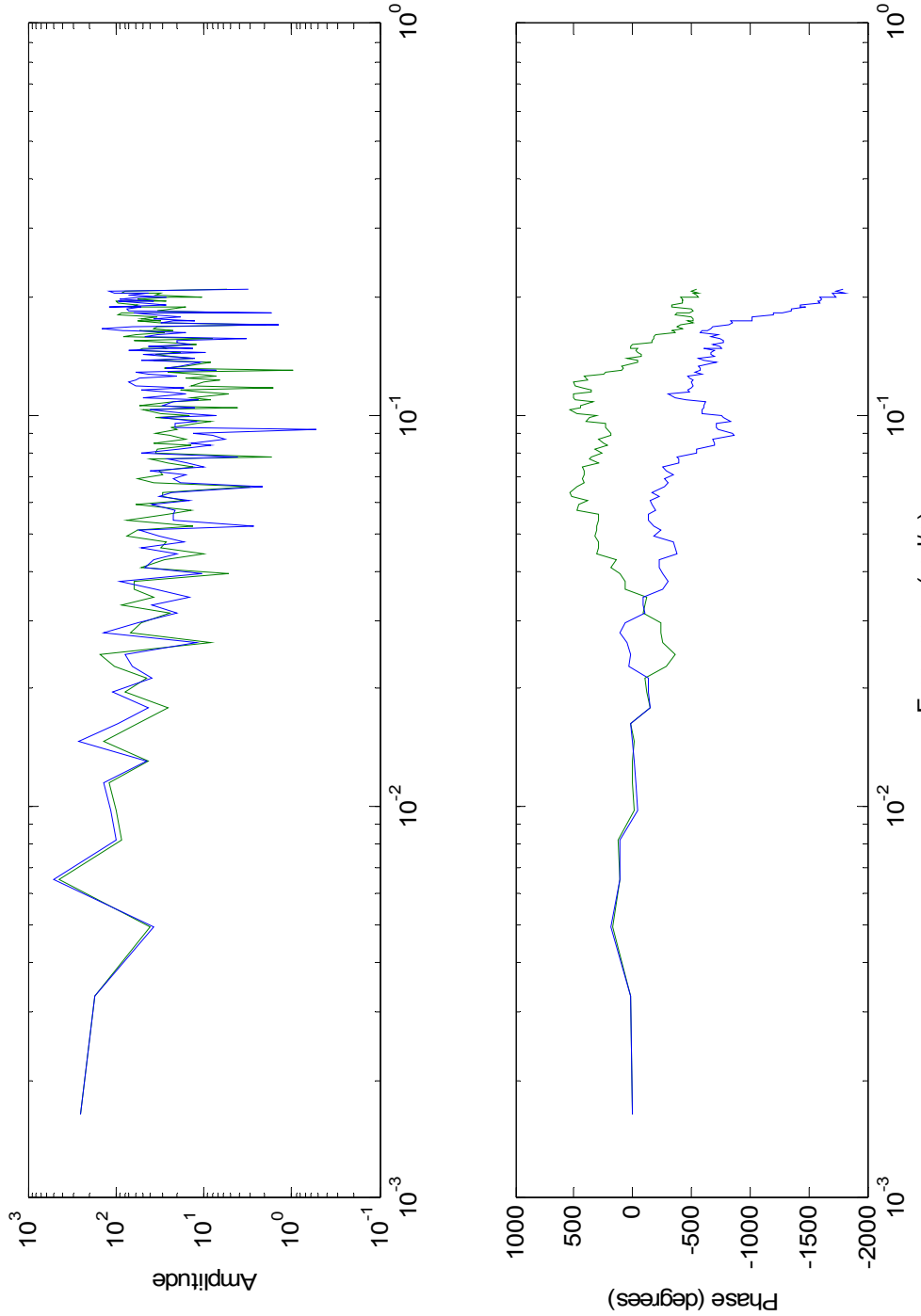

Frequency Function – Inside Temperature vs. AC Duty Cycle

```
n4s3 =
Discrete-time state-space model:
  x(t+Ts) = A x(t) + B u(t) + K e(t)
     y(t) = C x(t) + D u(t) + e(t)

A =
                    x1                  x2                  x3
   x1    0.9759 +/- 2.831e+11  -0.02625 +/- 3.214e+11  0.002302 +/- 6.859e+10
   x2   -0.1922 +/- 5.168e+12    0.4219 +/- 2.176e+12    0.3488 +/- 1.084e+12
   x3   0.06496 +/- 1.019e+13  -0.08368 +/-  1.06e+12     0.231 +/- 2.079e+12

B =
                OutsideTemp              DutyCycle
   x1  0.0009866 +/- 1.076e+10   -0.03179 +/- 1.298e+11
   x2    0.05506 +/- 1.488e+11    -0.2371 +/- 1.144e+12
   x3     -0.125 +/- 3.844e+11   -0.08221 +/- 1.707e+12

C =
                         x1                  x2                  x3
   InsideTemp      26.13 +/- 2.823e+13      1.775 +/- 1.178e+13  -0.004073 +/- 4.979e+12

D =
              OutsideTemp    DutyCycle
   InsideTemp           0           0

K =
                InsideTemp
   x1  0.01643 +/-  3.73e+10
   x2   0.0312 +/- 3.417e+11
   x3   0.0936 +/- 5.169e+11

Name: n4s3
Sample time: 15 minutes

Parameterization:
   FREE form (all coefficients in A, B, C free).
   Feedthrough: none
   Disturbance component: estimate
   Number of free coefficients: 21
   Use "idssdata", "getpvec", "getcov" for parameters and their uncertainties.

Status:
Estimated using N4SID on time domain data "ze".
Fit to estimation data: 90.71% (prediction focus)
FPE: 0.01882, MSE: 0.01223
More information in model's "Report" property.
```

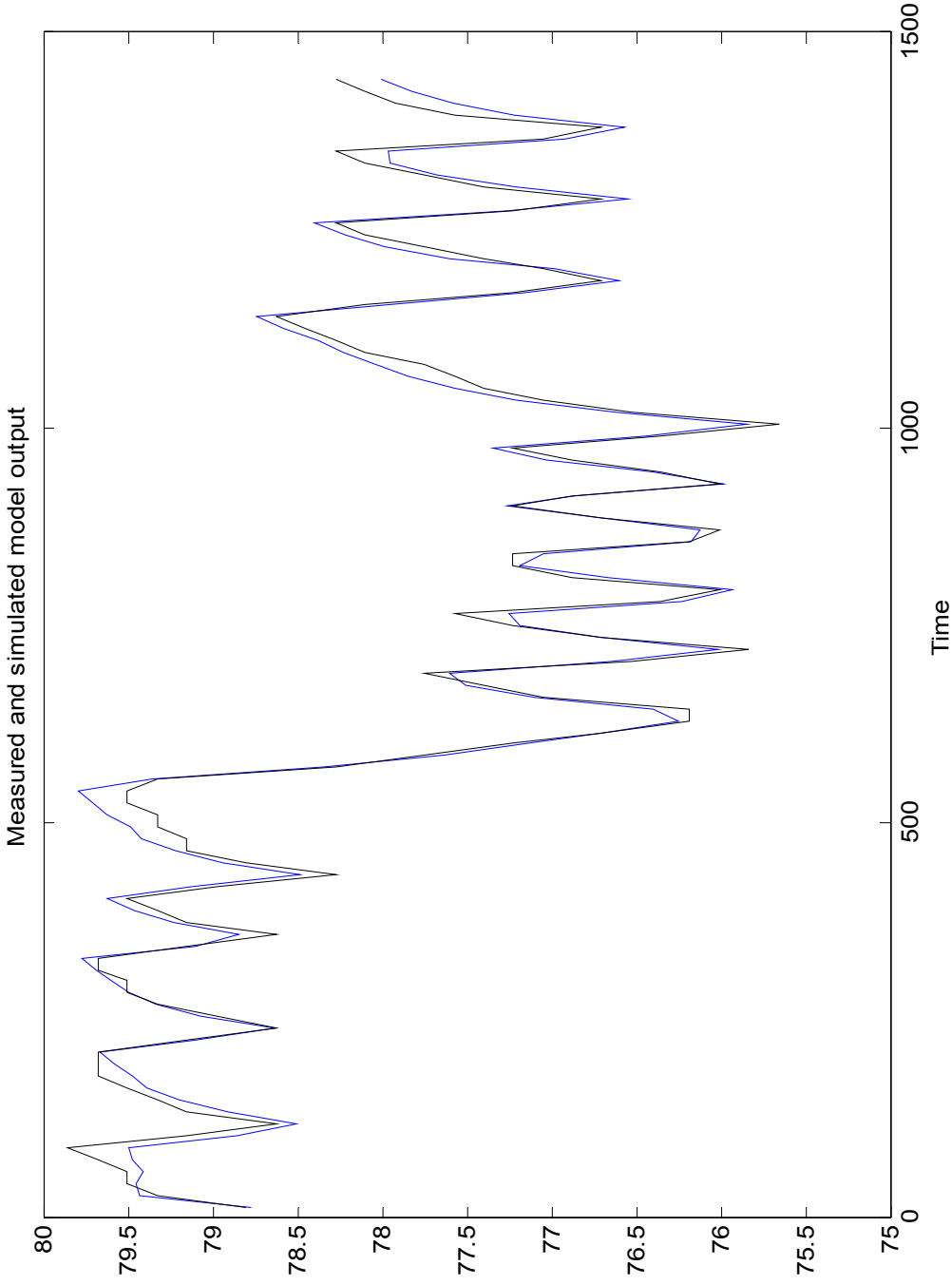

Discrete-time State-space Model Output with Parameter Estimation Data

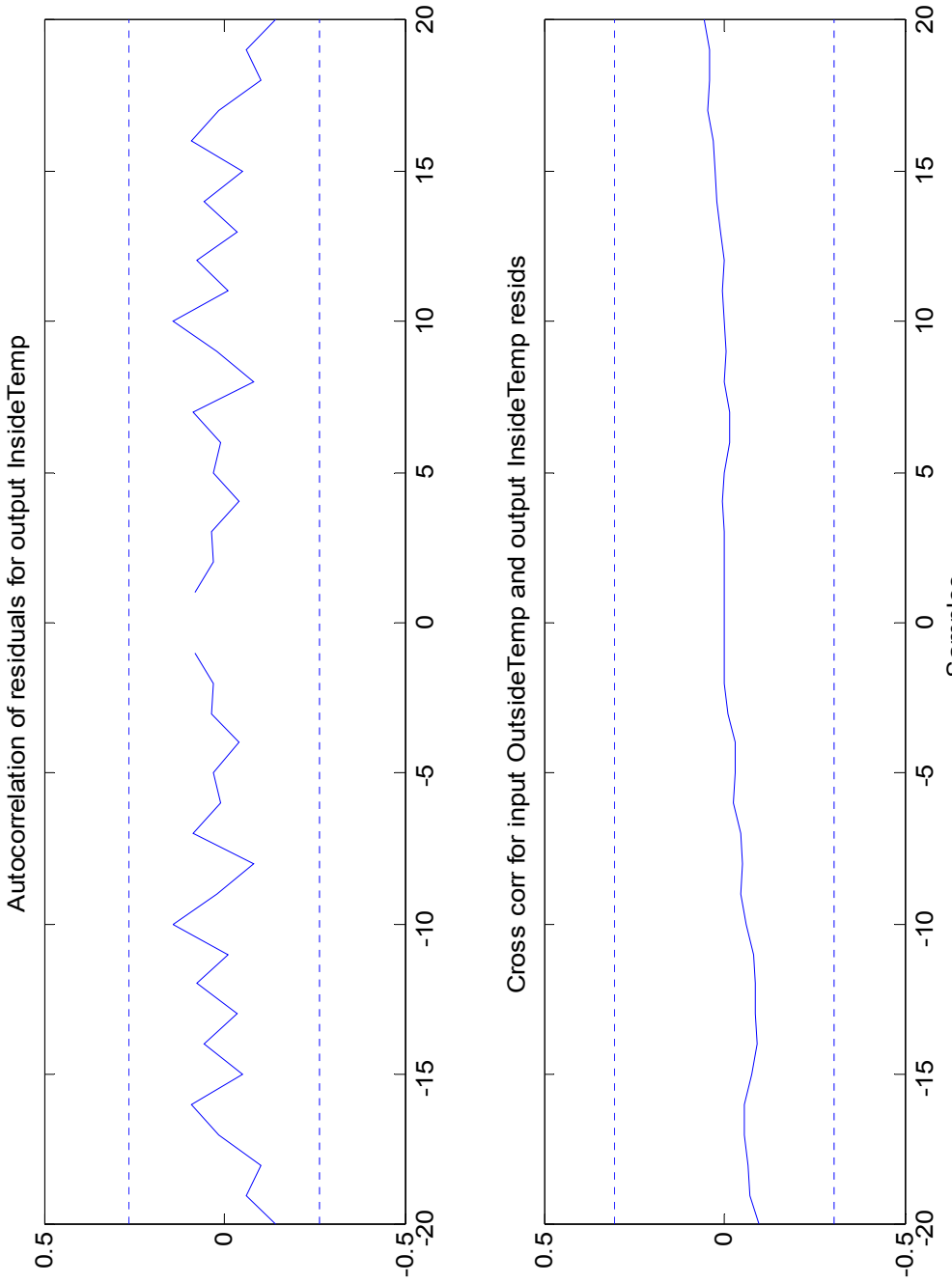

Discrete-time State-space Model Residuals with Parameter Estimation Data

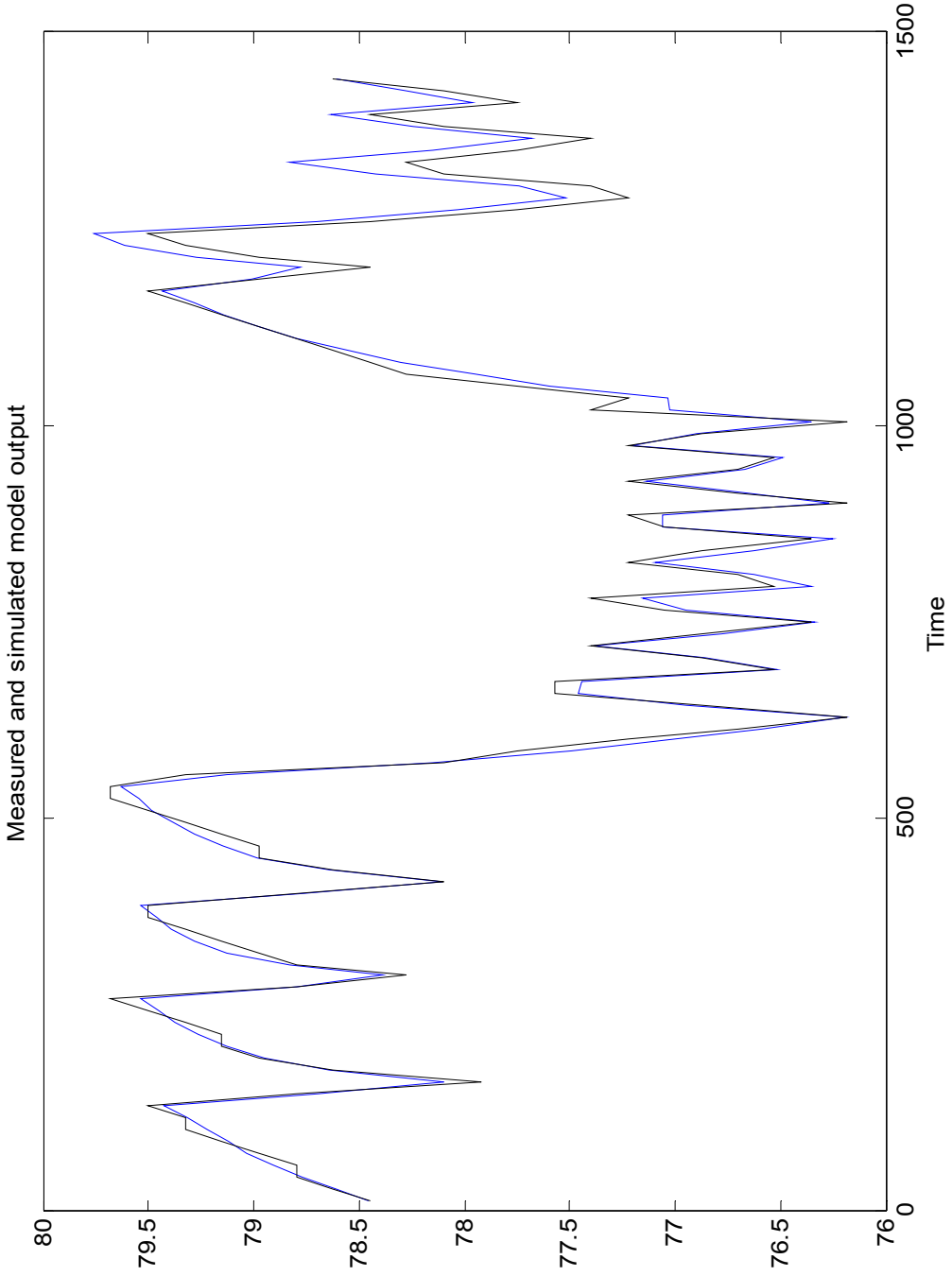

Discrete-time State-space Model Output with Parameter Validation Data

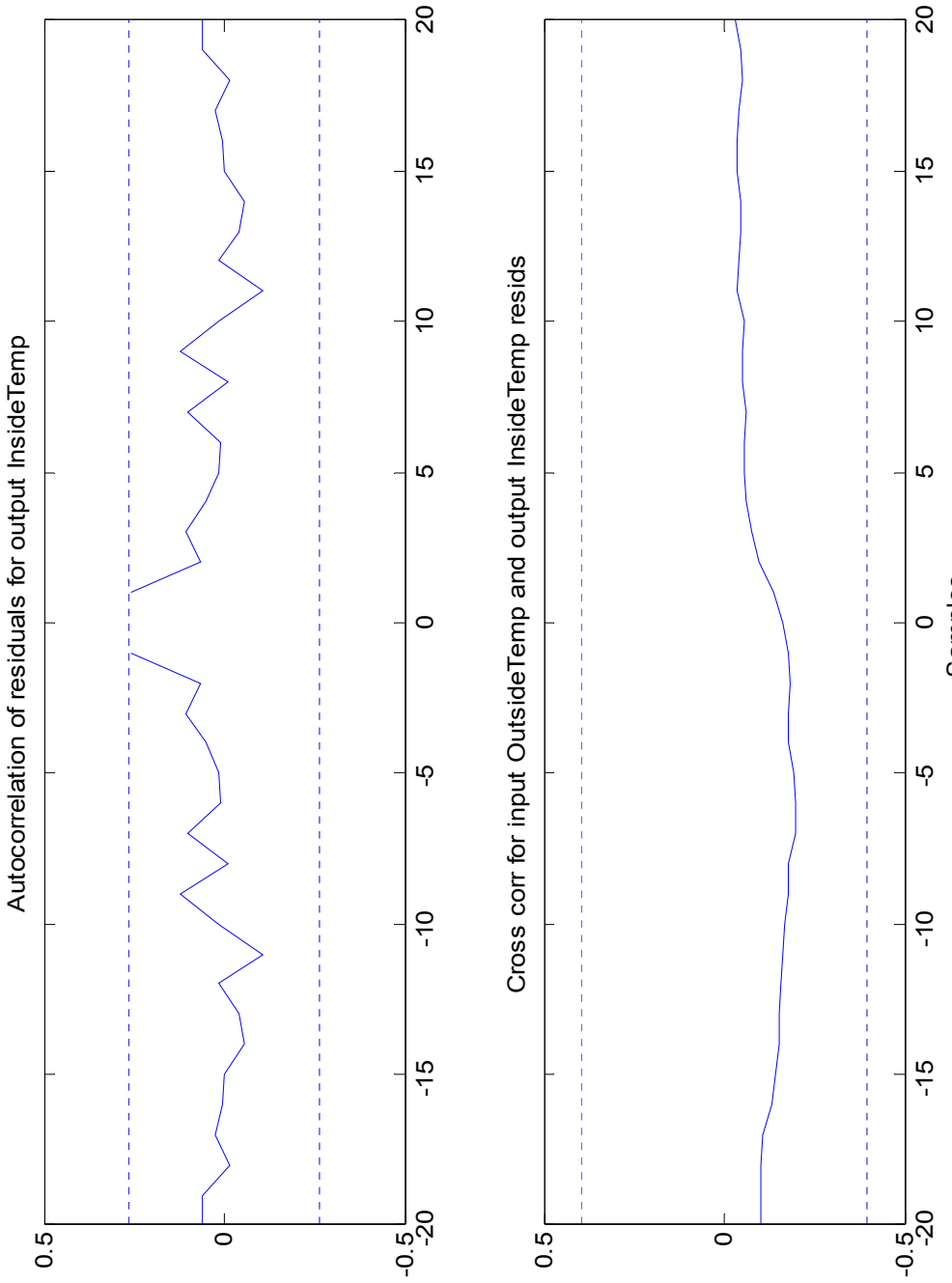

Discrete-time State-space Model Residuals with Parameter Validation Data

Hammerstein-Wiener model with 1 output and 2 inputs
Linear transfer function matrix corresponding to the orders:
  nb = [2 2]
  nf = [3 3]
  nk = [2 2]
Input nonlinearity estimators:
  For input 1: pwlinear with 10 units
  For input 2: pwlinear with 1 unit
Output nonlinearity estimator: poly1d of degree 5
Loss function: 0.0060491
Sampling interval: 1
Estimated by PEM

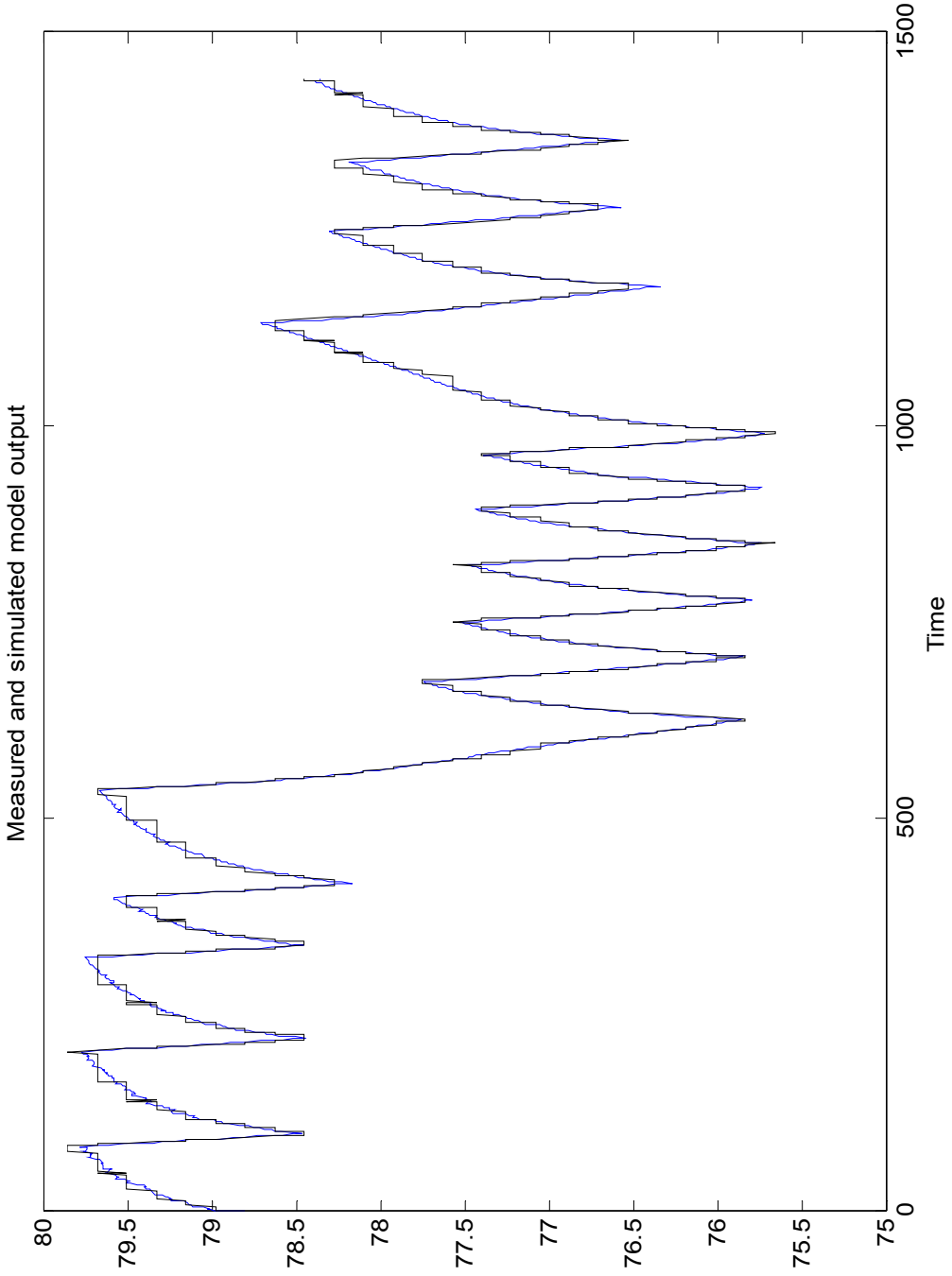

Hammerstein-Wiener Model Output with Parameter Estimation Data

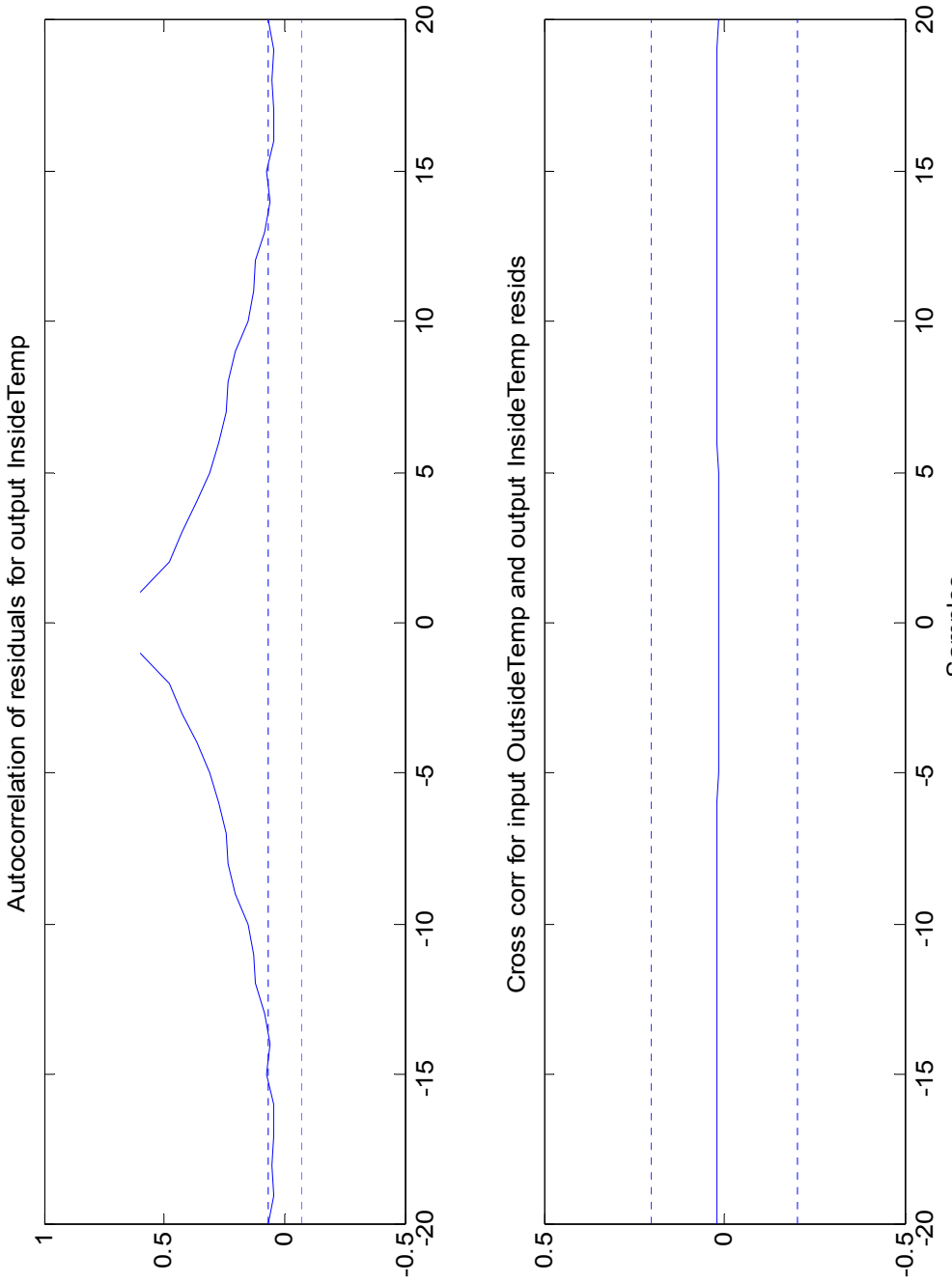

Hammerstein-Wiener Model Residuals with Parameter Estimation Data

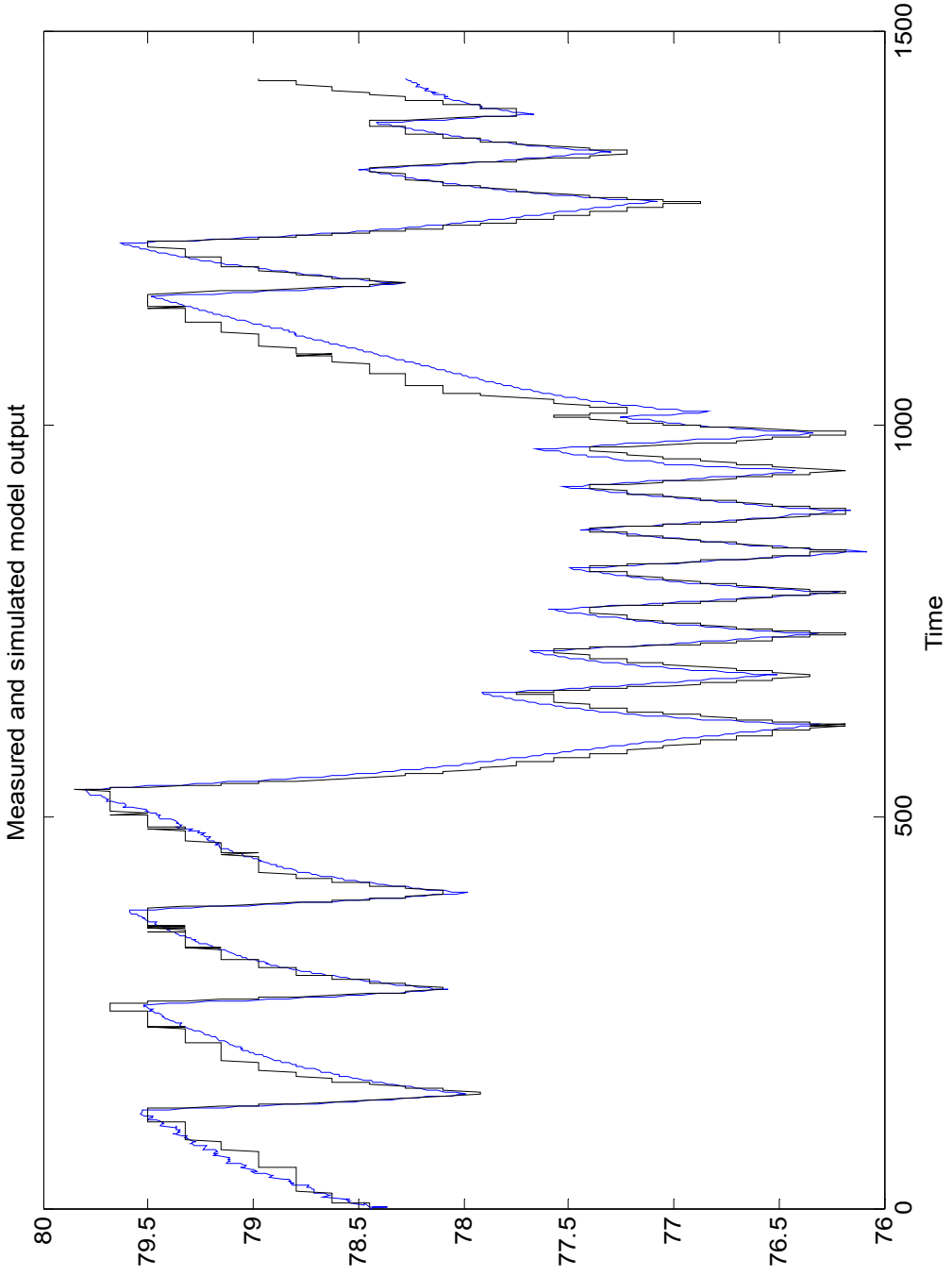

Hammerstein-Wiener Model Output with Parameter Validation Data

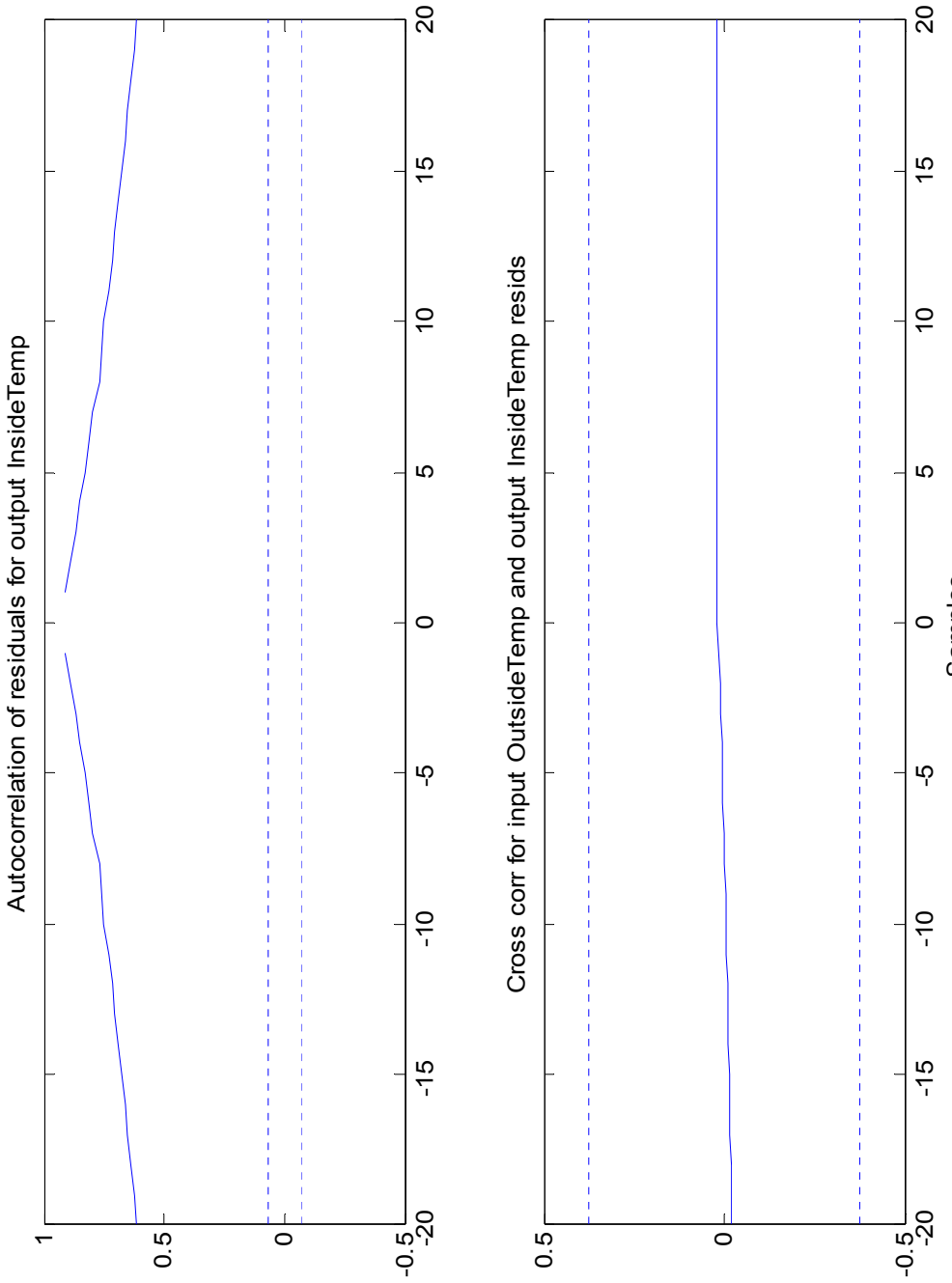

Hammerstein-Wiener Model Residuals with Parameter Estimation Data